NUMERICAL EVALUATION OF THE BOUNDARY LAYER APPROXIMATION FOR SOUND ATTENUATION BY SOLID PARTICLES IN WATER

DOUGLAS G. MERCER

ISBN 0-315-55042-2

NUMERICAL EVALUATION OF THE BOUNDARY LAYER APPROXIMATION FOR SOUND ATTENUATION BY SOLID PARTICLES IN WATER

by

© Douglas G. Mercer

A thesis submitted to
the School of Graduate Studies
in partial fulfillment of the
requirements for the degree of Master of Science

Department of Physics
Memorial University of Newfoundland
May 1989

St. John's Newfoundland Canada

ABSTRACT

Sound scattering and attenuation by small solid spheres in viscous fluids at ultrasonic frequencies is investigated theoretically. The approach is based upon that of Allegra and Hawley [1972], and Pierce [1981], and involves separating the sound field into different modes, which include strongly damped thermal compression and viscous shear wave modes, in addition to the usual weakly damped acoustic modes. A simplification of the computational problem is then sought by obtaining approximate expressions for the (six) boundary conditions at the fluid-scatterer interface, through the use of a suitable boundary layer approximation. We find that the radial stress at the boundary in the fluid may be approximated as the dynamic pressure, and that the thermal waves generated at the boundary are purely radial to an excellent approximation. This result for the thermal waves implies that in a partial wave expansion of the attenuation, thermal effects only appear in the isotropic term, and higher order, nonisotropic terms may be treated in the viscous thermally non-conducting limit with high accuracy. Numerical results are compared to Allegra and Hawley's measurements for aqueous suspensions of polystyrene spheres, and reasonable agreement is obtained in the appropriate limit.

ACKNOWLEDGEMENTS

First, I would like to thank Dr. Alex Hay for his help and encouragement above and beyond the call of duty, first for suggesting the thesis topic, and then for helping significantly in its production. I would also like to thank Dr. Brian Sanderson and Dr. Ian Webster for several discussions, and for encouragement. Mr. Sheng Jin-yu gave good advice both on thesis production and on several theoretical matters in sound scattering. Many other people, both in the Oceanography Group and the Physics Department gave much "encouragement" and support.

I wish to acknowledge the generous support in the form of an NSERC postgraduate scholarship for two years, a bursary from Memorial University of Newfoundland, and grant support from Dr. A.E. Hay.

I dedicate this thesis to my mother and my father.

TABLE OF CONTENTS

LIST OF TABLES

LIST OF FIGURES

LIST OF SYMBOLS

$\vec{\mathbf{A}}$	vector potential
A_n	constant, equation (2.3.1b)
a	particle radius
B_n	constant, equation (2.3.1c)
b_c , b_t	equations (2.1.17), (2.1.18)
C_n	constant, equation (2.3.1d)
C_p , C_v	specific heats
c	phase speed of compressional wave
c_s	phase speed of shear wave
c_1'	equation (2.1.3f)
d_s	viscous boundary layer thickness
d_t	thermal boundary layer thickness
e_{ij}	rate of strain tensor for the fluid
f	frequency
f_∞	form factor, equation (2.3.22)
h_n	spherical Hankel function
I	intensity
j_n	spherical Bessel function
n_n	spherical Neumann function
Im	imaginary part of ...
K	thermal conductivity

k_c , k_t, k_v	wavenumbers for the acoustic, thermal and viscous modes respectively
p	pressure
P_n (cos θ)	Legendre polynomial
r	radial coordinate
Re	real part of ...
S	entropy
s	k_v a
T	temperature
t	k_t a
U	specific internal energy
$\vec{u}$	displacement in the solid
$\vec{v}$	velocity in the fluid
X	root of Kirchoff dispersion relation
x	k_c a
x_i	Cartesian coordinates
α	attenuation coefficient
α_n	nth term of equation (2.3.19)
β	thermal dilatation (2.1.3f)
γ	ratio of specific heats C_p / C_v
δ_{ij}	Kronecker delta tensor
ϵ	volume fraction of particles in suspension
ϵ_t , ϵ_v	thermal and viscous scaling factors
θ	polar angle coordinate
λ'	Lamé constant
μ'	Lamé constant
ρ	density

σ	thermal diffusivity $(K/\rho_0 C_p)$
σ_{ij}	stress tensor for fluid (prime denotes solid)
ϕ	azimuthal angle coordinate
Φ	viscous dissipation function
ϕ_c	scalar potential for compressional wave
ϕ_t	scalar potential for thermal wave
Π	power
ξ_{ij}	strain tensor for solid
ω	angular frequency $2\pi f$

CHAPTER 1. INTRODUCTION

This thesis considers the problem of absorption and scattering of sound energy by a small solid elastic particle in a fluid. This problem is of interest in oceanography for suspended sediment transport studies, for the related problem of tracing water motion and turbulence by tracking particles suspended in the fluid, and for other problems relating to the interaction of acoustic waves with particulate matter in the ocean.

Many suspensions are so dilute that the total scattering and attenuation effects are merely the sum of the contributions from individual particles, with negligible interaction between the particles, thus leaving no noticeable multiple scattering effects. Therefore it is useful to consider the scattering from a single particle, independent of any other particles in the fluid, and we do so.

The particular aspect of the overall problem which is considered here is the absorption of energy due to the molecular diffusion of heat and momentum at the boundary between the solid scatterer and the surrounding fluid, which act to remove energy from sound waves propagating through a suspension, in addition to that lost through scattering. To simplify the formulation of the problem, and to understand better the physical mechanisms operating at the fluid-particle interface we apply boundary layer approximations in the thin regions near the surface of the sphere that are affected by viscosity and thermal conductivity, in the fluid and in the solid, and examine the results to see where such approximations are justified.

1.1. Historical Background

1.1.1. Scattering Theory Without Absorption

In 1877 Rayleigh [1945] considered the problem of sound scattering by a small spherical particle, solving for the case in which the acoustic wavelength is much greater than the scatterer circumference. In 1948 Morse [1986] generalized the problem to encompass all wavelengths, but assumed the scatterer to be rigid. Then Faran [1951] allowed the scatterers to be elastic, thus permitting longitudinal and shear waves in the solid. His theoretical work agreed well with his experimental results for long cylinders, which showed that the backscattered pressure amplitude is a minimum if the sound frequency corresponds to a scatterer free-body resonance frequency. Hickling [1962] and Hickling and Wang [1966] used Faran's formulation to calculate the backscattered intensity from spheres in water, for spheres of various materials. They also considered the case of the spheres being rigid and movable (this means the sphere has finite density, but is perfectly rigid, allowing no acoustic waves in the interior). Experimental measurements of backscatter amplitudes with spherical scatterers were made by Neubauer et al. [1974] for aluminum and tungsten carbide spheres, for a wide frequency range. Hay and Schaafsma [1989] have reported measurements of total scattering cross-section in suspensions of spherical particles. Both sets of results agree well with Faran's theory.

1.1.2. Scattering Theory With Absorption

Lord Rayleigh [1945] observed that the zeroth order term in the partial wave expansion of the perturbed pressure field was due to compressional differences between the two media, while the first order or dipole term was due to density

differences. In 1910 Sewell found that the dipole term was due to the relative motion of the solid and fluid, and should produce a viscous loss. He then calculated the viscous absorption due to a solid immovable sphere. This derivation was simplified in 1932 by Lamb [1945] who extended this work to include a movable sphere. Elasticity was included in 1941 by Epstein, who was only able to obtain qualitative agreement with experimental data. Urick [1948] obtained measurements in the long wavelength region from suspensions of kaolin and sand, which were in good agreement with losses predicted from viscous drag at the particle surface, based upon the theory of Lamb [1945]. Isakovitch [1948] noted possible thermal loss mechanisms at the scatterer boundary.

Then Epstein and Carhart [1953] performed a detailed analysis for fluid spheres in fluid media, including both viscous and thermal effects. This was generalized to the solid sphere case by Allegra and Hawley [1972], who noticed a formal resemblance in the equations for a fluid sphere immersed in a fluid to those of a solid sphere in a fluid. They also obtained experimental data for several different fluid emulsions in water, and suspensions of polystyrene spheres in water, showing that thermal effects can be significant. Hay and Burling [1982] recast the Allegra and Hawley theory in terms of Faran's [1951] phase shifts for the partial scattered waves, and obtained an expression for the relative importance of viscous and thermal effects at long wavelengths. Hay and Mercer [1985] obtained explicit expressions for the phase shifts in the intermediate and short wavelength regions, including only viscous effects, valid for frequencies and scatterer sizes such that the viscous boundary layer thickness was much less than the particle radius. The existence of a viscous boundary layer in the fluid allowed a simplification of the radial viscous dependence, allowing a simplified solution that was not very restrictive. Hay and Mercer [1989] showed that the attenuation coefficient obtained using their expressions for the phase shifts is in

agreement with Urick's [1948] result in the appropriate limit.

1.2. Purpose and Organization of Thesis

The purpose of this thesis is to apply a boundary layer approximation to the problem of sound scattering and attenuation from a solid sphere in water, where the wavelength of the sound is much greater than the particle radius. By doing so we hope to simplify calculation of attenuation and scattering effects, and we also wish to see which mechanisms are important in attenuation and which may be neglected. In doing so, we adapt a method used by Pierce [1981] which has distinct advantages in interpretation over the previously used exact treatment of Allegra and Hawley [1972].

Chapter 2 reviews the work of Allegra and Hawley [1972], and presents a derivation of the governing equations for the fluid and solid using the method of Pierce [1981]. In Chapter 3 we review basic boundary layer theory. Then we show some numerical results based on the Allegra and Hawley theory. This is followed by a derivation of two boundary layer approximations. We denote the simpler one by the first boundary layer approximation, where we apply various simplifications to the radial stress boundary condition in the fluid to see what mechanisms are important. The second is a formal derivation using the method of Pierce [1981], which we adapt to the formulation of Allegra and Hawley [1972] in terms of potentials. We examine numerical results using both the first and the second boundary layer approximation, and in each case compare these results to the exact results based on the Allegra and Hawley [1972] theory, in aqueous suspensions of polystyrene spheres. Chapter 4 concludes with the useful information we have obtained from the above analysis.

CHAPTER 2. THEORY OF SCATTERING AND ATTENUATION

In this Chapter we review the scattering and attenuation theory of Allegra and Hawley [1972]. First we present the governing equations in both the solid scatterer and the surrounding fluid. We solve for wave equations, which involves separating the sound field into a weakly damped acoustic wave, a strongly damped thermal wave and a strongly damped viscous shear wave in the fluid, together with weakly damped compression and shear waves, and a strongly damped thermal wave, in the solid. For each of these waves we find modal relationships between field quantities, using the method presented by Pierce [1981]. Then we present the six boundary conditions at the fluid-solid interface, which couple the various modes together. Then each of the modes is represented by a series expansion in terms of a complete set of orthogonal eigenfunctions. This results in six equations involving the nth-order undetermined coefficients in the eigenfunction expansion, one equation for each boundary condition. The relationship between the measured quantitiy of interest, the attenuation coefficient, and the amplitude coefficients of the scattered wave, is presented. This Chapter ends with a discussion of the inviscid, nonconducting limit at long wavelengths.

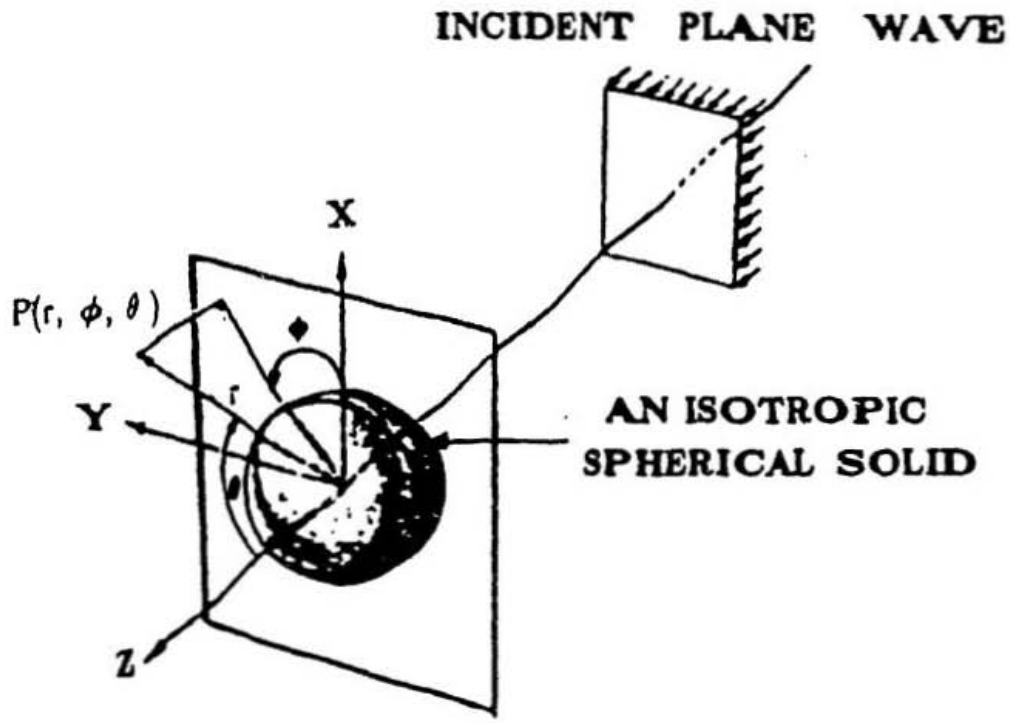

Figure 2.1. The geometry of scattering of an acoustic wave by a sphere.

2.1. General Problem

In our most general case the fluid is viscous, thermally conducting, and has a Newtonian rheology. The solid scatterer is a homogeneous, elastic, and thermally conducting sphere. The incident plane wave propagates in the positive z direction (Figure 2.1.). The coordinate system is spherical, with coordinates (r, θ, ϕ). The origin of the coordinate system is at the center of the sphere, which has radius a and equilibrium density ρ_0'. In all cases we are primarily interested in the total scattered energy, and in the energy absorbed as the incident wave passes by the sphere.

For the solid scatterer, the equations of motion are conservation of mass [Allegra and Hawley, 1972],

$$\frac{\partial \rho'}{\partial t} + \vec{\nabla} \cdot (\rho' \dot{\vec{u}}) = 0 \qquad (2.1.1a)$$

conservation of momentum [Landau and Lifshitz, 1986, p.87],

$$\rho' \ddot{u}_j + \rho' (\dot{\vec{u}} \cdot \vec{\nabla}) \dot{u}_j = \frac{\partial \sigma'_{ij}}{\partial x_i} \qquad (2.1.1b)$$

and conservation of energy [Allegra, 1970; see also Landau and Lifshitz, 1986, p.137],

$$\rho' \frac{\partial U'}{\partial t} + \rho' \dot{u}_i \frac{\partial U'}{\partial x_i} + p' \vec{\nabla} \cdot \dot{\vec{u}} = \Phi + K' \nabla^2 T' \qquad (2.1.1c)$$

where ξ_{ij} is the strain tensor defined below, $\vec{u}$ is the displacement vector, T' is the temperature, ρ' is the density, p' is the pressure, K' is the thermal conductivity, U' is the specific internal energy, Φ is the viscous dissipation function, and the x_i are Cartesian coordinates. Note that the Einstein summation convention is used, that primed quantities refer to the solid, unless noted otherwise, and that the overdots denote differentiation with respect to time.

In equation (2.1.1b), σ'_{ij} is the stress tensor for an elastic isotropic solid and

may be written

$$\sigma'_{ij} = \lambda' \xi_{ii} \delta_{ij} + 2 \mu' \xi_{ij} \tag{2.1.2a}$$

where

$$\xi_{ij} = \frac{1}{2} \left(\frac{\partial u_i}{\partial x_j} + \frac{\partial u_j}{\partial x_i} \right) . \tag{2.1.2b}$$

Here δ_{ij} is the Kronecker delta tensor, and λ' and μ' are the Lamé constants of the solid.

We may write the solid stress tensor as

$$\sigma'_{ij} = (\lambda' + \frac{2}{3} \mu') \xi_{ii} \delta_{ij} + 2 \mu' \xi'_{ij} , \tag{2.1.2c}$$

where

$$\xi'_{ij} = \xi_{ij} - \frac{1}{3} \xi_{ii} \delta_{ij} \quad \text{and} \quad \xi'_{ii} = 0.$$

In this form the first term is the bulk modulus times the relative change in volume. Thus

$$p' = - (\lambda' + \frac{2}{3} \mu') \xi_{ii} \tag{2.1.2d}$$

and

$$\sigma'_{ij} = - p' \delta_{ij} + 2 \mu' \xi'_{ij} . \tag{2.1.2e}$$

Nonlinear effects are neglected in our treatment, since we are interested in small amplitude forcing and response. Due to this we ignore all terms which are second order or larger in small quantities (see Appendix 1). Equations (2.1.1) simplify to

$$\frac{\partial \rho'}{\partial t} + \rho_0' \vec{\nabla} \cdot (\dot{\vec{u}}) = 0 , \tag{2.1.3a}$$

$$\rho_0' \ddot{\vec{u}} = - \vec{\nabla} p' + \frac{\mu'}{3} \vec{\nabla} (\vec{\nabla} \cdot \vec{u}) + \mu' \nabla^2 \vec{u} , \tag{2.1.3b}$$

and

$$\rho_0' \frac{\partial U'}{\partial t} + p_0' \vec{\nabla} \cdot \dot{\vec{u}} = + K' \nabla^2 T' , \tag{2.1.3c}$$

where ρ_0' and p_0' are the equilibrium density and pressure respectively.

There are seven unknowns (ρ', p', U', T', and $\vec{u}$), but only five equations. The two additional equations are provided by two implicit dynamic equations of state [Allegra, 1970, page 15]:

$$\vec{\nabla} p' = \frac{c_1'^2}{\gamma'} \vec{\nabla} \rho' + \frac{c_1'^2 \beta' \rho_0'}{\gamma'} \vec{\nabla} T' \tag{2.1.3d}$$

and

$$\dot{U}' = \frac{1}{\rho_0'^2} \left[p_0' - \frac{\rho_0' (\gamma' - 1) C_v'}{\beta'} \right] \dot{\rho}' + C_v' \dot{T}' . \tag{2.1.3e}$$

Here β' and γ' are

$$\beta' = -\frac{1}{\rho_0'} \left(\frac{\partial \rho'}{\partial T'} \right)_p \tag{2.1.3f}$$

and

$$\gamma' = \frac{C_p'}{C_v'} , \tag{2.1.3g}$$

while c_1' is defined by

$$c_1'^2 = \frac{(\lambda' + 2/3\ \mu')}{\rho_0'} . \tag{2.1.3h}$$

C_p' and C_v' are the specific heats at constant pressure and volume, respectively.

Similarly, the linearized equations governing sound waves in the fluid are conservation of mass,

$$\frac{\partial \rho}{\partial t} + \rho_0 \vec{\nabla} \cdot \vec{v} = 0 \tag{2.1.4a}$$

conservation of momentum,

$$\rho_0 \frac{\partial \vec{v}}{\partial t} = - \vec{\nabla} p + \mu_0 \left[\nabla^2 \vec{v} + \frac{1}{3} \vec{\nabla} (\vec{\nabla} \cdot \vec{v}) \right] \tag{2.1.4b}$$

and conservation of energy,

$$\rho_0 \frac{\partial U}{\partial t} + p_0 \vec{\nabla} \cdot \vec{v} = K \nabla^2 T , \tag{2.1.4c}$$

or equivalently

$$\rho_0 T_0 \frac{\partial S}{\partial t} = K \nabla^2 T , \tag{2.1.4d}$$

where in the fluid $\vec{\mathbf{v}}$ is the velocity, μ_0 is the molecular shear viscosity, ρ is the density, U is the specific internal energy, S is the entropy, T is the temperature, and K is the thermal conductivity. Entropy is related to energy by the linearized relation

$$T_0 \frac{\partial S}{\partial t} = \frac{\partial U}{\partial t} + p_0 \vec{\nabla} \cdot \vec{\mathbf{v}} . \qquad (2.1.4e)$$

Again, to close the system of equations we use the two thermodynamic equations of state [Pierce, 1981, page 515]

$$\rho = \frac{1}{c^2} p - \left(\frac{\rho_0 \beta T_0}{C_p} \right) S , \qquad (2.1.4f)$$

and

$$T = \left(\frac{\beta T_0}{\rho_0 C_p} \right) p + \left(\frac{T_0}{C_p} \right) S , \qquad (2.1.4g)$$

where we use entropy instead of energy in the thermodynamic relationships for ease of calculation, and where c is the adiabatic sound speed. We use energy for our calculations in the solid instead of entropy to facilitate comparison with the derivation of Allegra and Hawley [1972].

2.1.1. Allegra-Hawley Formulation

Now we simplify the governing equations following the approach used by Allegra and Hawley [1972]. For the solid, placing $\vec{\nabla} p'$ from (2.1.3d) into equation (2.1.3b) and $\dot{U}'$ from (2.1.3e) into equation (2.1.3c) gives

$$\rho_0' \ddot{\vec{u}} = - \left[\frac{{c_1'}^2}{\gamma} \vec{\nabla} \rho' + \frac{{c_1'}^2 \rho_0' \beta'}{\gamma} \vec{\nabla} T' \right] + \frac{\mu'}{3} \vec{\nabla} (\vec{\nabla} \cdot \vec{u}) + \mu' \nabla^2 \vec{u} , \qquad (2.1.5a)$$

and

$$\frac{\dot{\rho}'}{\rho_0'} \left[p_0' - \frac{\rho_0' (\gamma' - 1) C_v'}{\beta'} \right] + \rho_0' C_v' \dot{T}' + p_0' \vec{\nabla} \cdot \dot{\vec{u}} = K' \nabla^2 T' . \qquad (2.1.5b)$$

We eliminate ρ' by using the mass conservation equation (2.1.3a), and assuming a

time dependance $e^{-i\omega t}$ for perturbation quantities, we obtain the following equations for the solid:

$$\omega^2 \vec{u} + \left(\frac{c_1'^2}{\gamma'} + \frac{\mu'}{3\rho_0'} \right) \vec{\nabla}(\vec{\nabla}\cdot\vec{u}) - \frac{c_1'^2\beta'}{\gamma'} \vec{\nabla} T' + \frac{\mu'\nabla^2\vec{u}}{\rho_0'} = 0 \qquad (2.1.6a)$$

and

$$(-i\omega) \left[\frac{(\gamma'-1)}{\beta'} \right] \vec{\nabla}\cdot\vec{u} - i\omega T' - \gamma'\sigma'\nabla^2 T' = 0, \qquad (2.1.6b)$$

where $\vec{u}$ is the displacement vector.

Similarly, for the fluid we eliminate S and p from (2.1.4b) and (2.1.4c) using (2.1.4f) and (2.1.4g), and then eliminate ρ using (2.1.4a) to get

$$\omega^2\vec{v} + \left(\frac{c^2}{\gamma} - \frac{i\omega\mu_0}{3\rho_0} \right) \vec{\nabla}(\vec{\nabla}\cdot\vec{v}) + \frac{i\omega c^2\beta}{\gamma} \vec{\nabla} T - \frac{i\omega\mu_0}{\rho_0}\nabla^2\vec{v} = 0 \qquad (2.1.7a)$$

and

$$\left[\frac{(\gamma-1)}{\beta} \right] \vec{\nabla}\cdot\vec{v} - i\omega T - \gamma\sigma\nabla^2 T = 0. \qquad (2.1.7b)$$

Using Helmholtz's Theorem [Arfken, 1970, p. 67], we may represent the velocity field in the fluid and the displacement field in the solid by scalar potentials $\bar{\phi}$ and vector potentials $\vec{A}$ in the following manner:

$$\vec{v} = -\vec{\nabla}\bar{\phi} + \vec{\nabla}\times\vec{A}, \qquad (2.1.8)$$

$$\vec{u} = -\vec{\nabla}\bar{\phi}' + \vec{\nabla}\times\vec{A}', \qquad (2.1.9)$$

where

$$\bar{\phi} = \phi_c + \phi_t, \qquad (2.1.10)$$

and ϕ_c and ϕ_t are scalar potentials for the compression and thermal waves defined below, and where

$$\phi_c = \phi_0 + \dot{\phi}, \qquad (2.1.11)$$

ϕ_0 and $\dot{\phi}$ being the scalar potentials for the incident and scattered compressional waves in the fluid.

Because the problem is axially symmetric $\vec{A} = (0, 0, A_\phi)$ and

$\vec{A}' = (0 , 0 , A_\phi')$ [Faran, 1951]. If we assume wavelike solutions, the four equations (2.1.7) reduce to three Helmholtz equations (Appendix 2),

$$\begin{aligned} \nabla^2 \phi_c + k_c^2 \phi_c &= 0, \\ \nabla^2 \phi_t + k_t^2 \phi_t &= 0, \\ \nabla^2 A_\phi + k_s^2 A_\phi &= 0, \end{aligned} \tag{2.1.12}$$

where $\vec{\nabla} \cdot \vec{A} = 0$. The wavenumbers resulting from this reduction are

$$k_c^2 \approx \frac{\omega^2}{c^2} \left\{ 1 - \frac{i\omega}{c^2} \left[\frac{4\mu_0}{3\rho_0} + (\gamma - 1)\sigma \right] \right\}^{-1}, \tag{2.1.13}$$

$$k_t^2 \approx \frac{i\omega}{\sigma}, \tag{2.1.14}$$

$$k_s^2 \equiv \frac{i\omega\rho_0}{\mu_0}, \tag{2.1.15}$$

In addition, a relation between the temperature and the scalar potentials is produced as follows:

$$T = \frac{(b_c \phi_c + b_t \phi_t)}{(- i \omega)}. \tag{2.1.16}$$

Here b_c and b_t are given by

$$b_c = \left(- \frac{\gamma}{c^2 \beta} \right) \left[\omega^2 - \left(\frac{c^2}{\gamma} - \frac{4 i \omega \mu_0}{3 \rho_0} \right) k_c^2 \right], \tag{2.1.17}$$

and

$$b_t = \left(- \frac{\gamma}{c^2 \beta} \right) \left[\omega^2 - \left(\frac{c^2}{\gamma} - \frac{4 i \omega \mu_0}{3 \rho_0} \right) k_t^2 \right]. \tag{2.1.18}$$

There are three waves: the usual weakly damped compression wave (2.1.13), a highly damped thermal compression wave (2.1.14), and a highly damped viscous shear wave (2.1.15). In obtaining equations (2.1.13) and (2.1.14) from (2.1.7), it has been assumed that $| k_c / k_t | \ll 1$, $| k_c / k_s | \ll 1$, and $| k_c | \approx \omega / c$. For water the viscous wavenumber condition holds for $f \ll 10^{11}$ Hz (see Table 2.1), which is not unduly restrictive. The thermal wavenumber condition holds for $f \ll 10^{14}$ Hz, and is even less restrictive.

For a solid, the same procedure yields [Hay and Burling, 1982]

$$k_c'^2 \approx \frac{\omega^2}{c'^2}\left[1 - \frac{i\,\omega\,\sigma'}{c'^2}\,(\gamma'-1)\,\frac{(\lambda' + 2\,\mu'/3)}{(\lambda' + 2\,\mu')}\right]^{-1}, \qquad (2.1.19)$$

$$k_t'^2 \approx \frac{i\,\omega}{\sigma'}, \qquad (2.1.20)$$

$$k_s'^2 \equiv \frac{\rho_0'\omega^2}{\mu'}, \qquad (2.1.21)$$

and

$$T' = b_c'\,\phi_c' + b_t'\,\phi_t', \qquad (2.1.22)$$

where

$$b_c' = \frac{-\gamma'}{c_1'^2\,\beta'}\left[\omega^2 - \left(\frac{c_1'^2}{\gamma'} + \frac{4\,\mu'}{3\,\rho_0'}\right) k_c'^2\right], \qquad (2.1.23)$$

$$b_t' = \frac{-\gamma'}{c_1'^2\,\beta'}\left[\omega^2 - \left(\frac{c_1'^2}{\gamma'} + \frac{4\,\mu'}{3\,\rho_0'}\right) k_t'^2\right]. \qquad (2.1.24)$$

In this case there are again three waves: a compression wave weakly damped by thermal diffusion (2.1.19), a highly damped thermal compression wave (2.1.20), and an undamped shear wave (2.1.21). The shear wave is undamped because viscous dissipation in the solid has been ignored (see equation 2.1.1c).

As in the fluid, equations (2.1.19) and (2.1.20) have been obtained by assuming that $|k_c'| \approx \omega/c'$ and $|k_c'/k_t'| \ll 1$. For example, for quartz and polystyrene in water, the thermal condition holds for $f \ll 10^{14}$ Hz (refer to Table 2.2). This restricts γ' to be close tc 1, instead of a frequency restriction as in the fluid. We use quartz as an example because of its relevance to sediment transport, and we use polystyrene because comparisons will be made with measurements in polystyrene suspensions.

Because $|k_c/k_t| \ll 1$ and $|k_c'/k_t'| \ll 1$, then $|b_c/b_t| \ll 1$ and $|b_c'/b_t'| \ll 1$. Also, for most solid or fluid particles in water, $k_c \approx O(k_c')$, so that $|b_c/b_t'| \ll 1$ and $|b_c'/b_t| \ll 1$ as well.

Table 2.1. Physical properties of water at 20 °C, taken from Allegra and Hawley [1972].

Water		
density	ρ_0	0.998 g cm $^{-3}$
thermal conductivity	K	1.41×10^{-3} cal^{0}C^{-1}cm^{-1}s^{-1}
specific heat	C_p	1.000 cal^{0}C^{-1}g^{-1}
thermal exp. coeff.	β	2.1×10^{-4} °C
	$\gamma-1$	5.77×10^{-3}
viscosity	μ_0	1.002×10^{-2} g cm $^{-1}$ s $^{-1}$
speed of sound	c	1483 m s $^{-1}$

Table 2.2. Physical properties of polystyrene at 20 °C. taken from Allegra and Hawley [1972].

Polystyrene		
density	ρ_0'	1.055 g cm $^{-3}$
thermal conductivity	K'	0.27×10^{-3} cal^{0}C^{-1}cm^{-1}s^{-1}
specific heat	C_p'	0.287 cal^{0}C^{-1}g^{-1}
thermal exp. coeff.	β'	2.64×10^{-4} °C
	$\gamma'-1$	0.069
comp. wave speed	c'	2380 m s $^{-1}$
shear wave speed	c_s'	1097 m s $^{-1}$

Table 2.3. Physical properties of quartz at 20 °C, taken from Hay and Burling [1982].

Quartz		
density	ρ_0'	2.65 g cm $^{-3}$
thermal conductivity	K'	8.4×10^{-3} cal^{0}C^{-1}cm^{-1}s^{-1}
specific heat	C_p'	0.192 cal^{0}C^{-1}g^{-1}
thermal exp. coeff.	β'	3.4×10^{-5} °C
	$\gamma'-1$	5.2×10^{-3}
comp. wave speed	c'	5100 m s $^{-1}$
shear wave speed	c_s'	3200 m s $^{-1}$

2.1.2. Decomposition Into Acoustic, Thermal And Viscous Fields

In this section we present an alternate derivation which shows some physical interactions more clearly, and which is used in the boundary layer approximations. This derivation is based largely on the treatment of Pierce [1981, pp.519-523] for fluids, and is here adapted also to solids. The governing equations and thermodynamic identities are separated into three modes: an acoustic mode, a thermal mode, and a viscous mode.This yields three dispersion relationships between modes, both for the solid and the fluid. We will first solve for the fluid case.

We have a plane-wave disturbance of frequency ω in a homogeneous, time independent medium, where each field quantity is represented by Ψ and varies with t and $\vec{x}$ as

$$\Psi(\vec{x}, t) = \mathrm{Re}\ \psi \exp[i(\vec{k}\cdot\vec{x} - \omega t)] \tag{2.1.25}$$

where $\vec{k}$ is the same for each Ψ, and ψ is independent of $\vec{x}$ and t and is generally complex, as is $\vec{k}$.

We seek values of $\vec{k}$ which allow (2.1.25) to be a solution of the governing equations, thus getting the dispersion relationship $k(\omega)$. We substitute $\vec{\nabla} = i\vec{k}$, $\partial/\partial t = -i\omega$, and p, S, or $\vec{v}$ as appropriate into the governing equations (2.1.4), thus obtaining for (2.1.4a, b, and d)

$$\omega\left(\frac{p}{c^2} - \frac{\rho_0 \beta T_0}{C_p} S\right) - \rho_0 \vec{k}\cdot\vec{\mathbf{v}} = 0\,, \tag{2.1.26a}$$

$$-i\omega\rho_0\vec{\mathbf{v}} = -i\vec{k}p - \mu_0(k^2\vec{\mathbf{v}} + 1/3\vec{k}(\vec{k}\cdot\vec{\mathbf{v}}))\,, \tag{2.1.26b}$$

and

$$i\omega S = \sigma k^2\left(S + \frac{\beta}{\rho_0} p\right) \tag{2.1.26c}$$

where p is the complex pressure amplitude, $\vec{\mathbf{v}}$ is the velocity amplitude, and S is the entropy amplitude, and where (2.1.4d) and (2.1.4e) have been used to elim-

inate ρ and T. The vector and scalar products of $\vec{k}$ with (2.1.3b) give respectively

$$(-i\omega\rho_0 + \mu_0 k^2)(\vec{k}\times\vec{v}) = 0 \qquad (2.1.27a)$$

and

$$(\omega\rho_0 + i(4/3)\mu_0 k^2)\vec{k}\cdot\vec{v} = k^2 p \ . \qquad (2.1.27b)$$

Equation (2.1.27a) implies that either

$$\vec{k}\times\vec{v} = 0 \ , \qquad (2.1.28a)$$

or

$$k^2 = i\omega\frac{\rho_0}{\mu_0} \qquad (2.1.28b)$$

(a) Viscous Mode

Consider (2.1.28b) first. Substituting this equation in (2.1.27b) and in (2.1.26a,c), it can be shown that k^2 must be purely real (which would contradict (2.1.28b)), unless $\vec{k}\cdot\vec{v} = 0$. This implies, using (2.1.26), that for this mode T, ρ, p, and S are all zero. Thus we have a mode which is transverse and solenoidal, which produces no pressure, temperature, density, or entropy perturbations, and for which the wavenumber depends only on the viscosity. This is the viscous mode. Summarizing, it has the following properties: the dispersion relation,

$$k_v^2 = i\omega\frac{\rho_0}{\mu_0} \qquad (2.1.29a)$$

which is identical to Allegra and Hawley's relation (2.1.15); the polarization relation,

$$\vec{k}_v\cdot\vec{v}_v = 0 \qquad (2.1.29b)$$

which implies

$$\vec{\nabla}\cdot\vec{v}_v = 0 \qquad (2.1.29c)$$

and

$$p_e = S_e = T_e = \rho_e = 0 . \qquad (2.1.29d)$$

The relations (2.1.29d) are an example of the additional information regarding field quantities provided by Pierce's approach.

Next we consider the condition $\vec{k} \times \vec{v} = 0$. To simplify the algebra, let us make the following abbreviations

$$X = \frac{c^2 k^2}{\omega^2} \qquad (2.1.30a)$$

$$\epsilon_e = i\frac{4}{3}\frac{\mu_0 \omega}{\rho_0 c^2} \qquad (2.1.30b)$$

and

$$\epsilon_t = \frac{iK\omega}{\rho_0 c^2 C_p} \qquad (2.1.30c)$$

Equation (2.1.27b) and (2.1.26c), with $\vec{k} \cdot \vec{v}$ taken from (2.1.26a), represent two simultaneous equations for S and p, which can be rewritten with the above abbreviations (2.1.30) and with the identity $\gamma - 1 = \beta^2 T_0 c^2 / C_p$ [Pierce, 1981, p.30] as

$$(1 + \epsilon_t X) S + (\epsilon_t X)\frac{\beta p}{\rho_0} = 0 \qquad (2.1.31a)$$

$$-(\gamma - 1)(1 + \epsilon_e X) S + (1 + \epsilon_e X - X)\frac{\beta p}{\rho_0} = 0 \qquad (2.1.31b)$$

For a nontrivial solution we require that the determinant of the coefficients vanish. This produces a quadratic called Kirchoff's dispersion relation [Truesdell, 1953]

$$(-\epsilon_t + \gamma \epsilon_e \epsilon_t) X^2 + (\epsilon_e + \gamma \epsilon_t - 1) X + 1 = 0 . \qquad (2.1.32)$$

For water, $|\epsilon_e| \approx 3.8 \times 10^{-12} f$, and $|\epsilon_t| \approx 4.02 \times 10^{-13} f$. Therefore, for our frequency range $f \leq 100$ MHz, both ϵ_e and ϵ_t are much less than 1. Thus we solve (2.1.32) to lowest order, obtaining the following approximate dispersion relations

$$X_- = 1 + \epsilon_e + (\gamma - 1)\epsilon_t , \qquad (2.1.33a)$$

$$X_+ = -\frac{1}{\epsilon_t} + (\gamma - 1)\left[1 - \frac{\epsilon_s}{\epsilon_t}\right] . \qquad (2.1.33b)$$

where the subscripts denote positive and negative roots.

(b) Acoustic Mode

The dispersion relation in (2.1.33a) gives

$$k_c^2 = \frac{\omega^2}{c^2}\left\{1 + \frac{i\,\omega}{c^2}\left[\frac{4\,\mu_0}{3\,\rho_0} + (\gamma - 1)(\frac{C_p\,K}{\rho_0})\right]\right\} \qquad (2.1.34)$$

This result is the same as (2.1.13), which is Allegra and Hawley's dispersion relation for compression waves in the fluid, since the imaginary term is much less than one for water at frequencies less than 100 MHz. Hence the use of the subscript c in the wavenumber.

Since $\vec{k}\times\vec{v} = 0$, these waves are longitudinal. To obtain relations between the different field quantities, we ignore terms of first or higher order in ϵ_t or ϵ_s. From (2.1.31a) and (2.1.33a), we get

$$S = -\epsilon_t \frac{\beta p}{\rho_0}. \qquad (2.1.35)$$

so $S_c \approx 0$. In a similar manner, we obtain the following from equation (2.1.33b)

$$\rho_0 \frac{\partial \vec{v}_c}{\partial t} \approx -\vec{\nabla} p_c \qquad (2.1.36a)$$

and from equation (2.1.4f)

$$T_c \approx \left(\frac{T_0 \beta}{\rho_0 C_p}\right) p_c \qquad (2.1.36b)$$

and from equation (2.1.4e)

$$\rho_c \approx \frac{p_c}{c^2} . \qquad (2.1.36c)$$

(c) Thermal Mode

The other dispersion relation (2.1.33b) becomes, after dropping all but the first term (since $\gamma \approx 1$ and $|\epsilon_t| \ll 1$),

$$k_t^2 = i\frac{\rho_0 C_p}{K}\omega = i\frac{\omega}{\sigma} \tag{2.1.37a}$$

which is the same as the Allegra-Hawley thermal wave dispersion relation, (2.1.14). As for the acoustic mode

$$\vec{\nabla}\times\vec{v}_t = 0\,, \tag{2.1.37b}$$

and for the relations between field quantities we neglect terms of order 1 or higher in ϵ_s and ϵ_t. From (2.1.33b) and (2.1.31 a or b)

$$\frac{\beta p}{\rho_0} = (\gamma - 1)(\epsilon_t - \epsilon_s)\, S \tag{2.1.37c}$$

and thus, we have $p_t \approx 0$. With $p_t \approx 0$ and using (2.1.4e), we get

$$\rho_t \approx -\left(\frac{\rho_0 \beta T_0}{C_p}\right) S_t\,, \tag{2.1.37d}$$

and from equation (2.1.4f)

$$T_t \approx \left(\frac{T_0}{C_p}\right) S_t \tag{2.1.37e}$$

Then through a tedious derivation (see Appendix 3) it is found that

$$\vec{v}_t \approx \left(\frac{\beta T_0 K}{\rho_0 C_p^{\,2}}\right)\vec{\nabla} S_t\,. \tag{2.1.37f}$$

Note that combining the velocity and temperature modal relationships results in

$$\vec{v}_t \approx \left(\frac{\beta K}{\rho_0 C_p}\right)\vec{\nabla}\, T_t \tag{2.1.37g}$$

which implies flow from cold regions into warmer ones. As explained by Pierce [1981, p.523], this can be understood from the fact that at a local temperature maximum the diffusion equation predicts that the temperature must decrease with time. Since the thermally induced pressure is negligible, thermodynamic considerations require that the density simultaneously increase with time, which in turn requires the mass flow from cold to warm regions implied by (2.1.37g).

Now we present the equivalent results for the solid case, which are obtained

in the same manner. The governing equations for a solid are again (2.1.3).

As for the fluid, replace the time derivative by $-i\omega$ and let $\vec{\nabla} = i\,\vec{k}'$ to obtain the following relations

$$\vec{k}' \cdot \vec{u} = i\frac{\rho'}{\rho_0'} \tag{2.1.38a}$$

$$(\omega^2\rho_0' - \mu' k'^2)\vec{u} = i\vec{k}'\left[c_1'^2\frac{\rho'}{\gamma'} + \frac{c_1'^2\beta'\rho_0'T'}{\gamma'}\right] + \frac{\mu'}{3}\vec{k}'(\vec{k}' \cdot \vec{u}) \tag{2.1.38b}$$

and

$$i\omega\left[\frac{\rho_0' C_p' T'}{\gamma'} - \frac{(\gamma' - 1)C_p'\rho'}{\beta'\gamma'}\right] = K' k'^2 T' . \tag{2.1.38c}$$

(a) Shear Wave Mode

As for the fluid, the shear wave mode is obtained by taking $\vec{k}' \cdot \vec{u}_s = 0$, from which it is seen, using (2.1.38) that

$$k_s'^2 = \omega^2\frac{\rho_0'}{\mu'} \tag{2.1.39a}$$

which is the same as Allegra and Hawley's dispersion relation (2.1.21), and

$$p_s' = \rho_s' = T_s' = 0 \tag{2.1.39b}$$

For the case $\vec{k}' \times \vec{u} = 0$, we again substitute for $\vec{k}' \cdot \vec{u}$ from (2.1.38a) in equations (2.1.38b and c), to get two equations in two unknowns; ρ' and T'. That is,

$$(\gamma' - 1)\frac{\rho'}{\rho_0'} - (1 + \gamma'\epsilon_t' X')\beta' T' = 0 \tag{2.1.40a}$$

$$[\gamma' - (\epsilon_s'\gamma' + 1)X']\frac{\rho'}{\rho_0'} - X'\beta' T' = 0 \tag{2.1.40b}$$

with the following abbreviations

$$X' = \frac{c_1'^2 k'^2}{\omega^2} , \tag{2.1.41a}$$

$$\epsilon_s' = \frac{4\mu'}{3\rho_0' c_1'^2} , \tag{2.1.41b}$$

$$\epsilon_t' = i\frac{\sigma'\omega}{c_1'^2} . \tag{2.1.41c}$$

As before, for a nontrivial solution to exist the determinant of the coefficients must equal zero. This determinant is

$$1 + (\gamma' \epsilon_t' - 1 - \epsilon_s') X' - \epsilon_t' (1 + \gamma' \epsilon_s') X'^2 = 0 \qquad (2.1.42)$$

and on solving for the roots we get

$$\frac{2}{X'} = (1 - \gamma' \epsilon_t' + \epsilon_s') \pm [(1 - \gamma' \epsilon_t' + \epsilon_s')^2 + 4\epsilon_t' (1 + \gamma' \epsilon_s')]^{1/2} \qquad (2.1.43)$$

which is identical to Allegra's result.

For a solid, ϵ_s' is not a small quantity, while $|\epsilon_t'|$ is small over the frequency range of interest. For example, for polystyrene, $|\epsilon_t'| \approx 10^{-13} f$, but $\epsilon_s' \approx 0.395$ (see Table 2.2). Therefore we may approximate (2.1.43) by keeping only terms in the square root of first or lower order in $\epsilon_t'/(1 + \epsilon_s')$.

(b) Acoustic Mode

The positive root reduces, to first order (Appendix 4), to

$$\frac{1}{X'_+} \approx 1 + \epsilon_s' - \frac{\epsilon_t' (1 + \gamma' \epsilon_s')}{1 + \epsilon_s'} . \qquad (2.1.44)$$

If we write X_+ in terms of frequencies and wavespeeds, we obtain

$$k_c'^2 = \frac{\omega^2}{c'^2} \left[1 + i \sigma' \omega \left(\frac{c_1'^2}{c'^4} \right) (\gamma' - 1) \right] \qquad (2.1.45a)$$

which is equivalent, to first order in the imaginary term, to Allegra and Hawley's result (2.1.19).

Let us consider the polarization relation. We have

$$\nabla \times \vec{u}'_c = 0 \qquad (2.1.45b)$$

For the modal relations between field quantities we keep terms of order zero or lower in ϵ_t'. Using equations (2.1.40a or b) and (2.1.3d), we get

$$\rho'_c \approx \frac{p'_c}{c_1'^2} , \qquad (2.1.45c)$$

then we substitute (2.1.3d), (2.1.38a), and (2.1.45c) into (2.1.38c) to obtain

$$\vec{u}_c' \approx \frac{c'^2}{\rho_0' \omega^2 c_1'^2} \vec{\nabla} p_c' \,. \tag{2.1.45d}$$

We also use (2.1.3d) and (2.1.45c) to get

$$U_c' \approx \frac{p_0'}{\rho_0'^2 c_1'^2} p_c' \tag{2.1.45e}$$

$$T_c' \approx \frac{(\gamma' - 1)}{\rho_0' \beta' c_1'^2} p_c' \tag{2.1.45f}$$

(c) Thermal Mode

For the negative root, we have

$$\frac{1}{X_-'} \approx -\epsilon_t' \frac{(1 + \gamma' \epsilon_s')}{1 + \epsilon_s'} \tag{2.1.46}$$

$$\approx -\epsilon_t' \left(1 + \frac{(\gamma' - 1)\epsilon_s'}{1 + \epsilon_s'} \right)$$

Substituting (2.1.46a) in either of equations (2.1.40) gives

$$\frac{\rho'}{\rho_0'} \approx -\frac{\beta' T'}{1 + \gamma' \epsilon_s'} \tag{2.1.47}$$

An approximate dispersion relation may be obtained from (2.1.46) if

$$\frac{(\gamma' - 1)\epsilon_s'}{(1 + \epsilon_s')} \ll 1 \tag{2.1.48}$$

which does hold for the materials that we are interested in (Tables 2.2 and 2.3), since γ' is very close to one. This gives the dispersion relation (see Appendix 5)

$$k_t'^2 = \frac{i\omega}{\sigma'} \tag{2.1.49a}$$

Summarizing, we have

$$\vec{\nabla} \times \vec{u}_t = 0 \,, \tag{2.1.49b}$$

$$\rho_t' \approx \frac{-\rho_0' \beta'}{1 + \gamma' \epsilon_s'} T_t' \,, \tag{2.1.49c}$$

and using (2.1.3d)

$$p_t' = \frac{\epsilon_s'}{1 + \gamma' \epsilon_s'} \rho_0' \beta' c_1'^2 T_t' \,. \tag{2.1.49d}$$

We derive the velocity relation in a derivation analogous to the fluid case

(2.1.37g)

$$\vec{u}_t' \approx \frac{\sigma' \beta'}{-i\,\omega} \frac{{c_1'}^2}{{c'}^2} \vec{\nabla} T_t' , \tag{2.1.49e}$$

while the energy relation is found using (2.1.3e) and (2.1.49c)

$$U_t' = \frac{1}{1 + \gamma' \epsilon_s'} \left[C_p' (1 + \epsilon_s') - \frac{\beta' p_0'}{\rho_0'} \right] T_t' . \tag{2.1.49f}$$

As can be seen, the differences in form between the liquid and solid thermal waves are obvious, with the most important effect for our purposes being the fact that the thermal pressure wave is not negligible in the solid.

2.2. Boundary Conditions

Consider the boundary at $r = a$ in our coordinate system, which is the interface between the solid and the fluid. The boundary conditions at the surface of the sphere are continuity of velocity, stress, temperature and heat flux. By symmetry, velocity and stress in the azimuthal ϕ direction are zero, and we are reduced to six boundary conditions. These are [Epstein and Carhart, 1953;Allegra and Hawley, 1972]

(a) continuity of radial velocity

$$v_r = v_r' , \tag{2.2.1a}$$

(b) continuity of tangential velocity

$$v_\theta = v_\theta' , \tag{2.2.1b}$$

(c) continuity of temperature

$$T = T' , \tag{2.2.1c}$$

(d) continuity of heat flux

$$K \frac{\partial T}{\partial r} = K' \frac{\partial T'}{\partial r} , \tag{2.2.1d}$$

(e) continuity of radial stress

$$\sigma_{rr} = \sigma'_{rr} \,, \tag{2.2.1e}$$

(f) and continuity of tangential stress

$$\sigma_{r\theta} = \sigma'_{r\theta} \,. \tag{2.2.1f}$$

Equivalently, for the fluid the stress tensor is [Batchelor, 1967, pp.141-7]

$$\sigma_{ij} = -p\ \delta_{ij} + 2\mu_0 \left(e_{ij} - \frac{1}{3}\ e_{ii}\ \delta_{ij} \right) , \tag{2.2.2}$$

where $p = (1 / 3)\ \sigma_{ii}$ and

$$e_{ij} = \frac{1}{2} \left(\frac{\partial\ v_i}{\partial\ x_j} + \frac{\partial\ v_j}{\partial\ x_i} \right) .$$

Therefore the required stress tensor components are

$$\sigma_{rr} = -p - \frac{2}{3}\ \mu_0\ \vec{\nabla} \cdot \vec{v} + 2\ \mu_0\ \frac{\partial\ v_r}{\partial\ r} \,, \tag{2.2.3}$$

$$\sigma'_{rr} = -p' - \frac{2}{3}\ \mu'\ \vec{\nabla} \cdot \vec{u} + 2\ \mu'\ \frac{\partial\ u_r}{\partial\ r} \,, \tag{2.2.4}$$

$$\sigma_{r\theta} = \mu_0 \left[r \frac{\partial}{\partial r} \left(\frac{v_\theta}{r} \right) + \frac{1}{r}\ \frac{\partial v_r}{\partial \theta} \right] , \tag{2.2.5}$$

and

$$\sigma'_{r\theta} = \mu' \left[r \frac{\partial}{\partial r} \left(\frac{u_\theta}{r} \right) + \frac{1}{r}\ \frac{\partial u_r}{\partial \theta} \right] . \tag{2.2.6}$$

2.3. Matrix Solution

2.3.1. Partial Wave Expansion

Series solutions of equations (2.1.12) for the fluid, which are independent of the angle ϕ, are [Epstein and Carhart, 1953; Allegra and Hawley, 1972],

$$\phi_0 = \sum_{n=0}^{\infty} i^n\ (2\ n + 1)\ j_n\ (k_c\ r)\ P_n\ (\cos \theta) \,, \tag{2.3.1a}$$

$$\dot{\phi} = \sum_{n=0}^{\infty} i^n\ (2\ n + 1)\ A_n\ h_n\ (k_c\ r)\ P_n\ (\cos \theta) \,, \tag{2.3.1b}$$

$$\phi_t = \sum_{n=0}^{\infty} i^n\ (2\ n + 1)\ B_n\ h_n\ (k_t\ r)\ P_n\ (\cos \theta) \,, \tag{2.3.1c}$$

$$A_\phi = - \sum_{n=0}^{\infty} i^n \, (2 n + 1) \, C_n \, h_n \, (k_s \, r) \, \frac{d \, P_n \, (\cos \theta)}{d \, \theta} , \quad (2.3.1d)$$

where $j_n(z)$ is a spherical Bessel function of the first kind, $h_n(z)$ is a spherical Hankel function of the first kind, and $P_n(\cos\theta)$ is a Legendre polynomial. ϕ_0 represents the incident wave, which must remain finite at the origin in the absence of the scatterer and therefore has radial dependance $j_n(k_c\, r)$. $\dot{\phi}$, ϕ_t, and A_ϕ represent the scattered compression, thermal, and viscous waves, which must propagate outward at large $k_c\, r$ and therefore are expressed in terms of $h_n(kr)$.

For the solid scatterer, the solutions for the scalar and vector potentials which are finite at the origin are

$$\phi_c' = \sum_{n=0}^{\infty} i^n \, (2 n + 1) \, A_n' \, j_n \, (k_c' \, r) \, P_n \, (\cos \theta) , \quad (2.3.2a)$$

$$\phi_t' = \sum_{n=0}^{\infty} i^n \, (2 n + 1) \, B_n' \, j_n \, (k_t' \, r) \, P_n \, (\cos \theta) , \quad (2.3.2b)$$

$$A_\phi' = - \sum_{n=0}^{\infty} i^n \, (2 n + 1) \, C_n' \, j_n \, (k_s' \, r) \, \frac{d \, P_n \, (\cos \theta)}{d \, \theta} . \quad (2.3.2c)$$

Appendix 2 shows why the form of equation (2.3.2c) differs from (2.3.2a and b).

2.3.2. Partial Wave Boundary Conditions

Defining $x = k_c \; a$, $s = k_s \; a$, $t = k_t \; a$, and substituting the equations (2.3.1) and (2.3.2) into the boundary conditions (2.2.1) gives

(a) Radial velocity

$$\begin{aligned} x \, j_n'(x) + x \, A_n \, h_n'(x) + t \, B_n \, h_n'(t) - C_n \, n \, (n + 1) \, h_n \, (s) \\ = - i \, \omega [\, x' \, A_n' \, j_n'(x') + t' \, B_n' \, j_n'(t') \\ - C_n' \, n \, (n + 1) \, j_n \, (s')] \end{aligned} \quad (2.3.3a)$$

(b) Tangential velocity

$$\begin{aligned} j_n \, (x) + A_n \, h_n \, (x) + B_n \, h_n \, (t) - C_n \, [\, h_n \, (s) + s \, h_n'(s)] \\ = - i \, \omega \{ \, A_n' \, j_n \, (x') + B_n' \, j_n \, (t') \\ - C_n' [\, j_n \, (s') + s' \, j_n'(s')] \} \end{aligned} \quad (2.3.3b)$$

(c) Temperature

$$b_c \left[j_n(x) + A_n h_n(x) \right] + b_t B_n h_n(t) = -i\omega \left[b_c' A_n' j_n(x') + b_t' B_n' j_n(t') \right] \quad (2.3.3c)$$

(d) Heat Flux

$$b_c \left[x j_n'(x) + A_n x h_n'(x) \right] + B_n b_t t h_n'(t) = -i\omega \frac{K'}{K} \left[A_n' b_c' x' j_n'(x') + B_n' b_t' t' j_n'(t') \right] \quad (2.3.3d)$$

(e) Radial Stress

$$\begin{aligned} &\left[-i\omega\rho_0 a^2 + 2\mu_0 n(n+1) \right] j_n(x) - 4\mu_0 x j_n'(x) \\ &\quad + A_n \left\{ \left[-i\omega\rho_0 a^2 + 2\mu_0 n(n+1) \right) h_n(x) - 4\mu_0 x h_n'(x) \right\} \\ &+ B_n \left[\left(-i\omega\rho_0 a^2 + 2\mu_0 n(n+1) \right) h_n(t) - 4\mu_0 t h_n'(t) \right] \\ &\quad + C_n 2\mu_0 n(n+1) \left[h_n(s) - s h_n'(s) \right] \\ &= A_n' \left\{ \left[-\omega^2 \rho_0' a^2 + 2\mu' n(n+1) \right] j_n(x') - 4\mu' x' j_n'(x') \right\} + \\ &\quad B_n' \left[\left(-\omega^2 \rho_0' a^2 + 2\mu' n(n+1) \right) j_n(t') - 4\mu' t' j_n'(t') \right] \\ &\quad + C_n' 2\mu' n(n+1) \left[j_n(s') - s' j_n'(s') \right] \end{aligned} \quad (2.3.3e)$$

(f) Tangential Stress

$$\begin{aligned} &\mu_0 \left\{ x j_n'(x) - j_n(x) + A_n \left[x h_n'(x) - h_n(x) \right] + \right. \\ &\qquad \left. B_n \left[t h_n'(t) - h_n(t) \right] \right. \\ &\left. - C_n \left[-s h_n'(s) + \left(-\frac{s^2}{2} + n^2 + n - 1 \right) h_n(s) \right] \right\} \\ &\quad = \mu' \left\{ A_n' \left[x' j_n'(x') - j_n(x') \right] + B_n' \left[t' j_n'(t') - j_n(t') \right] \right. \\ &\qquad \left. - C_n' \left[-s' j_n'(s') + \left(-\frac{s'^2}{2} + n^2 + n - 1 \right) j_n(s') \right] \right\} \end{aligned} \quad (2.3.3f)$$

Note that the primes on j_n and h_n denote differentiation with respect to the argument. The above results are identical with those of Allegra and Hawley [1972], except for a sign change in the viscous term in the fluid, and the shear term in the solid, in (2.3.3f), which Davis [1979] and Hay and Burling [1982] have observed.

It should be noted for $n = 0$, that every term in the tangential stress and velocity contains $dP_0(\cos\theta)/d\theta$ as a multiplicative factor, which vanishes identically, and therefore there are only four boundary conditions to satisfy

instead of six. Furthermore, C_0 and C_0' disappear from the remaining equations.

2.3.3. Attenuation Coefficients

Attenuation of the incident sound wave is due both to energy scattered by the sphere to infinity (i.e., r such that $k_c\, r \gg 1$) , and to absorption in or near the sphere. The scattered energy is contained in the scattered compressional wave $\dot{\phi}$. In the farfield we may use the intensity expression for a plane wave [Pierce, 1981, p.516], neglecting thermal and viscous effects;

$$I = < p\ \vec{v} > = \frac{\rho_0\, c\ |\ \vec{v}\ |^2}{2}\,, \tag{2.3.4}$$

where the brackets $< >$ denote taking the average over a wave period.

To find the scattered power $\dot{\Pi}$ we integrate (2.3.4) over a large sphere centered on the scatterer. For large r, $|\ \vec{v}\ | \rightarrow |\ \dot{v}_r\ |$, so

$$\dot{\Pi} = 2\pi\, \rho_0\, c\ r^2 \int_0^{\pi} |\ \dot{v}_r\ |^2 \sin\theta\, d\,\theta. \tag{2.3.5}$$

Now $\dot{v}_r$ is given by

$$\dot{v}_r = -\frac{\partial\, \dot{\phi}_r}{\partial\, r} = -\sum_{n=0}^{\infty} i^n\ (\,2\,n\,+\,1\,)\, A_n\, \frac{\partial h_n\,(\,k_c\, r\,)}{\partial r} P_n\ (\,\cos\,\theta\,). \tag{2.3.6}$$

At large distances [Arfken, 1970, p.524]

$$\frac{\partial h_n\ (\,k_c\ r\,)}{\partial r} \rightarrow i^{-n}\, \frac{e^{\,i\,k_c\ r}}{r}. \tag{2.3.7}$$

and therefore

$$\dot{\Pi} = 2\pi\rho_0 c \int_0^{\pi} \sum_{m,n=0}^{\infty} (2n+1)(2m+1) A_n\, A_m^{*}\, P_n(\cos\theta) P_m(\cos\theta)\, \sin\theta\, d\,\theta, \tag{2.3.8}$$

where A_m^{*} denotes the complex conjugate of A_m. By orthogonality [Arfken, 1970, pp. 432-6]

$$\int_0^{\pi} P_n\ (\,\cos\,\theta\,)\, P_m\ (\,\cos\theta\,)\, \sin\theta\, d\,\theta = \frac{2}{2n\,+\,1}\delta_{mn} \tag{2.3.9}$$

and therefore (2.3.8) becomes

$$\hat{\Pi} = 4\,\pi\,\rho_0\,c\,\sum_{n=0}^{\infty}\,(2n+1)\,|\,A_n\,|^2. \tag{2.3.10}$$

To determine the energy absorbed, the total velocity potential at infinity is written in terms of incoming and outgoing waves. First, we let $r \to \infty$, and consider the asymptotic approximations to the spherical Bessel functions [Arfken, 1970, p. 524];

$$j_n\,(k_c\,r) \to (-1)^n\,\frac{\sin(k_c\,r + n\frac{\pi}{2})}{k_c\,r} \tag{2.3.11a}$$

$$h_n\,(k_c\,r) \to (-i)^{n+1}\,\frac{e^{i\,k_c\,r}}{k_c\,r}\,. \tag{2.3.11b}$$

Therefore using equation (2.1.11) the total radial velocity component becomes

$$v_r = -\frac{\partial\,\phi_0}{\partial r} - \frac{\partial\dot{\phi}}{\partial r} \tag{2.3.12}$$

or

$$\lim_{r\to\infty} v_r = -\frac{1}{r}\sum_{n=0}^{\infty}(2n+1)P_n(\cos\theta)\left\{\left[A_n+\frac{1}{2}\right]e^{ik_c r}+(-1)^n\,\frac{e^{-ik_c r}}{2}\right\}. \tag{2.3.13}$$

Here $e^{i\,k_c\,r}$ represents the outgoing wave and $e^{-i\,k_c\,r}$ the incoming wave. The difference between the incoming and outgoing power at infinity is the power absorbed by the sphere: that is, calculating the power as before,

$$\begin{aligned}\Pi_A &= \Pi_{incoming} - \Pi_{outgoing} \\ &= 4\,\pi\,\rho_0\,c\,\sum_{n=0}^{\infty}\,(2n+1)\left[\frac{1}{4} - \left|A_n + \frac{1}{2}\right|^2\right]\end{aligned} \tag{2.3.14}$$

or

$$\Pi_A = -\,4\,\pi\,\rho_0\,c\,\sum_{n=0}^{\infty}\,(2n+1)\left[\mathrm{Re}\;A_n + |\,A_n\,|^2\right]. \tag{2.3.15}$$

Then for the total power removed from the incident wave by one particle we have

$$\Pi_{tot} = \Pi_A + \hat{\Pi} = -\,4\,\pi\,\rho_0\,c\,\sum_{n=0}^{\infty}\,(2n+1)\,\mathrm{Re}\;A_n\,, \tag{2.3.16}$$

Expressions equivalent to (2.3.10), (2.3.15), and (2.3.16) are given elsewhere [e.g. Morse and Ingard, 1968, p.427; Hay and Mercer, 1985].

We are considering dilute suspensions, for which the total attenuation should be the sum of contributions from individual particles, so if n is the particle number density, then the power loss per unit volume is $\Delta\Pi = n\ (\ \Pi_A + \dot{\Pi}\ )$. To obtain the attenuation per unit pathlength this quantity is divided by the incident wave intensity, which for a plane wave with unit amplitude velocity potential is

$$I = \frac{\rho_0\ c\ k_c^2}{2}$$

from (2.3.4), so the attenuation coefficient is

$$\alpha_I = \frac{\Delta\Pi}{I} = -\frac{4\ \pi\ n}{k_c^2} \sum_{n=0}^{\infty} (\ 2n\ +\ 1\ )\ \mathrm{Re}A_n\ . \qquad (2.3.17)$$

A few points should be noted. First, for uniformly sized particles the volume fraction ϵ can be related to the number density through the following equation;

$$n = \frac{\epsilon}{(4/3)\ \pi\ a^3}. \qquad (2.3.18)$$

Second, we should relate the attenuation coefficient for intensity α_I to the attenuation coefficient for pressure α_p. Since I is proportional to p^2, the two coefficients are related by $\alpha_I = 2\ \alpha_p$. If we let $\alpha = \alpha_p$, then

$$\alpha = -\frac{3}{2}\ \frac{\epsilon}{k_c^2 a^3} \sum_{n=0}^{\infty} (\ 2n\ +\ 1\ )\ \mathrm{Re}A_n\ . \qquad (2.3.19)$$

2.4. The Viscous Nonconducting Limit

Now suppose that absorption due to heat conduction can be ignored in comparison to viscous losses. Hay and Burling [1982] have shown that in the long wavelength limit this should be true for aqueous suspensions provided the acoustic frequency is such that the thicknesses of the thermal and viscous boundary

layers are less than the particle radius, and provided the particle grain densities are greater than 1.3–1.7 g cm $^{-3}$. This is born out by Urick's [1948] experimental results at megacycle frequencies with suspensions of sand and kaolin.

Based upon an analysis by Lamb [1945] of the rigid sphere case, Urick [1948] obtained

$$2\alpha = \epsilon \left[\frac{1}{6} k_c^4 a^3 + k(\sigma - 1)^2 \frac{D}{D^2 + (\sigma + C)^2} \right] \tag{2.4.1}$$

for $x \ll 1$ and $x \ll a/\delta_v$, and where δ_v is the viscous boundary layer thickness given by

$$\delta_v = \left(\frac{2\mu_0}{\rho_0 \omega} \right)^{1/2} \tag{2.4.2}$$

and

$$\sigma = \frac{\rho_0'}{\rho_0} \tag{2.4.3}$$

$$C = \frac{1}{2} + \frac{9\delta_v}{4a} \tag{2.4.4}$$

$$D = \frac{9\delta_v}{4a} \left(1 + \frac{\delta_v}{a} \right) . \tag{2.4.5}$$

The first term of (2.4.1) is the loss due to scattering. The second term represents absorption of energy due to viscous dissipation in the vicinity of the scatterer, and is caused by velocity differences between the scatterer and the fluid.

CHAPTER 3 BOUNDARY LAYER APPROXIMATIONS

In this Chapter we review laminar boundary layer theory, and discuss some of the general properties of boundary layers. Then we discuss the applicability of the usual boundary layer approach to our problem. We present experimental data obtained by Allegra and Hawley [1972], together with a discussion of the applicability of a boundary layer approximation to this data set. We examine the radial stress boundary condition in the fluid, and derive an approximate form. We call this the first boundary layer approximation. Then a more general form is derived, which affects all six boundary conditions, which we call the second boundary layer approximation. In each case, approximate results are compared to the exact theory. The approximation results are compared to exact plots based upon the Allegra and Hawley theory.

3.1.1. Laminar Boundary Layer Theory

Prandtl [1905] proposed that there exist layers near boundaries where viscous effects are significant, and that outside these layers the inviscid equations hold. The basic idea is that as we approach a boundary, the no-slip condition requires that the flow decrease to zero. At some point, regardless of the Reynolds number of the exterior flow, the flow speed becomes small enough that viscous effects become significant relative to inertial effects. The region where this holds is called the boundary layer, and at high Reynolds number it is a thin layer next to the boundary. This theory is not mathematically rigorous in general, but it

has proved useful in many cases.

Viscous terms are comparable to inertial terms when

$$\left| \vec{v} \cdot \vec{\nabla} \vec{v} \right| \approx \left| \frac{\mu_0}{\rho_0} \nabla^2 \vec{v} \right| . \tag{3.1.1}$$

To illustrate the basic properties we consider a flat plate with an infinite fluid above it, where the origin is at the left edge of the plate and the x-axis coincides with the surface, while the positive y-axis points up into the fluid. Vorticity is created at the surface of the plate, and is advected downstream by the exterior flow before it can diffuse far from the boundary, and is therefore confined to a thin layer near the boundary, especially in fluids with low viscosity.

We also restrict ourselves to two-dimensional steady flow and an incompressible fluid, where we have a farfield flow $\vec{V} = (U(x), 0)$. Let us scale the boundary layer thickness by δ, the scale over which the exterior fluid velocity changes along a streamline by L, the scale of the exterior velocity by U_0, and we scale the velocity normal to the boundary, in the boundary layer, by V_0. Then the continuity equation

$$\frac{\partial u}{\partial x} + \frac{\partial v}{\partial y} = 0 \tag{3.1.2}$$

shows that $V_0 \approx U_0 \delta / L$. Using this and scaling (3.1.1) we find that

$$\frac{\delta}{L} \approx \left(\frac{\rho_0 U_0 L}{\mu_0} \right)^{-\frac{1}{2}} \tag{3.1.3}$$

$$\approx R_e^{-1/2} .$$

The boundary layer thickness varies as the inverse square root of the Reynolds number R_e for the exterior flow, and tends to zero as R_e tends to infinity.

The basic procedure of the boundary layer appoach is first to derive the inviscid equations far from the boundary, then to derive the approximate equations in the boundary layer (for high Reynolds number), and then to join the two

regions using suitable matching conditions. Across the boundary layer we scale the pressure by a factor P_b, while in the inviscid exterior we scale it by P_0.

The equations in the boundary layer are the continuity equation (3.1.2) together with the x and y components of the Navier-Stokes equation (with their scales included) as follows,

$$\begin{array}{cccccc} u\frac{\partial u}{\partial x} + v\frac{\partial u}{\partial y} & & = -\frac{1}{\rho_0}\frac{\partial p}{\partial x} + \frac{\mu_0}{\rho_0}\frac{\partial^2 u}{\partial x^2} & + & \frac{\mu_0}{\rho_0}\frac{\partial^2 u}{\partial y^2} \\ \frac{U_0^2}{L} & \frac{U_0 V_0}{\delta} \approx \frac{U_0^2}{L} & \frac{P_0}{\rho_0 L} & & \frac{\mu_0 U_0}{\rho_0 L^2} & \frac{\mu_0 U_0}{\rho_0 \delta^2} \end{array} \qquad (3.1.4)$$

where $U_0 V_0/\delta \approx U_0^2/L$ from the continuity equation, and

$$\begin{array}{cccccc} u\frac{\partial v}{\partial x} + v\frac{\partial v}{\partial y} & & = -\frac{1}{\rho_0}\frac{\partial p}{\partial y} + \frac{\mu_0}{\rho_0}\frac{\partial^2 v}{\partial x^2} & + & \frac{\mu_0}{\rho_0}\frac{\partial^2 v}{\partial y^2} \\ \frac{U_0^2 \delta}{L^2} & \frac{U_0^2 \delta}{L^2} & \frac{P_b}{\rho_0 \delta} & & \frac{\mu_0 U_0 \delta}{\rho_0 L^3} & \frac{\mu_0 U_0}{\rho_0 \delta L} \end{array} \qquad (3.1.5)$$

We consider the case when $R_e >> 1$, so that $\delta << L$ (see 3.1.3).

In this case the y momentum equation is at most of size δ/L relative to the x-momentum equation (3.1.4), except for the pressure term. Therefore $\partial p/\partial y \approx 0$. Also, the second term on the right hand side of (3.1.4) is negligible compared to the third term. Thus the boundary layer equations are

$$u\frac{\partial u}{\partial x} + v\frac{\partial u}{\partial y} \approx -\frac{1}{\rho_0}\frac{\partial p}{\partial x} + \frac{\mu_0}{\rho_0}\frac{\partial^2 u}{\partial y^2}, \qquad (3.1.6a)$$

$$\frac{\partial u}{\partial x} + \frac{\partial v}{\partial y} = 0, \qquad (3.1.6b)$$

and

$$\frac{\partial p}{\partial y} \approx 0. \qquad (3.1.6c)$$

Since $\partial p/\partial y \approx 0$ in the boundary layer, we may extend the pressure in the exterior flow across the boundary layer to the surface.

At the boundary $y = 0$,

$$u = v = 0 \qquad (3.1.7a)$$

and in the farfield

$$u \to U(x) \text{ as } y \to \infty . \tag{3.1.7b}$$

3.1.2 Oscillatory Boundary Layers

Let us consider a periodic flow characterized by high Reynolds number, where the oscillatory motion in the flow might be caused by a moving boundary [Batchelor, 1967,p.353], but will be taken here to be due to a sound wave propagating parallel to the boundary. We investigate when it is possible to linearize the equations of motion in this case, and the consequences.

For the case where there is no mean flow, to linearize the Navier-Stokes' equation we assume that

$$\left| \frac{\partial \vec{v}}{\partial t} \right| >> \left| \vec{v} \cdot \vec{\nabla} \vec{v} \right| . \tag{3.1.8}$$

If we scale $\vec{v}$ by U_0, the time by the angular frequency ω, and the distance over which $\vec{v}$ changes significantly by $1 / k_c$, then (3.1.8) implies that

$$\frac{U_0 k_c}{\omega} = \frac{U_0}{c} << 1 \tag{3.1.9}$$

Vorticity arises from viscous diffusion away from the boundary, and for periodic flow the vorticity generated is alternately positive and negative over one period. Thus if vorticity does not travel far from the boundary in this time, then no net vorticity is generated, and the layers of positive and negative vorticity are confined to a thin region next to the boundary where they diffuse together and cancel [Batchelor, 1967, p.353].

Since the time available for diffusion of vorticity (of one sign) away from the boundary is $T \equiv \pi/\omega$ (half the wave period), then by dimensional analysis we have a length scale $\delta = \left(\frac{2\mu_0}{\rho_0 \omega} \right)^{1/2}$. Since we consider a flow with a high Reynolds

number, and

$$R_c = \frac{\rho_0 U_0}{\mu_0 k_c} = \frac{U_0}{c} \frac{1}{(\delta k_c)^2} \tag{3.1.10}$$

then we obtain

$$\delta \ll \frac{1}{k_c} \quad . \tag{3.1.11}$$

So when $\delta \ll \frac{1}{k_c}$, the flow is irrotational over most of the field, and the velocity of the flow may be found from the speed and position of the boundary.

Let us consider an irrotational flow $\vec{V} = U(x)\, e^{i\omega t}\hat{x}$, where U is in general complex and varies along the boundary. For the irrotational flow exterior to the boundary layer we have

$$\frac{DU}{Dt} \equiv \frac{\partial U}{\partial t} + U\frac{\partial U}{\partial x} = -\frac{1}{\rho_0}\frac{\partial p}{\partial x} \tag{3.1.12}$$

resulting in the x-component of the boundary layer equations

$$\frac{\partial u}{\partial t} = \frac{\partial}{\partial t}\left(U\ e^{i\omega t}\right) + \frac{\mu_0}{\rho_0}\frac{\partial^2 u}{\partial y^2} \, . \tag{3.1.13}$$

The boundary conditions are that

$$u \to U e^{i\omega t} \quad \text{as} \quad y \to \infty \tag{3.1.14a}$$

and

$$u = 0 \quad \text{at} \quad y = 0 \, . \tag{3.1.14b}$$

If we convert to coordinates moving with the fluid far from the boundary, this is equivalent to a flat plate oscillating in a fluid at rest, which has solution [Batchelor, 1967, p.354]

$$u(x, y, t) = U(x)\, e^{i\omega t}\ (1 - e^{(1+i)y/\delta})$$

where

$$\delta = \left(\frac{2\mu_0}{\rho_0 \omega}\right)^{\frac{1}{2}} \, . \tag{3.1.15}$$

From (3.1.1), the boundary layer approximation should apply when δ is much smaller than the wavelength, which places a limitation on the acoustic frequency ω. That is, using (3.1.16), equation (3.1.11) becomes

$$\omega << \frac{c^2 \rho_0}{2\mu_0} \tag{3.1.16}$$

Recall that in the previous chapter we found that the viscous wavenumber was given by

$$k_s = (1+i)\left(\frac{\omega\rho_0}{2\mu_0}\right)^{\frac{1}{2}} \tag{3.1.17}$$

$$= \frac{(1+i)}{\delta} .$$

We identify the reciprocal of the imaginary part of the wavenumber with the e-folding scale for the viscous wave, and see that it is identical to the viscous boundary layer thickness.

3.1.3. The Effects of Boundary Curvature

Suppose we have a curved boundary with radius of curvature a. Then the boundary layer theory will be locally applicable if the gradients normal to the surface are much larger than those tangential to it [Tritton, 1977, p.101]. We obtain approximate expressions for the local gradients in Cartesian coordinates.

For a boundary layer of thickness δ we have (see Figure 3.1)

$$\frac{\partial}{\partial y} \approx \frac{1}{\delta} \tag{3.1.18a}$$

and

$$\frac{\partial}{\partial x} \approx \frac{1}{x_\delta} \tag{3.1.18b}$$

where x_δ is defined by

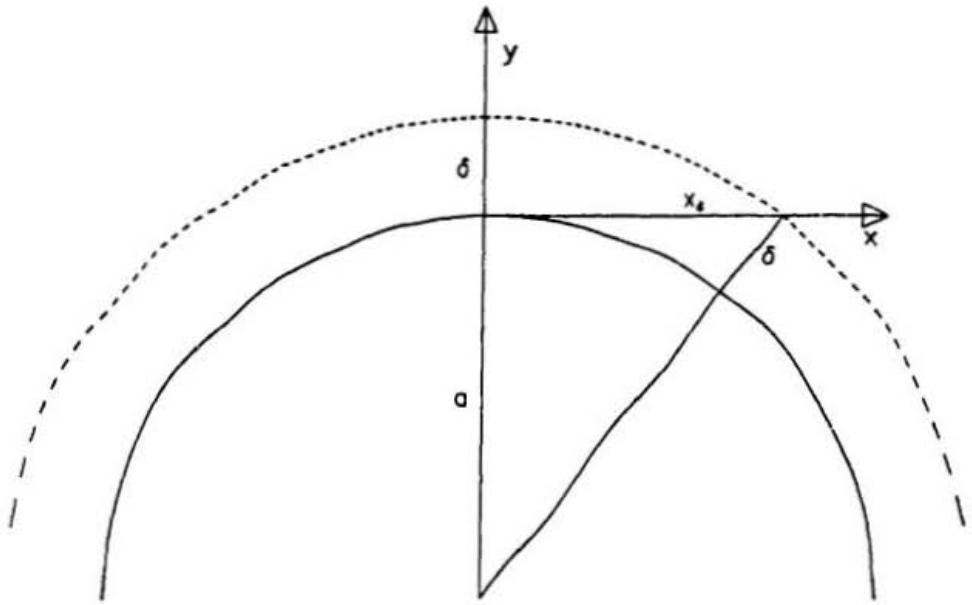

Figure 3.1. Curved Boundary Layer.

$$x_\delta = [(a+\delta)^2 - a^2]^{1/2} \qquad (3.1.19)$$
$$= (2a\,\delta)^{1/2}\left(1 + \frac{\delta}{2a}\right)^{1/2} .$$

For the boundary layer approximation to be applicable we require $\partial/\partial y >> \partial/\partial x$ which implies that $\delta/x_\delta << 1$. So

$$\left(\frac{\delta}{2a}\right)^{1/2}\left(1+\frac{\delta}{2a}\right)^{1/2} << 1 \qquad (3.1.20)$$

and we find that

$$\left(\frac{\delta}{2a}\right)^{1/2} << 1 \qquad (3.1.21)$$

and therefore

$$\frac{\delta}{a} << 2 \ . \qquad (3.1.22)$$

Thus for a boundary layer approximation to hold we expect that $\delta << a$. The boundary curvature therefore imposes a constraint on the size of an immersed body, in addition to the frequency constraint found earlier (3.1.16). Furthermore, since our variable s from the last chapter is

$$s = k_t a \qquad (3.1.23)$$
$$= (1+i)\frac{a}{\delta}$$

then we expect that the boundary layer approximation will work when $|s| \gg 1$.

3.1.4. Thermal Boundary Layers

Thermal diffusion of heat away from a boundary in a flow is similar to diffusion of vorticity, in that heat is advected downstream before it can extend far from the boundary, resulting in a thin layer with a high heat flux next to the boundary, particularly for fluids with low thermal conductivity [Schlichting, 1968, p.263].

As an example we consider a two-dimensional flow, as before. The flow is assumed to be incompressible and steady with constant properties. The governing equations are continuity (3.1.2), momentum (3.1.4 and 3.1.5), and energy as follows:

$$\left(u\frac{\partial T}{\partial x} + v\frac{\partial T}{\partial y}\right) = \sigma\left(\frac{\partial^2 T}{\partial x^2} + \frac{\partial^2 T}{\partial y^2}\right) + \frac{\mu_0}{\rho_0 C_p}\Phi\,, \qquad (3.1.24a)$$

where the viscous dissipation function Φ is given by

$$\Phi = 2\left[\left(\frac{\partial u}{\partial x}\right)^2 + \left(\frac{\partial v}{\partial y}\right)^2\right] + \left(\frac{\partial v}{\partial x} + \frac{\partial u}{\partial y}\right)^2 . \qquad (3.1.24b)$$

In a manner analogous to that in section (3.1.1), we obtain the boundary layer equations for a flat plate. The resulting momentum equations are identical to those in the viscous nonconducting case (3.1.6a and c), so the same scaling and approximations hold.

Let us scale the energy equation (3.1.24). As before let the farfield flow be $\vec{V} = U(x)\hat{x}$, with scale U_0. L is the length scale in the x-direction as before, and the boundary layer thickness is scaled by δ_t. From the continuity equation,

$$V_0 \approx \frac{\delta_t}{L} U_0 \tag{3.1.25}$$

in the thermal boundary layer. If we give a scale ΔT for the temperature, equation (3.1.24) scales like

$$\begin{array}{cccc} u\frac{\partial T}{\partial x} & + v\frac{\partial T}{\partial y} & = \sigma\frac{\partial^2 T}{\partial x^2} & + \sigma\frac{\partial^2 T}{\partial y^2} \\ U_0\frac{\Delta T}{L} & U_0\frac{\Delta T}{L} & \sigma\frac{\Delta T}{L^2} & \sigma\frac{\Delta T}{\delta^2} \end{array} \tag{3.1.26}$$

$$\begin{array}{ccccccc} + \frac{\mu_0}{\rho_0 C_p}\left(\frac{\partial u}{\partial x}\right)^2 & + \frac{\mu_0}{\rho_0 C_p}\left(\frac{\partial v}{\partial y}\right)^2 & + \frac{\mu_0}{\rho_0 C_p}\left(\frac{\partial v}{\partial x} & + & \frac{\partial u}{\partial y}\right)^2 \\ \frac{\mu_0}{\rho_0 C_p}\left(\frac{U_0}{L}\right)^2 & \frac{\mu_0}{\rho_0 C_p}\left(\frac{U_0}{L}\right)^2 & \frac{\mu_0}{\rho_0 C_p}\left(\frac{U_0\delta}{L^2}\right. & & \left.\frac{U_0}{\delta}\right)^2 \end{array}$$

Since $\delta_t \ll L$, within the boundary layer we have

$$u\frac{\partial T}{\partial x} + v\frac{\partial T}{\partial y} = \sigma\frac{\partial^2 T}{\partial y^2} + \frac{\mu_0}{\rho_0 C_p}\left(\frac{\partial u}{\partial y}\right)^2 . \tag{3.1.27}$$

Our boundary layer assumption is that in a thin region near the boundary, advective and diffusive terms are comparable in magnitude, which implies

$$\frac{U_0}{L} \approx \frac{\sigma}{\delta_t^2} \tag{3.1.28}$$

and this can be rearranged to give

$$\left(\frac{\delta_t}{L}\right)^2 \approx \frac{1}{P_r R_e} . \tag{3.1.29}$$

$P_r \equiv \frac{\mu_0}{\rho_0 \sigma}$ is the Prandtl number and is the ratio of the kinematic diffusivities of momentum and heat. Since $\delta_t \ll L$, we require $P_r R_e \gg 1$.

Thus the boundary layer equations for a thermal boundary layer on a flat plate are the continuity equation (3.1.6b) the momentum equations (3.1.6a,c) and the energy equation (3.1.27), together with boundary conditions as for viscous boundary layers together with continuity of temperature or heat flux.

The momentum and continuity equations are independent of thermal effects so that the solution for the viscous boundary layer in the flow is the same as

before. In addition, the thermal field is dependant on the flow but does not affect it, because buoyancy effects have been ignored. Thus we may solve the viscous boundary layer problem without worrying about thermal effects, then solve the thermal problem, and superpose solutions.

3.1.5. Thermoviscous Acoustic Boundary Layers

The decomposition of the exterior flow into acoustic, thermal and viscous modes, which are uncoupled except at boundaries [Pierce, 1981, p.519], provides a solution in principle to the thermoviscous problem we are considering. The acoustic field can be represented by an eigenfunction expansion, where the eigenfunctions are the complete set of eigensolutions to Helmholtz's equation for each mode in the particular geometry of the problem being considered. The unknown coefficients in the expansion may then be obtained by satisfying the conditions of continuity of velocity, stress, temperature, and heat flux at the boundary, and the problem is reduced to solving for these coefficients.

A boundary layer approximation to the governing equations, of the type presented in the preceding sections, is therefore not necessarily useful in this instance, except indirectly. Instead, approximate forms of the boundary conditions themselves are needed to simplify the problem.

Thus far we have considered the boundary layers in the fluid. Under appropriate conditions, a thermal boundary layer will also be present in the solid. However, it is not evident that the thermal wave in the solid decays rapidly inwards. The thermal wave in the solid scatterer is given by (2.3.2b)

$$\phi_t' = \sum_{n=0}^{\infty} i^n \, (2n + 1) \, B_n' \, j_n \, (k_t' r) \, P_n \, (\cos \theta) \, . \qquad (3.1.30)$$

In general, we may write $j_n \, (k_t' r)$ as the following sum

$$j_n \, (k_t' r) = h_n^{(1)} \, (k_t' r) + h_n^{(2)} \, (k_t' r) \, , \qquad (3.1.31)$$

where $h_n^{(1)}$ and $h_n^{(2)}$ are Hankel functions of the first and second kind [Arfken, 1970, p.522]. Asymptotically, for $|k_t' r| >> 1$, this becomes [Arfken, 1970, p.524]

$$j_n(k_t' r) \approx \frac{1}{2k_t' r}\left\{(-i)^{n+1} e^{i\frac{r}{\delta_t}} e^{-\frac{r}{\delta_t}} + (i)^{n+1} e^{-i\frac{r}{\delta_t}} e^{\frac{r}{\delta_t}}\right\} \quad (3.1.32)$$

For $r >> \delta_t$, the second term predominates. So near the boundary $r = a$ the thermal wave propagates radially inwards, and decays exponentially toward the center of the sphere. This suggests that a boundary layer approach might be useful inside the scatterer, provided however that $\delta_t << a$. Again, a constraint on the size of the scatterer is implied.

There is a very important consequence of the fact that thermal wave motion is predominantly radial in the boundary layer. Let us consider the fluid. For the thermal mode in the fluid the velocity is given by (2.1.37g).

$$\vec{v}_t = \frac{\beta K}{\rho_0 C_p}\vec{\nabla} T_t \quad (3.1.33)$$

Since $\vec{\nabla}_{\tan} T_t << \partial T_t / \partial r$ in the boundary layer, then the tangential component of the thermal velocity is negligible compared to the radial componemt. If we use Helmholtz's theorem we may write the thermal velocity as $\vec{v}_t = -\vec{\nabla}\phi_t$, where the vector potential is missing due to the modal relation $\vec{\nabla}\times\vec{v}_t = 0$. The fact that the tangential component of the thermal velocity is negligible in the boundary layer means that

$$\frac{\partial \phi_t}{\partial \theta} \approx 0 \quad \text{for all } \theta . \quad (3.1.34)$$

As noted before, we may write ϕ_t as the complete orthonormal series

$$\phi_t = \sum_{n=0}^{\infty} i^n (2n+1) B_n h_n(k_t r) P_n(\cos\theta) . \quad (3.1.35)$$

Thus (3.1.34) implies that

$$\phi_t = B_0 h_0(k_t r) , \quad (3.1.36)$$

so that the thermal potential contributes only to the $n = 0$ partial wave. This means that the viscous nonconducting case should be enough to describe the $n > 0$ terms, which greatly simplifies the problem. A similar result holds for the solid, using an analogous argument.

3.1.6. Allegra and Hawley's Results for Polystyrene Spheres

Allegra and Hawley [1972] measured the attenuation coefficient in aqueous suspensions of polystyrene spheres. Five suspensions were used, four being monodisperse (uniform size) and one being heterodisperse (non-uniform size). The monodisperse suspensions had polystyrene spheres of radii 0.653 μm , 0.504 μm, 0.178 μm, and 0.044 μm, while the single heterodisperse suspension had a nominal particle radius of 0.11 μm . Volume concentrations were stated to be about 10 % . Measurements were made at 20° C for sound frequencies ranging from around 3 MHz to around 100 MHz.

The quantity measured by Allegra and Hawley was the excess attenuation due to the suspended particles, which according to Allegra and Hawley is the intrinsic attenuation separated from diffraction losses via point by point comparison of signal amplitudes as a function of distance for water and for the suspension. Hawley [1967, p.81] determined experimentally that for polystyrene volume concentrations of up to at least 10 %, the attenuation was a linear function of the concentration, leading him to conclude that the total attenuation was a simple sum of the independant attenuation effects of each particle, and that particle-particle interaction and multiple scattering effects were negligible for this material at these volume concentrations.

The experimental and theoretical results obtained by Allegra and Hawley for polystyrene are reproduced in Appendix 6. These same experimental data, together with theoretical results computed using equations (2.3.3; our so-called

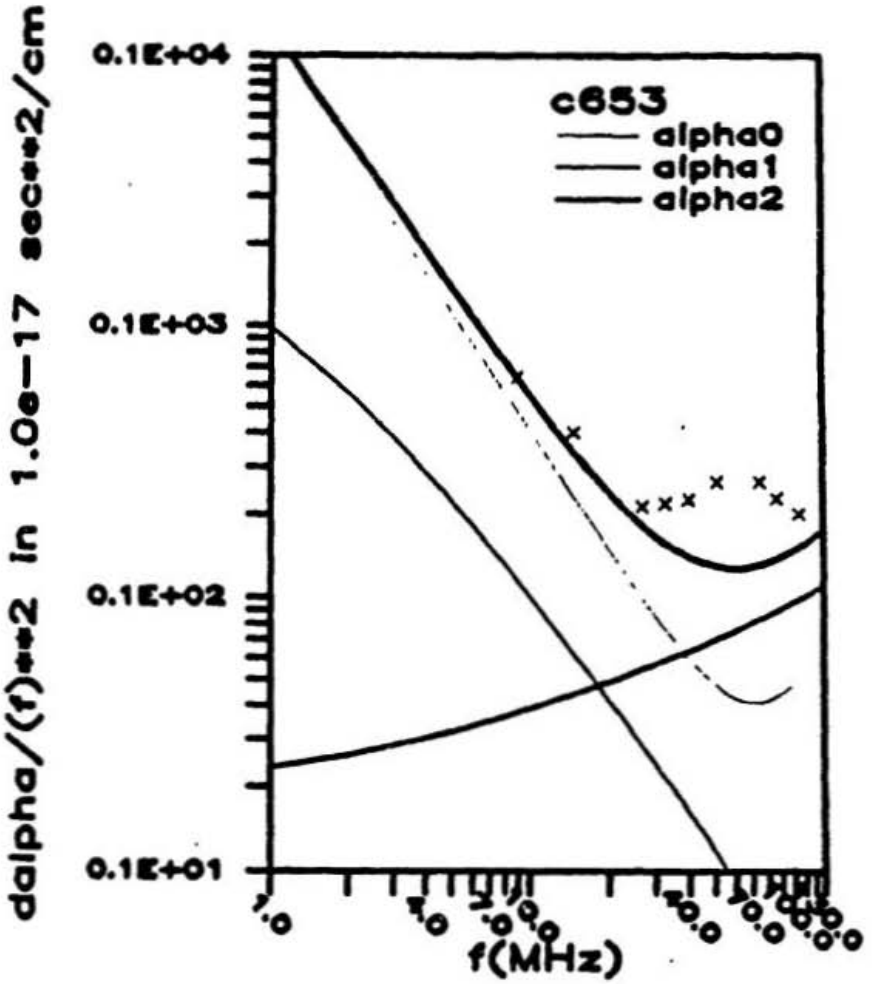

Figure 3.2. Excess attenuation versus frequency for an aqueous suspension of polystyrene spheres at 20^{o} C, $a = 0.653\ \mu m$. Points are measured excess attenuation . (Allegra and Hawley [1972]). The thickest line is the total theoretical attenuation, and the legend indicates which lines are α_0, α_1, and α_2, respectively.

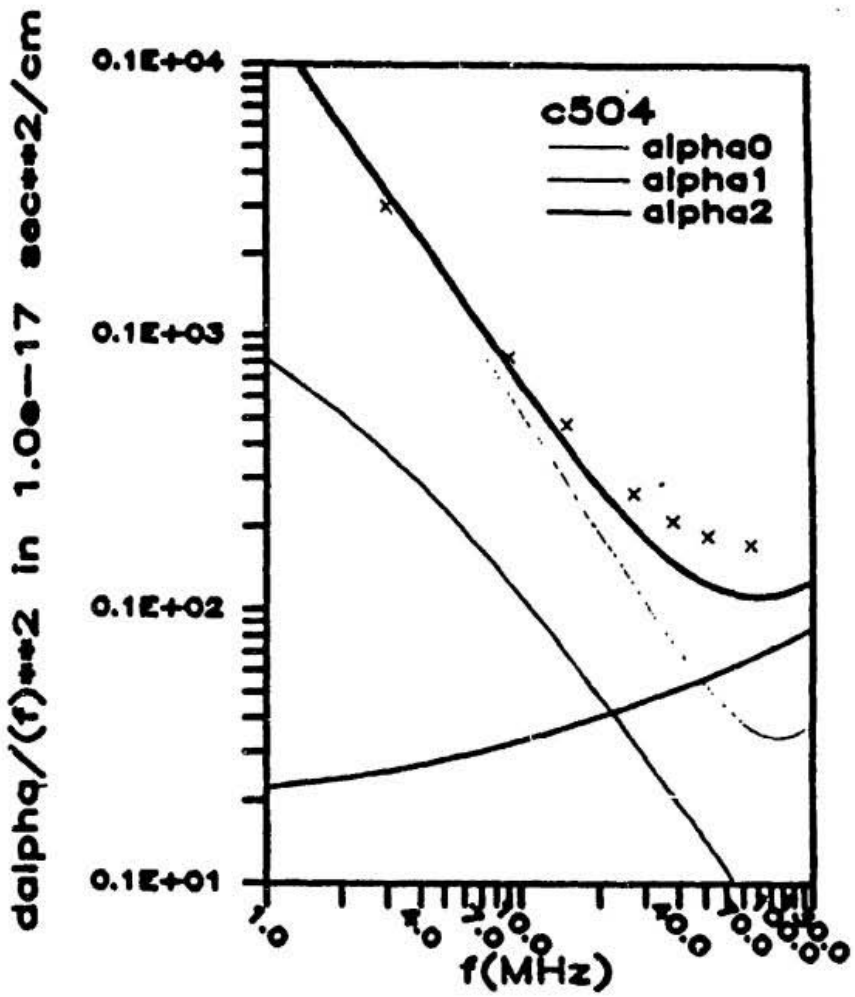

Figure 3.3. Excess attenuation versus frequency for an aqueous suspension of polystyrene spheres at 20° C, $a = 0.504\,\mu$m . Points are measured excess attenuation . (Allegra and Hawley [1972]). The thickest line is the total theoretical attenuation, and the legend indicates which lines are α_0, α_1, and α_2, respectively.

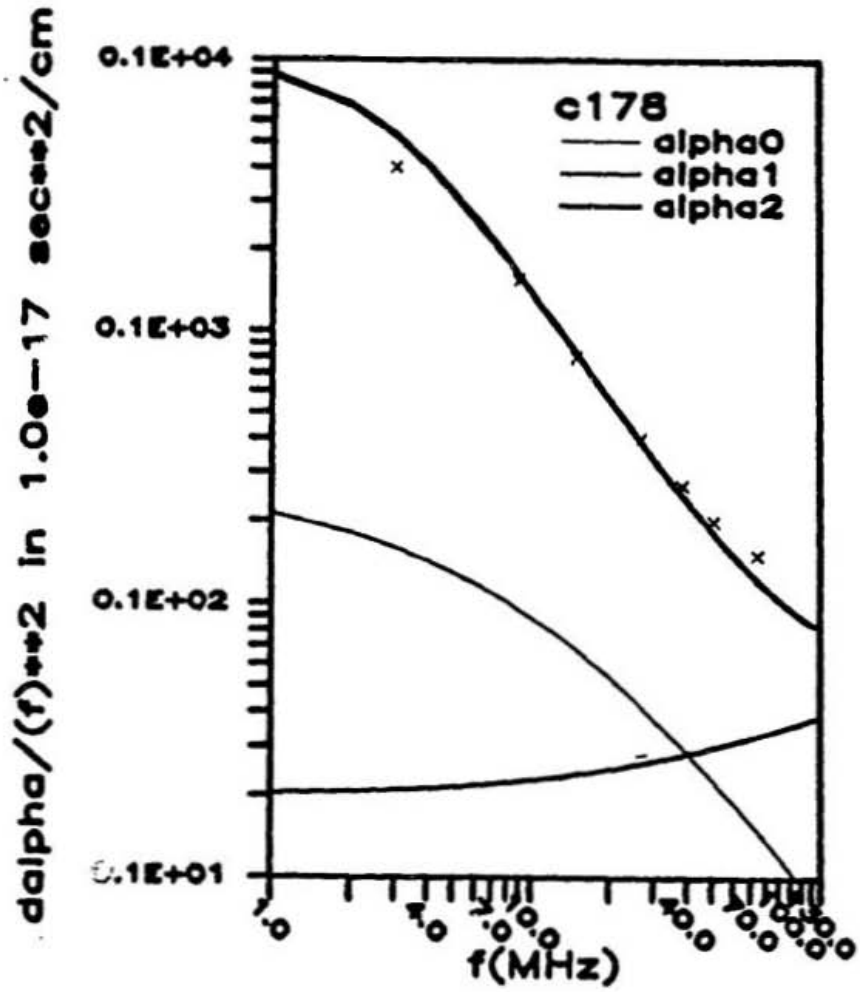

Figure 3.4. Excess attenuation versus frequency for an aqueous suspension of polystyrene spheres at 20° C, $a = 0.178\ \mu m$. Points are measured excess attenuation . (Allegra and Hawley [1972]). The thickest line is the total theoretical attenuation, and the legend indicates which lines are α_0, α_1, and α_2, respectively.

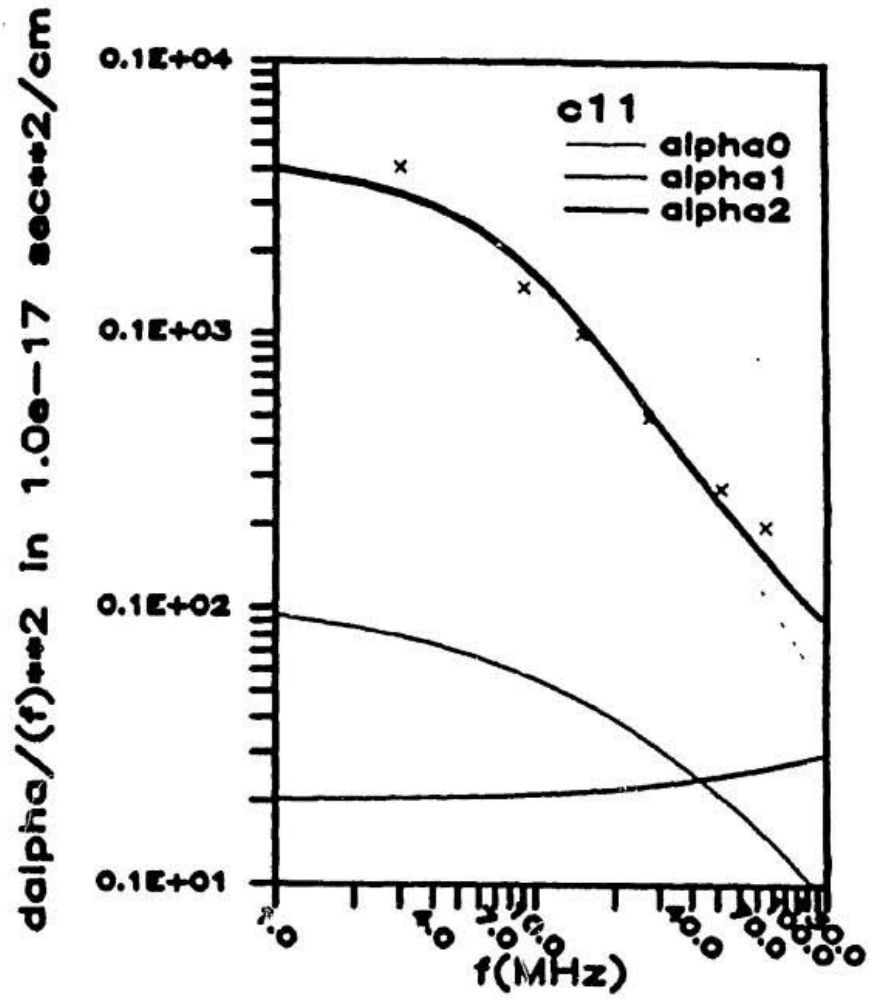

Figure 3.5. Excess attenuation versus frequency for an aqueous suspension of polystyrene spheres at 20° C, $a = 0.110\ \mu m$. Points are measured excess attenuation . (Allegra and Hawley [1972]). The thickest line is the total theoretical attenuation, and the legend indicates which lines are α_0, α_1, and α_2, respectively.

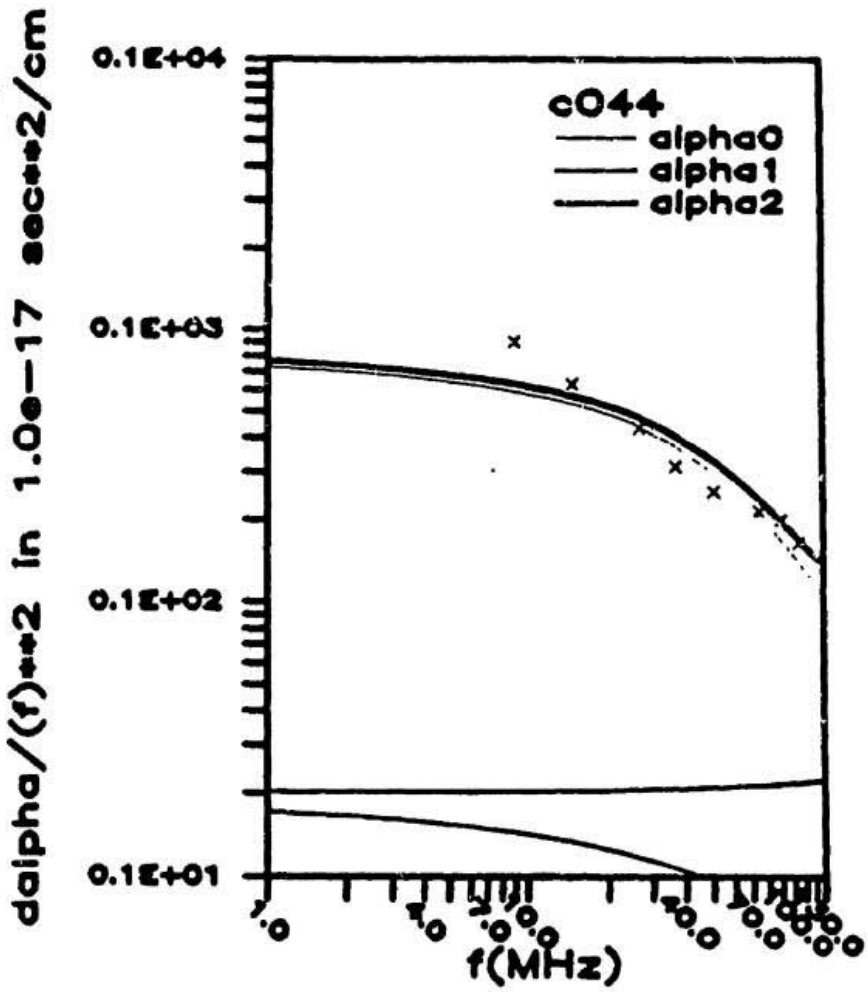

Figure 3.6. Excess attenuation versus frequency for an aqueous suspension of polystyrene spheres at 20° C, $a = 0.044\ \mu m$. Points are measured excess attenuation. (Allegra and Hawley [1972]). The thickest line is the total theoretical attenuation, and the legend indicates which lines are α_0, α_1, and α_2, respectively.

exact case), are shown in Figures 3.2 to 3.6, for a volume concentration $\epsilon = 0.1$. Only the contributions from terms $n = 0, 1$ and 2 are shown, because Allegra and Hawley [1972] found that for their particle sizes and frequencies the higher order terms were negligible. In Figures 3.2 to 3.6, the terms α_0, α_1, and α_2 represent the $n = 0, 1$ and 2 terms of the partial wave expansion. The total attenuation shown is the sum of α_0, α_1, and α_2.

The numerical method used was as follows. We solved the set of boundary conditions (2.3.3) for each n, to obtain the coefficient A_n, using the IMSL (International Mathematical and Statistical Library) Gaussian elimination subroutine LEQT1C. The attenuation coefficient α_n was obtained using equation (2.3.19) and A_n. In order to solve the system of equations numerically, it proved necessary to normalize the thermal terms. We did this by dividing every B_n term by $h_n(t)$, and dividing every B_n' term by $j_n(t')$, in equations (2.3.3). Otherwise we were faced with a numerical overflow problem. Finally the results for $n = 0$, 1, and 2 were plotted using the GRAFMAKER subset of the DI-3000 set of graphics software. All numerical calculations were made on a Digital Equipment Corporation VAX 8800 computer, with the VMS 4.7 operating system.

Comparing Figures 3.2-3.6 to Figures A5.1-A5.5, we find that for the $n = 0$ term our results decrease more rapidly with frequency than Allegra and Hawley's for all particle sizes. This results in lower total attenuation at high frequencies for the largest particles. The reason for this discrepancy is not known, since our calculations are based on the same equations as those of Allegra and Hawley [1972], except for the previously mentioned sign difference in the tangential stress boundary condition, which does not affect $n = 0$. With one exception, the $n = 1$ and $n = 2$ terms agreed well. The exception was the $n = 1$ term for particle radius $a = 0.044\ \mu m$ (Figures 3.6 and A5.5), where the Allegra and Hawley [1972] result is much larger than ours. We believe this to be an error in

their diagram for several reasons. First, our result provides a better fit to their data for this size. Second, the α_1 term tends to decrease with decreasing particle size in all of our graphs, and in all of their graphs, except the one in question. Third, as has been suggested, thermal effects should be insignificant for $n > 0$, which implies that the $n = 1$ term should match the corresponding term in the viscous nonconducting case. This turns out to be accurate for all results in the Figures being discussed, except for $a = 0.044\ \mu$m, for Allegra and Hawley [1972]. Thus we conclude that our α_1 term is correct in this instance.

We expect that a boundary layer approach will be useful for the Allegra and Hawley data set if the viscous and thermal boundary layer thicknesses are less than the particle radii. As has been shown, these thicknesses can be taken equal to the e-folding scales of the corresponding waves, which from the complex wavenumbers (2.1.14), (2.1.15), and (2.1.20) are:

$$\delta_t = \left(\frac{2\sigma}{\omega}\right)^{1/2}$$

$$\delta_s = \left(\frac{2\mu_0}{\rho_0\omega}\right)^{1/2}$$

$$\delta_t' = \left(\frac{2\sigma'}{\omega}\right)^{1/2}$$

Noting that $|s| = \sqrt{2}a/\delta_s$, $|t| = \sqrt{2}a/\delta_t$, $|t'| = \sqrt{2}a/\delta_t'$, the magnitudes of s, t, and t' should thus be much greater than unity. Table 2.3 gives the range of values of $|s|$, $|t|$ and $|t'|$ over the measured frequency range, for each particle size used. Clearly a boundary layer approximation should work well for the larger particles over most of the frequency range, and it should have the least validity for the lowest frequencies and for the smallest particles considered.

Table 3.1. Range of magnitudes of s for Allegra and Hawley's [1972] data set. a is the particle radius.

a (μ m)	$\lvert s \rvert$	
	f = 1 MHz	f = 100 MHz
0.653	1.68	16.8
0.504	1.29	12.9
0.178	0.457	4.57
0.110	0.282	2.82
0.044	0.113	1.13

Table 3.2. Range of magnitudes of t for Allegra and Hawley's [1972] data set. a is the particle radius.

a (μm)	$\lvert t \rvert$	
	f = 1 MHz	f = 100 MHz
0.653	4.35	43.5
0.504	3.36	33.6
0.178	1.19	11.9
0.110	0.734	7.34
0.044	0.293	2.93

Table 3.3. Range of magnitudes of t' for Allegra and Hawley's [1972] data set. a is the particle radius.

a (μm)	$\lvert t' \rvert$	
	f = 1 MHz	f = 100 MHz
0.653	5.48	54.8
0.504	4.23	42.3
0.178	1.49	14.9
0.110	0.923	9.23
0.044	0.369	3.69

3.2. First Boundary Layer Approximation

3.2.1. Viscous Nonconducting Limit

The basic approach to be followed here is to examine the validity of several approximations to the radial stress boundary condition in the fluid, in the viscous nonconducting case. Because of the well-known importance of the $n = 1$ term to the viscous absorption cross-section, this approach is taken for $n = 1$ initially. First we obtain the boundary conditions, in partial wave form, in the viscous non-conducting limit by taking equations (2.3.3), removing both the temperature and heat flux boundary conditions, and dropping thermal mode terms from the other boundary conditions. The radial stress boundary condition in the fluid, σ_{rr}, is then the left hand side of (modified) equation (2.3.3e),

$$\begin{aligned}\sigma_{rr} = &[-i\,\omega\,\rho_0\,a^2 + 2\,\mu_0\,n(n+1)]\,j_n(x) - 4\,\mu_0\,x\,j_n'(x) \\ &+ A_n\,\{[-i\,\omega\,\rho_0\,a^2 + 2\,\mu_0\,n(n+1)]\,h_n(x) - 4\,\mu_0\,x\,h_n'(x)\} \\ &+ C_n\,2\,\mu_0\,n(n+1)[h_n(s) - s\,h_n'(s)]\end{aligned} \tag{3.2.1}$$

We might simply approximate the radial stress in the fluid by the inviscid pressure field outside the boundary layer. This approach is suggested by laminar boundary layer theory, in which the pressure inside the boundary layer is approximately the same as the exterior pressure. In this case the radial stress σ_{rr} is just

$$\sigma_{rr} = -i\omega\rho_0 a^2[j_n(x) + A_n\,h_n(x)] \tag{3.2.2}$$

However, this approximation, when applied to polystyrene in water, results in α_1 being larger than both the exact result and Urick's result (see Figure 3.7) for the smallest ($a = 0.044\mu$m) and largest ($a = 0.653\mu$m) particles examined by Allegra and Hawley. For the small particle it is initially larger, while for the large particle the divergence from the exact case only becomes significant at high frequencies.

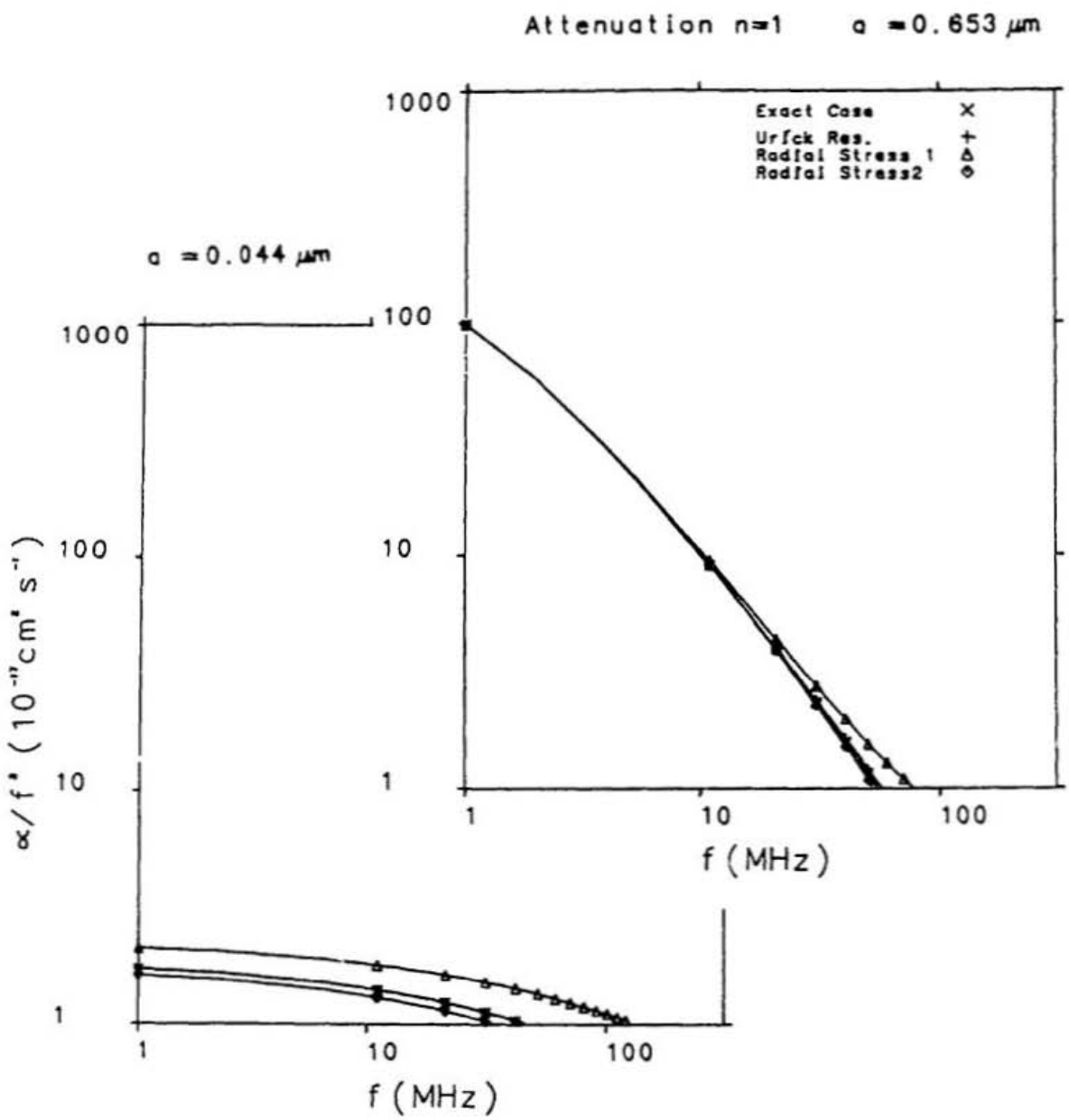

Figure 3.7. The $n = 1$ contribution to total attenuation, first boundary layer approximation, viscous non-conducting case, polystyrene spheres in water at 20 ^{0}C. Particle radii are given. The exact result (3.2.1), Urick's [1948] result (2.4.1; second term), and the first boundary layer approximations (3.2.2 and 3.2.3) are shown. Radial stress 1 is (3.2.2), Radial stress 2 is (3.2.3).

A somewhat less restrictive approximation is to leave the radial stress of the incident plane wave ϕ_0 unaffected but to maintain the approximation with respect to the other terms in σ_{rr}. That is:

$$\sigma_{rr} = [- i \omega \rho_0 a^2 + 2 \mu_0 n(n+1)] j_n(x) - 4 \mu_0 x j_n'(x) \qquad (3.2.3)$$
$$-i\omega\rho_0 A_n h_n(x)$$

When this approximation is used we obtain much better agreement with the exact case and with Urick's result (Figure 3.7).

This raises an interesting question. Why are viscous effects in the incident radial stress so important, while viscous effects in the radial stress due to the scattered wave are relatively unimportant? To examine this question, it is helpful to recognize that for Ailegra and Hawley's data set, $x \ll 1$ (for the largest particle, $a = 0.653\ \mu$m, so at the highest frequency considered, $f = 100$Mhz, we get $x_{max} = 0.277$). Noting that $\frac{\mu_0}{i\omega\rho_0 a^2} = \frac{1}{s^2}$, we expand (3.2.1) to order x^3, obtaining (for $n = 1$)

$$\frac{\sigma_{rr}}{-i\omega\rho_0 a^2} \approx \frac{x}{3} + \frac{x^3}{3}\left[-1 + \frac{8}{s^2}\right] + \qquad (3.2.4)$$
$$A_1\left\{\frac{x}{3} + \frac{x^3}{3}\left[-1 + \frac{8}{s^2}\right] + \right.$$
$$\left. i\left[\frac{1}{x^2}\left[-1 + \frac{12}{s^2}\right] - \frac{1}{2}\left[1 + \frac{4}{s^2}\right] + \frac{x^2}{8}\left[1 + \frac{4}{s^2}\right]\right]\right\}$$
$$- \frac{4}{s^2} C_1 \left[i\frac{e^{is}}{s}\right]\left[3i + s - \frac{1}{s}\right]$$

where the C_1 term is exact [Arfken, 1970, p.525]. We recall (see Table 3.1) that $|s|$ is not small at high frequencies. If we consider that part of (3.2.4) associated with the incident plane wave (the part not multiplied by A_1), it is inviscid to lowest order in small quantities, and thus viscous terms should be relatively unimportant. On the other hand, the scattered wave terms (the part multiplied by A_1) have a significant viscous component to lowest order, and this contribu-

tion to the attenuation should be measurably modified when viscous terms are dropped (see equation 3.2.2). As shown in Figure 3.7, the actual result is the opposite.

The α_2 term exhibits none of these difficulties. Both approximate forms of the radial stress match the exact case for both sizes, and for all frequencies considered (Figure 3.8).

3.2.2 Viscous Conducting Case

Again, the set of boundary conditions used is the general set of equations (2.3.3), and again the term to be modified is the radial stress in the fluid, σ_{rr}, given by the left hand side of equation (2.3.3e). Now, however, thermal terms are retained, and we are most interested in the $n = 0$ term, because it is this term which we expect will be most sensitive to thermal effects. Thus, the radial stress in the fluid at the boundary is

$$\begin{aligned}\sigma_{rr} = {} & [- i \omega \rho_0 a^2 + 2 \mu_0 n(n+1)] j_n(x) - 4 \mu_0 x j_n'(x) \\ & + A_n \{ [- i \omega \rho_0 a^2 + 2 \mu_0 n(n+1)] h_n(x) - 4 \mu_0 x h_n'(x) \} \\ & + B_n \{ [- i \omega \rho_0 a^2 + 2 \mu_0 n(n+1)] h_n(t) - 4 \mu_0 t h_n'(t) \} \\ & + C_n 2 \mu_0 n (n+1) [h_n(s) - s h_n'(s)]\end{aligned} \tag{3.2.5}$$

As in the last Section, we first assume that the radial stress in the fluid is given simply by the pressure. We recall from (2.1.37g) that the thermal pressure is expected to be negligible within the thermal mode, and we will, at least initially, assume that the thermal pressure is small compared to the acoustic pressure. In this approximation we obtain

$$\sigma_{rr} = -i \omega \rho_0 a^2 [j_n(x) + A_n h_n(x)] \tag{3.2.6}$$

which is the same as equation (3.2.2) for the viscous non-conducting limit.

The results for $n = 0$ are shown in Figure 3.9 as the plot of radial stress 3. Clearly the approximate attenuation is too small at low frequencies for both particle sizes, although the discrepancy decreases as the frequency increases.

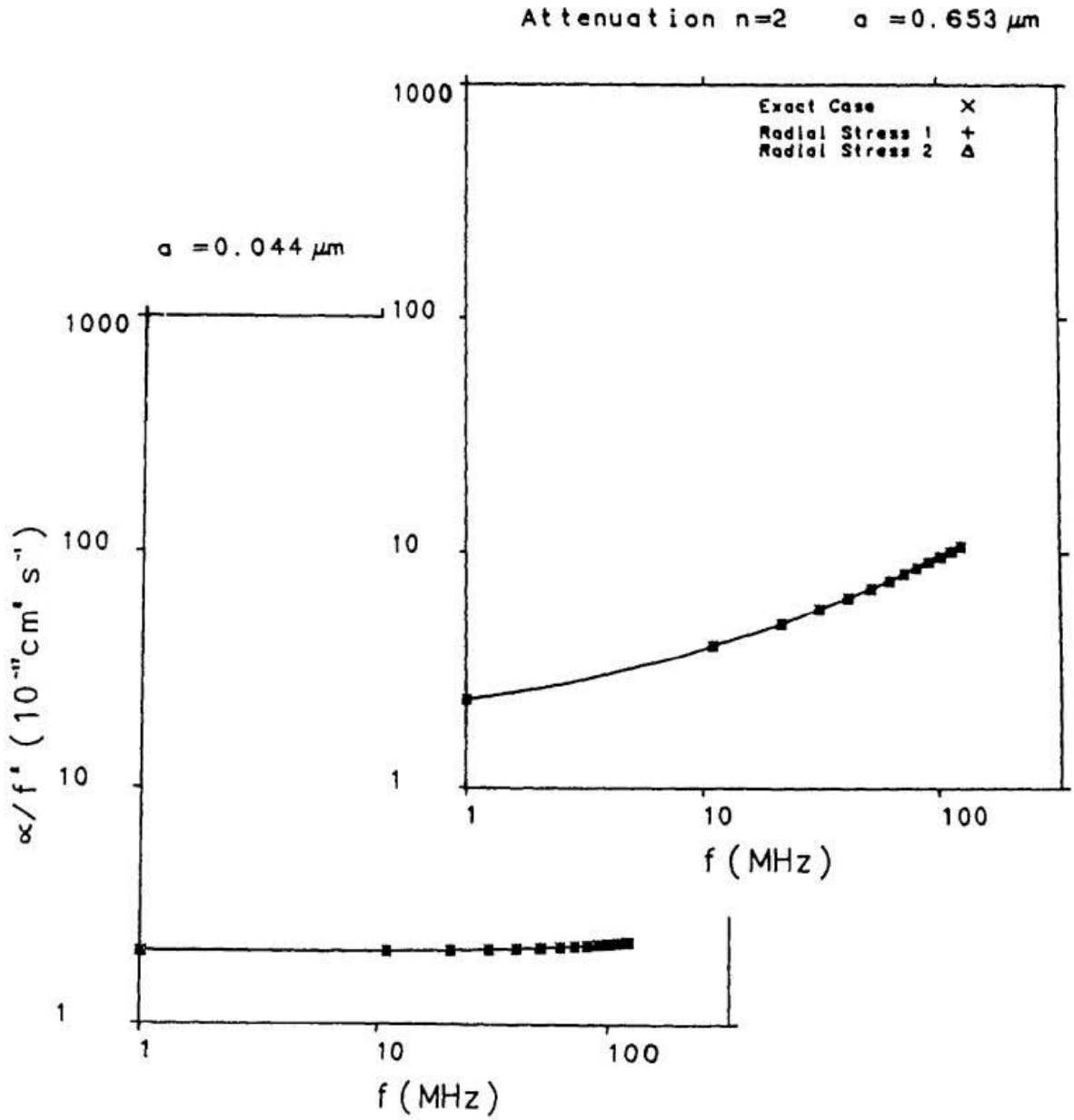

Figure 3.8. The $n = 2$ contribution to total attenuation, first boundary layer approximation, viscous non-conducting case, polystyrene spheres in water at 20 ^{0}C. Particle radii are given. The exact result (3.2.1) and the first boundary layer approximations (3.2.2 and 3.2.3) are shown. Radial stress 1 is (3.2.2), Radial stress 2 is (3.2.3).

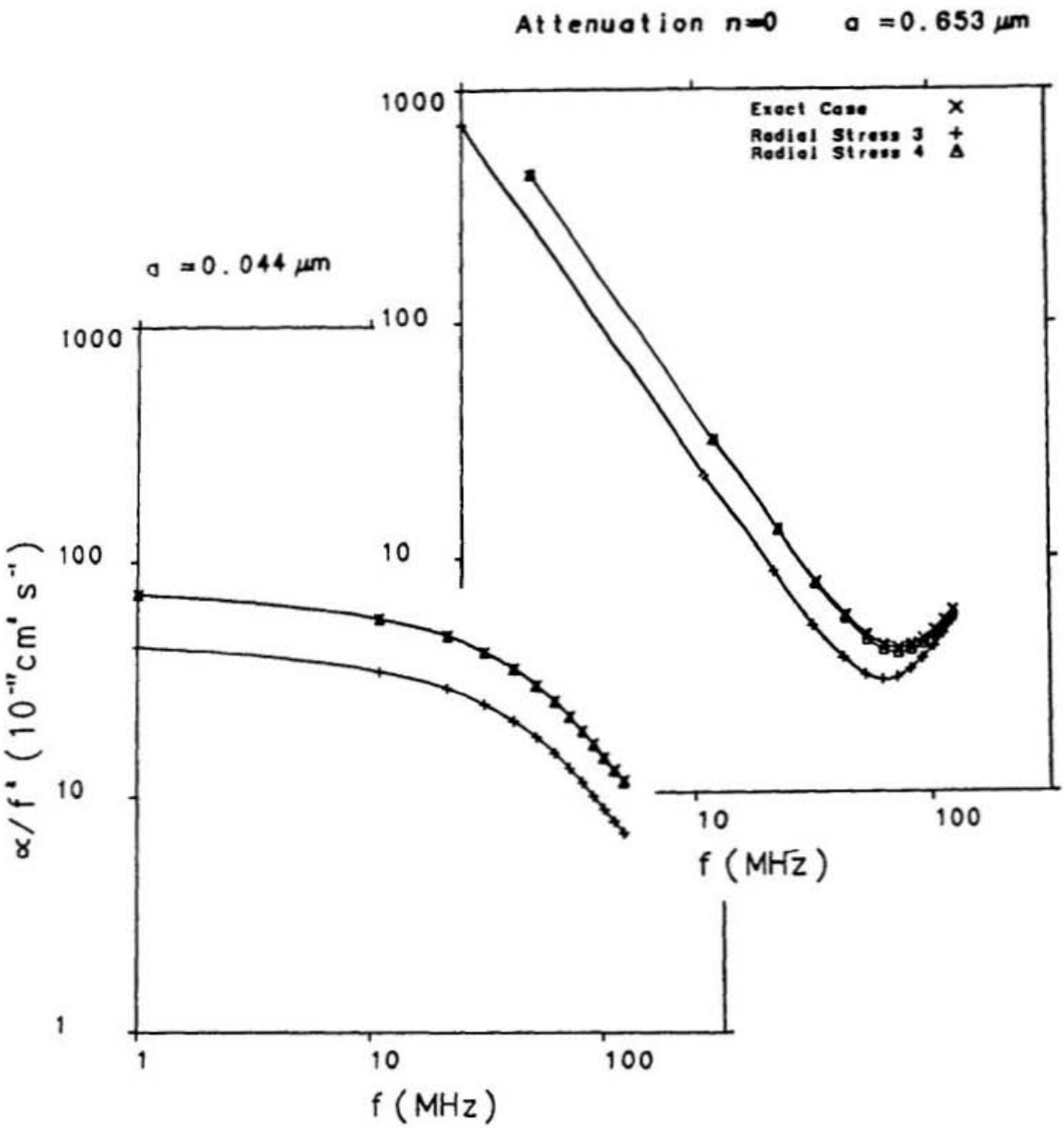

Figure 3.9. The $n = 0$ contribution to total attenuation, first boundary layer approximation, viscous conducting case, polystyrene spheres in water at 20 ^{0}C. Particle radii are given. The exact result (3.2.5), and the first boundary layer approximations (3.2.6 and 3.2.8) are shown. Radial stress 3 is (3.2.6), Radial stress 4 is (3.2.8).

The convergence to the exact result at high frequencies, however, is mostly due to the fact that, relative to the contribution of scattering to the attenuation, that from thermal absorption becomes negligible (see Figure A5.1). This suggests that thermal terms are not negligible in the radial stress.

We now reincorporate thermal effects, and make an approximation by assuming that the radial gradient of thermal quantities may be scaled by the boundary layer thickness. This produces the following equation for the radial stress in the fluid:

$$\sigma_{rr} = -i\omega\rho_0 a^2[j_n(x)+A_n h_n(x)] + (-i\omega\rho_0 a^2+2\mu_0 n(n+1)-4\mu_0 it)B_n h_n(t) \tag{3.2.7}$$

which, for $n = 0$ becomes

$$\sigma_{rr} = -i\omega\rho_0 a^2[j_0(x)+A_0 h_0(x)] + (-i\omega\rho_0 a^2-4\mu_0 it)B_0 h_0(t) \tag{3.2.8}$$

When this was done, agreement with the exact result was very good for both particles. This case is labelled radial stress 4 in Figure 3.9.

The results of the calculation for $n = 1$ and 2 using (3.2.7) are not shown because they are virtually identical to the first boundary layer approximation in the viscous nonconducting case (Figures 3.7 and 3.8). This shows that the aforementioned effective limitation of thermal effects to the α_0 term carries through to the boundary layer approximation. This indicates that the use of viscous nonconducting boundary conditions for $n > 0$ terms would be an excellent approximation.

To summarize, the first boundary layer approximation works well for α_0, the agreement with the exact case increasing as s, t, and t' increase, provided that the thermal pressure term in the fluid is retained. For α_1, agreement with the exact case is considerably improved when the viscous terms in the radial stress due to the incident plane wave are included. For α_2 the agreement is excellent

for both sizes and both approximations over the whole frequency range.

3.3. Second Boundary Layer Approximation

This is a more formal treatment which considers the thermal and viscous boundary layers in the fluid, as well as the thermal boundary layer in the solid, for all of the boundary conditions. The approach is primarily based upon the method Pierce [1981] used for boundary layers between two half-spaces separated by a plane interface.

3.3.1 Boundary Conditions in the 2nd Boundary Layer Approximation.

The modal relations in Section 2.1.2 indicate that in the fluid the pressure is approximately p_c, and that the viscous mode in the fluid and the shear wave mode in the solid have negligible effects on temperature or pressure.

We separate field quantities into the three modal components, and use the above simplifications, and the earlier result that the tangential component of the thermal velocity should be negligible, to re-express (2.2.1) as

$$v_{c,r} + v_{t,r} + v_{s,r} = v_{c,r}' + v_{t,r}' + v_{s,r}', \tag{3.3.1a}$$

$$v_{c,\theta} + v_{s,\theta} = v_{c,\theta}' + v_{s,\theta}', \tag{3.3.1b}$$

$$T_c + T_t = T_c' + T_t', \tag{3.3.1c}$$

$$K\left(\frac{\partial T_c}{\partial r} + \frac{\partial T_t}{\partial r}\right) = K'\left(\frac{\partial T_c'}{\partial r} + \frac{\partial T_t'}{\partial r}\right), \tag{3.3.1d}$$

$$\begin{aligned} p_t + \frac{2}{3}\mu_0\left[\vec{\nabla}\cdot\vec{\mathbf{v}}_c + \vec{\nabla}\cdot\vec{\mathbf{v}}_t\right] - 2\mu_0\left[\frac{\partial}{\partial r}(v_{c,r} + v_{t,r} + v_{s,r})\right] \\ = p_c' + p_t' + \frac{2}{3}\mu'\left[\vec{\nabla}\cdot\vec{\mathbf{u}}_c' + \vec{\nabla}\cdot\vec{\mathbf{u}}_t'\right] \\ - 2\mu'\left[\frac{\partial}{\partial r}(u_{c,r}' + u_{t,r}' + u_{s,r}')\right], \end{aligned} \tag{3.3.1e}$$

and

$$\mu_0\left[r\frac{\partial}{\partial r}\left(\frac{v_{s,t}}{r}\right)+\frac{1}{r}\frac{\partial v_{s,r}}{\partial\theta}+2\frac{\partial v_{c,t}}{\partial r}\right]$$
$$=\mu'\left[r\frac{\partial}{\partial r}\left(\frac{u_{s,t}'}{r}\right)+\frac{1}{r}\frac{\partial u_{s,r}'}{\partial\theta}+2\frac{\partial u_{c,t}'}{\partial r}\right]. \qquad (3.3.1f)$$

where the compression wave contribution to the tangential stress has been simplified as shown in Appendix 7, and the contribution of the tangential thermal velocities to the tangential stress has been ignored.

We now wish to represent equations (3.3.1) in potential form, and therefore need the relationships between modal field quantities and the potential functions. For the velocities of the three modes in the fluid we have

$$\vec{v}_c = -\vec{\nabla}\phi_c \ , \qquad (3.3.2a)$$
$$= -\frac{\partial\phi_c}{\partial r}\hat{r} - \frac{1}{r}\frac{\partial\phi_c}{\partial\theta}\hat{\theta}$$
$$\vec{v}_t = -\vec{\nabla}\phi_t \ , \qquad (3.3.2b)$$
$$= -\frac{\partial\phi_t}{\partial r}\hat{r} - \frac{1}{r}\frac{\partial\phi_t}{\partial\theta}\hat{\theta}$$

and

$$\vec{v}_s = \vec{\nabla}\times\vec{A} \ , \qquad (3.3.2c)$$
$$= \frac{1}{r\sin\theta}\frac{\partial}{\partial\theta}(A_\phi\sin\theta)\hat{r} - \frac{1}{r}\frac{\partial}{\partial r}(rA_\phi)\hat{\theta}$$

with similar relations for the solid.

The acoustic pressure in the fluid is found by substituting $\vec{v}_c = -\vec{\nabla}\phi_c$ into modal relation (2.1.36a) to obtain

$$p_c = -i\omega\rho_0\phi_c \qquad (3.3.3)$$

We have shown, using (2.1.37c), that the thermal pressure p_t is negligible.

For the acoustic temperature, we use (2.1.35b) and (3.3.3) to obtain

$$T_c = -i\omega\frac{T_0\beta}{C_p}\phi_c \qquad (3.3.4)$$
$$= \frac{-i\omega(\gamma-1)}{\beta c^2}\phi_c$$

using the thermodynamic identity [Allegra, 1970, p. 27]

$$\gamma - 1 = \frac{c^2 \beta^2 T_0}{C_p} \tag{3.3.5}$$

Here we identify the coefficient on the right hand side of (3.3.4) as an approximate form of $b_c/(-i\omega)$, where b_c is Allegra and Hawley's coefficient, equation (2.1.17). The approximate equivalence is shown in Appendix 8, and thus

$$b_c \approx -(\gamma-1)\frac{k_c^2}{\beta} \tag{3.3.6}$$

and (3.3.4) becomes $T_c = b_c \phi_c/(-i\omega)$.

The thermal mode temperature in the fluid is related to the potential ϕ_t by taking equation (2.1.37g) and substituting $\vec{v}_t = -\vec{\nabla}\phi_t$ into it to obtain

$$\begin{aligned} T_t &= -\frac{\rho_0 C_p}{\beta K}\phi_t \\ &= -\frac{k_t^2}{i\omega\beta}\phi_t \end{aligned} \tag{3.3.7}$$

where we recall that $\sigma = \frac{K}{\rho_0 C_p}$ and that $k_t^2 = i\omega/\sigma$. The coefficient on the right hand side of (3.3.7) is an approximation to Allegra and Hawley's thermal coefficient $b_t/(-i\omega)$, given in equation (2.1.18) (see Appendix 8). Thus

$$b_t \approx \frac{k_t^2}{\beta} \tag{3.3.8}$$

and (3.3.7) becomes $T_t = b_t \phi_t/(-i\omega)$. Thus we recover Allegra and Hawley's relation for the total temperature in the fluid, equation (2.1.18).

Now we derive similar relations for the wave modes in the solid. To get the potential form for the acoustic pressure p_c', we substitute $\vec{u}_c' = -\vec{\nabla}\phi_c'$ into the modal relation (2.1.45d) to obtain

$$\begin{aligned} p_c' &= -\omega^2 \rho_0' \frac{c_1^{2\prime}}{c^{\prime 2}}\phi_c' \\ &= \left(-\omega^2\rho_0' + \frac{4}{3}\mu' k_c^{\prime 2}\right)\phi_c' \end{aligned} \tag{3.3.9}$$

where the second expression is obtained using $k_c^{\prime 2} \approx \omega^2/c^{\prime 2}$.

The thermal pressure relation is obtained by substituting $\vec{u}' = -\vec{\nabla}\phi_c'$ into the modal relation (2.1.49e), and then substituting this into (2.1.49d) to obtain

$$p_t' = \rho_0' c'^2 k_t'^2 \left(\frac{\epsilon_s'}{1+\gamma' \epsilon_s'} \right) \phi_t' \qquad (3.3.10)$$

$$= \left(-\omega^2 \rho_0' + \frac{4}{3} \mu' k_t'^2 \right) \phi_t'$$

using (2.1.41b) and (2.1.3h). This can be approximated by

$$p_t' \approx \frac{4}{3} \mu' k_t'^2 \phi_t' \qquad (3.3.11)$$

We relate the acoustic temperature in the solid to the acoustic potential by substituting $\vec{u}_c' = -\vec{\nabla}\phi_c'$ into (2.1.45d) and combining this with (2.1.45f) to obtain

$$T_c' = -\frac{(\gamma' - 1)\omega^2}{\beta' \rho_0' c'^2} \phi_c' \qquad (3.3.12)$$

This is approximately the result obtained by Allegra and Hawley (see Appendix 8), and so $T_c' = b_c' \phi_c'$, with

$$b_c' \approx \frac{(1-\gamma')}{\beta'} \frac{\omega^2}{c'^2} \qquad (3.3.13)$$

The last relation we need is between the thermal mode temperature and ϕ_t'. We do this by using (2.1.49e) and the scalar potential to obtain

$$T_t' = \frac{k_t' c'^2}{\beta' c_1'^2} \phi_t' \qquad (3.3.14)$$

which is approximately the same as Allegra and Hawley's result (see Appendix 8), so that $T_t' = b_t' \phi_t'$, where

$$b_t' \approx \frac{c'^2}{c_1'^2} \frac{k_t'^2}{\beta'} \qquad (3.3.15)$$

and we recover Allegra and Hawley's relation (2.1.22) for the total temperature in the solid.

Now we proceed to substitute the above relations between potentials and

modal field quantities into equations (3.3.1). The resulting set of equations is

$$-\frac{\partial \phi_c}{\partial r} - \frac{\partial \phi_t}{\partial r} + \frac{1}{r\sin\theta}\frac{\partial}{\partial \theta}(A_\phi \sin\theta)$$
$$= -i\omega\left[-\frac{\partial \phi_c'}{\partial r} - \frac{\partial \phi_t'}{\partial r} + \frac{1}{r\sin\theta}\frac{\partial}{\partial \theta}(A_\phi' \sin\theta)\right] \qquad (3.3.16a)$$

$$-\frac{1}{r}\frac{\partial \phi_c}{\partial \theta} - \frac{1}{r}\frac{\partial}{\partial r}(rA_\phi) = -i\omega\left[-\frac{1}{r}\frac{\partial \phi_c'}{\partial \theta} - \frac{1}{r}\frac{\partial}{\partial r}(rA_\phi')\right] \qquad (3.3.16b)$$

$$b_c \phi_c + b_t \phi_t = -i\omega(b_c'\phi_c' + b_t'\phi_t') \qquad (3.3.16c)$$

$$K\left[b_c \frac{\partial \phi_c}{\partial r} + b_t \frac{\partial \phi_t}{\partial r}\right] = -i\omega K'\left[b_c'\frac{\partial \phi_c'}{\partial r} + b_t'\frac{\partial \phi_t'}{\partial r}\right] \qquad (3.3.16d)$$

$$-i\omega\rho_0\phi_c + \frac{2}{3}\mu_0\left[k_c^2\phi_c + k_t^2\phi_t\right]$$
$$+ 2\mu_0\left[\frac{\partial^2 \phi_c}{\partial r^2} + \frac{\partial^2 \phi_t}{\partial r^2} - \frac{\partial}{\partial r}\left\{\frac{1}{r\sin\theta}\frac{\partial}{\partial \theta}(A_\phi \sin\theta)\right\}\right]$$
$$= (-\omega^2\rho_0' + \frac{4}{3}\mu' k_c'^2)\phi_c' + (-\omega^2\rho_0' + \frac{4}{3}\mu' k_t'^2)\phi_t'$$
$$+ \frac{2}{3}\mu'\left[k_c'^2\phi_c' + k_t'^2\phi_t'\right]$$
$$+ 2\mu'\left[\frac{\partial^2 \phi_c'}{\partial r^2} + \frac{\partial^2 \phi_t'}{\partial r^2} - \frac{\partial}{\partial r}\left\{\frac{1}{r\sin\theta}\frac{\partial}{\partial \theta}(A_\phi' \sin\theta)\right\}\right] \qquad (3.3.16e)$$

$$\mu_0\left[r\frac{\partial}{\partial r}\left\{\frac{-1}{r^2}\frac{\partial}{\partial r}(rA_\phi)\right\} + \frac{1}{r^2}\frac{\partial}{\partial \theta}\left\{\frac{1}{\sin\theta}\frac{\partial}{\partial \theta}(A_\phi \sin\theta)\right\} - 2\frac{\partial}{\partial r}\left\{\frac{1}{r}\frac{\partial \phi_c}{\partial \theta}\right\}\right] \qquad (3.3.16f)$$
$$= \mu'\left[r\frac{\partial}{\partial r}\left\{\frac{-1}{r^2}\frac{\partial}{\partial r}(rA_\phi')\right\} + \frac{1}{r^2}\frac{\partial}{\partial \theta}\left\{\frac{1}{\sin\theta}\frac{\partial}{\partial \theta}(A_\phi' \sin\theta)\right\} - 2\frac{\partial}{\partial r}\left\{\frac{1}{r}\frac{\partial \phi_c'}{\partial \theta}\right\}\right]$$

Now we apply the second boundary layer approximation, which is to replace radial gradients of the thermal and viscous modes in the fluid, and of the thermal mode in the solid, by

$$\frac{\partial}{\partial r} \approx \left[\pm ik - \frac{1}{r} \right] \approx \pm ik \ . \tag{3.3.17}$$

at the boundary $r = a$. This comes from assuming a radial dependence of the form $e^{\pm ikr}/r$ for these waves near $r = a$, where the + sign represents outward propagation in the fluid, and the - sign inward propagation in the solid. Furthermore, we may assume that $|ka| >> 1$ for both thermal modes and the viscous mode, which implies that the second term in (3.3.17) may be neglected, as indicated.

We rewrite equations (3.3.16) using these approximations, obtaining

$$-\frac{\partial \phi_c}{\partial r} - ik_t \phi_t + \frac{1}{a \sin\theta} \frac{\partial}{\partial \theta}(A_\phi \sin\theta) = -i\omega \left[-\frac{\partial \phi_c'}{\partial r} + ik_t' \phi_t' + \frac{1}{a \sin\theta} \frac{\partial}{\partial \theta}(A_\phi' \sin\theta) \right] \tag{3.3.18a}$$

$$-\frac{1}{a} \frac{\partial \phi_c}{\partial \theta} - ik_c A_\phi = -i\omega \left[-\frac{1}{a} \frac{\partial \phi_c'}{\partial \theta} - \frac{1}{a} \frac{\partial}{\partial r}(rA_\phi') \right] \tag{3.3.18b}$$

$$b_c \phi_c + b_t \phi_t = -i\omega (b_c' \phi_c' + b_t' \phi_t') \tag{3.3.18c}$$

$$K \left[b_c \frac{\partial \phi_c}{\partial r} + ik_t b_t \phi_t \right] = -i\omega K' \left[b_c' \frac{\partial \phi_c'}{\partial r} - ik_t' b_t' \phi_t' \right] \tag{3.3.18d}$$

$$\begin{aligned} -i\omega \rho_0 \phi_c + \frac{2}{3} \mu_0 \left[k_c^2 \phi_c + k_t^2 \phi_t \right] \\ + 2\mu_0 \left[\frac{\partial^2 \phi_c}{\partial r^2} - k_t^2 \phi_t - \frac{\partial}{\partial r} \left\{ \frac{1}{r \sin\theta} \frac{\partial}{\partial \theta}(A_\phi \sin\theta) \right\} \right] \\ = (-\omega^2 \rho_0' + \frac{4}{3} \mu' k_c'^2) \phi_c' + (-\omega^2 \rho_0' + \frac{4}{3} \mu' k_t'^2) \phi_t' \\ + \frac{2}{3} \mu' \left[k_c'^2 \phi_c' + k_t'^2 \phi_t' \right] \\ + 2\mu' \left[\frac{\partial^2 \phi_c'}{\partial r^2} - k_t'^2 \phi_t' - \frac{\partial}{\partial r} \left\{ \frac{1}{r \sin\theta} \frac{\partial}{\partial \theta}(A_\phi' \sin\theta) \right\} \right] \end{aligned} \tag{3.3.18e}$$

$$\mu_0\left[k_e^2 A_\phi+\frac{1}{a^2}\frac{\partial}{\partial\theta}\left[\frac{1}{\sin\theta}\frac{\partial}{\partial\theta}(A_\phi\sin\theta)\right]-2\frac{\partial}{\partial r}\left(\frac{1}{r}\frac{\partial\phi_c}{\partial\theta}\right)\right]$$

$$=\mu'\left[-a\frac{\partial}{\partial r}\left(\frac{1}{r^2}\frac{\partial}{\partial r}(rA_\phi')\right)+\frac{1}{a^2}\frac{\partial}{\partial\theta}\left[\frac{1}{\sin\theta}\frac{\partial}{\partial\theta}(A_\phi'\sin\theta)\right]\right.$$

$$\left.-2\frac{\partial}{\partial r}\left(\frac{1}{r}\frac{\partial\phi_c'}{\partial\theta}\right)\right] \qquad (3.3.18f)$$

Next we present the approximated boundary conditions in partial wave form by expanding the potentials in terms of (2.3.1) and (2.3.2), and setting $r = a$. Note that in the boundary conditions for radial velocity, radial stress, and tangential stress we make use of Legendre's equation [e.g. Arfken, 1970, p.542].

$$\frac{1}{\sin\theta}\frac{d}{d\theta}\left(\sin\theta\frac{dP_n(\cos\theta)}{d\theta}\right)+n(n+1)P_n(\cos\theta)=0$$

Then the boundary conditions are

(a) radial velocity

$$x[j_n'(x)+A_n h_n'(x)]+itB_n h_n(t)-n(n+1)C_n h_n(s) \qquad (3.3.19a)$$
$$=(-i\omega)[x'A_n'j_n'(x')-it'B_n'j_n(t')-n(n+1)C_n'j_n(s')]$$

(b) tangential velocity

$$j_n(x)+A_n h_n(x)-isC_n h_n(s)$$
$$=(-i\omega)\{A_n'j_n(x')-C_n'[j_n(s')+s'j_n'(s')]\} \qquad (3.3.19b)$$

(c) temperature

$$b_c[j_n(x)+A_n h_n(x)]+b_t B_n h_n(t)=$$
$$(-i\omega)[b_c'A_n'j_n(t')+b_t'B_n'j_n(t')], \qquad (3.3.19c)$$

(d) heat flux

$$K\left[b_c x[j_n'(x)+A_n h_n'(x)]+itb_t B_n h_n(t)\right]=$$
$$(-i\omega)K'\left[b_c'x'A_n'j_n'(x')-it'b_t'B_n'j_n(t')\right], \qquad (3.3.19d)$$

(e) radial stress

$$[-i\omega\rho_0 a^2+2\mu_0 n(n+1)]j_n(x)-4\mu_0 x j_n'(x)$$

$$+ A_n[-i\omega\rho_0 a^2 + 2\mu_0 n(n+1)]h_n(x) - 4\mu_0 x h_n'(x)$$
$$- 2is\mu_0 n(n+1)C_n h_n(s)$$
$$= A_n'\{[-\omega^2\rho_0' a^2 + 2\mu' n(n+1)]j_n(x') - 4\mu' x' j_n'(x')\}$$
$$-\omega^2\rho_0' a^2 B_n' j_n(t') + 2\mu' n(n+1) C_n' [j_n(s') - s' j_n(s')] \quad (3.3.19e)$$

(f) and tangential stress

$$\mu_0\{[xj_n'(x) - j_n(x)] + [xh_n'(x) - h_n(x)]A_n$$
$$+ \frac{1}{2}(s^2 - n(n+1))C_n h_n(s)\}$$
$$= \mu'\{[x' j_n'(x') - j_n(x')]A_n'$$
$$+ C_n'[s' j_n'(s') - j_n(s')(-\frac{s'^2}{2} + n^2 + n - 1)]\} \quad (3.3.19f)$$

In the radial stress we have used the spherical Bessel equation

$$z^2 f_n''(z) + 2z f_n'(z) + (z^2 - n(n+1))f_n(z) = 0 \quad (3.3.20)$$

to eliminate second derivatives. We have also eliminated a term $\frac{-4}{3}\mu_0 x^2$ from the left hand side of equation (3.3.19e) compared to $-i\omega\rho_0$, because the ratio of these two terms is ϵ_s (equation 2.1.30b). This deletion is necessary to be consistent with the approximation to p_c made in Pierce's modal separation.

In addition, a term $-\frac{4}{3}\mu_0 t^2 B_n h_n(t)$ has been dropped from the left hand side of equation (3.3.19e), since if we substitute $\vec{v}_t = -\vec{\nabla}\phi_t$ into the momentum equation (2.1.26b), we obtain $p_t = (-i\omega\rho_0 + 4/3\mu_0 k_t^2)\phi_t$. The second term may be identified with the term we have dropped. The ratio of the second to the first term in p_t is $\frac{4}{3}\frac{k_t^2}{k_s^2} \approx 9$. This implies that the term we have dropped is of the same order as p_t, which is supposed to be negligible.

For $n = 0$ we obtain

(a) radial velocity

$$x[j_0'(x) + A_0 h_0'(x)] + itB_0 h_0(t) =$$
$$(-i\omega)[x' A_0' j_0'(x) - it' B_0' j_0(t')], \quad (3.3.21a)$$

(b) temperature

$$b_c\,[j_0(x) + A_0 h_0(x)] + b_t\, B_0 h_0(t) = (-i\omega)\,[b_c' A_0' j_0(t') + b_t' B_0' j_0(t')]\,, \tag{3.3.21b}$$

(c) heat flux

$$b_c\, x\,[j_0'(x) + A_0 h_0'(x)] + itb_t\, B_0 h_0(t) = (-i\omega)\frac{K'}{K}\,[b_c' x' A_0' j_0'(x') - it' b_t' B_0' j_0(t')]\,, \tag{3.3.21c}$$

(d) and radial stress

$$(-i\omega\rho_0 a^2)\,j_0(x) + \left[(-i\omega\rho_0 a^2)h_0(x) - 4\mu_0 x h_0'(x)\right]A_0 = \left\{(-\omega^2\rho_0' a^2)\,j_0(x') - 4\mu' x'\,j_0'(x')\right\}A_0' - \omega^2\rho_0' a^2 B_0' j_0(t') \tag{3.3.21d}$$

Note that the temperature condition (3.3.21b) is identical to the exact condition (2.3.3c).

For $n > 0$, as discussed previously, we drop the thermal boundary conditions, and the thermal mode terms in the boundary conditions. Therefore equations (3.3.19) become

(a) radial velocity

$$x\,[j_n'(x) + A_n h_n'(x)] - n(n+1)C_n h_n(s) = (-i\omega)\,[x' A_n' j_n'(x') - n(n+1)C_n' j_n(s')] \tag{3.3.22a}$$

(b) tangential velocity

$$j_n(x) + A_n h_n(x) - isC_n h_n(s) = (-i\omega)\,\{A_n' j_n(x') - C_n'\,[j_n(s') + s' j_n'(s')]\} \tag{3.3.22b}$$

(c) radial stress

$$[-i\omega\rho_0 a^2 + 2\mu_0 n(n+1)]\,j_n(x) - 4\mu_0 x j_n'(x) + \left[(-i\omega\rho_0 a^2 + 2\mu_0 n(n+1))h_n(x) - 4\mu_0 x h_n'(x)\right]A_n - 2\mu_0 isn(n+1)C_n h_n(s) = \left[(-\omega^2\rho_0' a^2 + 2\mu' n(n+1))\,j_n(x') - 4\mu' x'\,j_n'(x')\right]A_n' \tag{3.3.22c}$$

$$+ C_n' 2\mu' n(n+1)[j_n(s') - s' j_n'(s')]$$

(d) and tangential stress

$$\mu_0\{[xj_n'(x) - j_n(x)] + [xh_n'(x) - h_n(x)]A_n + (s^2 - n(n+1))C_n h_n(s)\}$$
$$= \mu'\{[x'j_n'(x') - j_n(x')]A_n' + C_n'[s'j_n'(s') - j_n(s')(-\frac{1}{2}s'^2 + n^2 + n - 1)]\} \qquad (3.3.22d)$$

3.3.2. Results For the Second Boundary Layer Approximation

We wish to examine the effects of the second boundary layer approximation on the different boundary conditions separately. Our computational procedure was therefore to take the set of exact boundary conditions (2.3.3), and replace one with its approximate counterpart from equations (3.3.21) or (3.3.22). Each computational run therefore involved one approximate and three exact boundary conditions.

The results for $n = 0$ are shown in Figure 3.10. The approximate radial velocity condition (3.3.21a) yields values for the attenuation which are too large in comparison with the exact case, but this difference decreases with increasing particle size and increasing frequency. This behaviour is expected because δ_t / a becomes smaller with increasing frequency and particle size. When the heat flux boundary condition is approximated, for small particle radii the quantities t and t' are so small (Tables 3.2 and 3.3) that the accuracy of the approximation is not expected to be good. In fact negative values of attenuation were obtained for the smallest particle at the lowest frequencies. However, at the high frequency end for $a = 0.044\mu$m, there is an indication of convergence with the exact case, and for $a = 0.653\mu$m, the approximate and exact results are nearly the same at high frequencies. The approximate radial stress is the same as was obtained in the first boundary layer approximation (Figure 3.9). The temperature condition is unaffected by the approximation for $n = 0$, so this result has to match the exact

case, and therefore is not plotted in Figure 3.10.

For $n = 1$ the radial stress boundary condition is approximated only in that the thermal mode terms have been dropped, and is not shown because it is then identical with the exact case, as previously mentioned. When we approximate the radial velocity boundary condition, for the small particle (Figure 3.11) we find a large difference which decreases for higher frequencies, and for the large particle we find a rapid convergence to the exact result, as expected. The approximate radial stress boundary condition produces negative attenuation for the small particle over the whole frequency range, and for the large particle (Figure 3.12) there is negative attenuation at the lower frequencies, but there is convergence towards the exact case at high frequencies. The tangential stress boundary condition, when approximated, yields poor agreement for the small particle, but agreement improves with increasing frequency for the large particle (see Figure 3.11). The results for $n = 1$ are poorer than the thermal approximations for $n = 0$ because, for the same frequency and particle size, the viscous boundary layer is 2-3 times thicker than the thermal boundary layer in the fluid.

The approximate boundary conditions for $n = 2$ produce good agreement with the exact case, except for the approximated tangential velocity condition. We obtain negative attenuation values for the small particle, but for the large particle rapid convergence to the exact case occurs as the frequency increases (Figure 3.13).

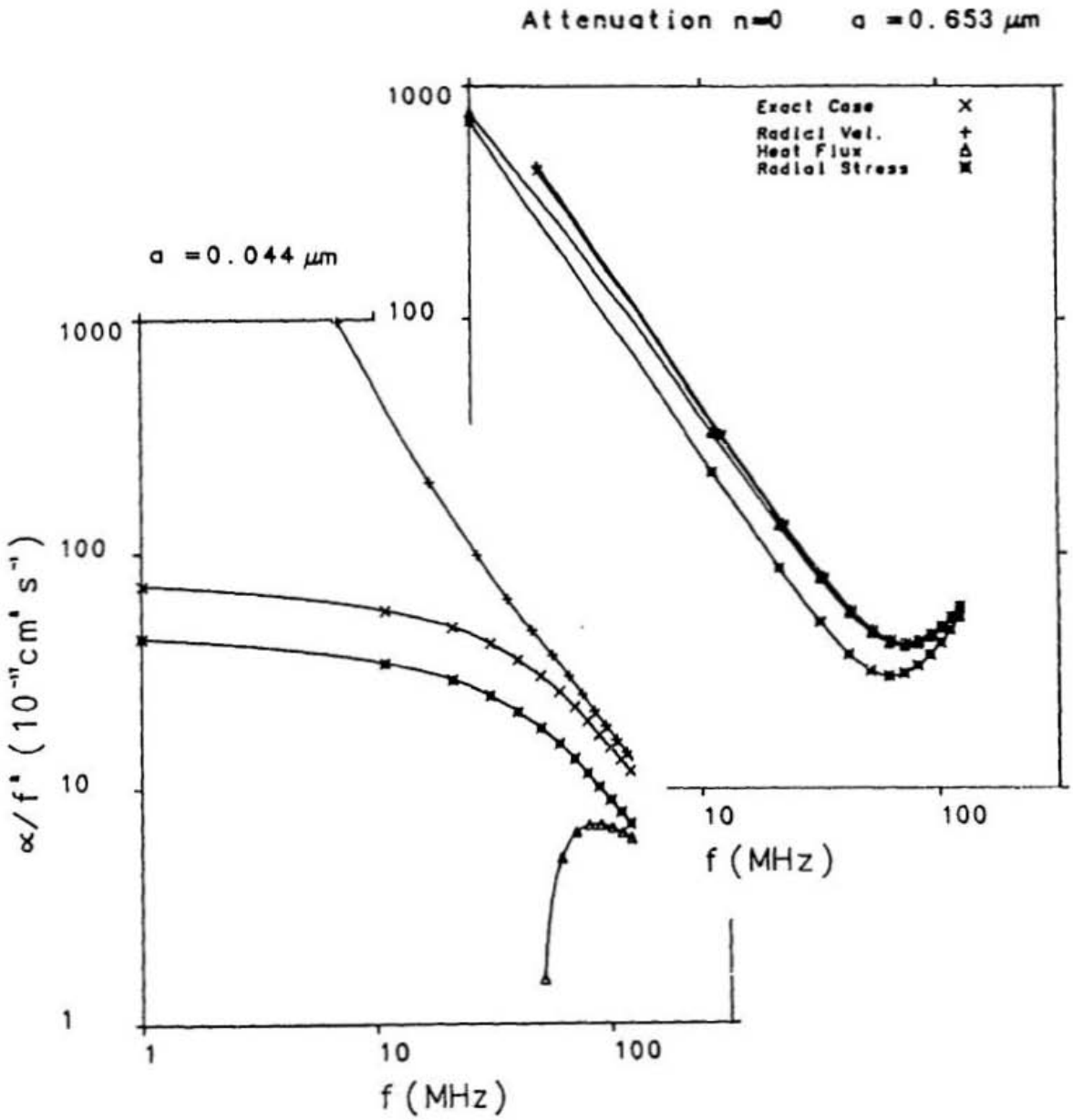

Figure 3.10. The $n = 0$ contribution to total attenuation, second boundary layer approximation, viscous conducting case, polystyrene spheres in water at 20 ^{0}C. Particle radii are given. The exact result (2.3.3), and the second boundary layer approximations (3.3.21) are shown.

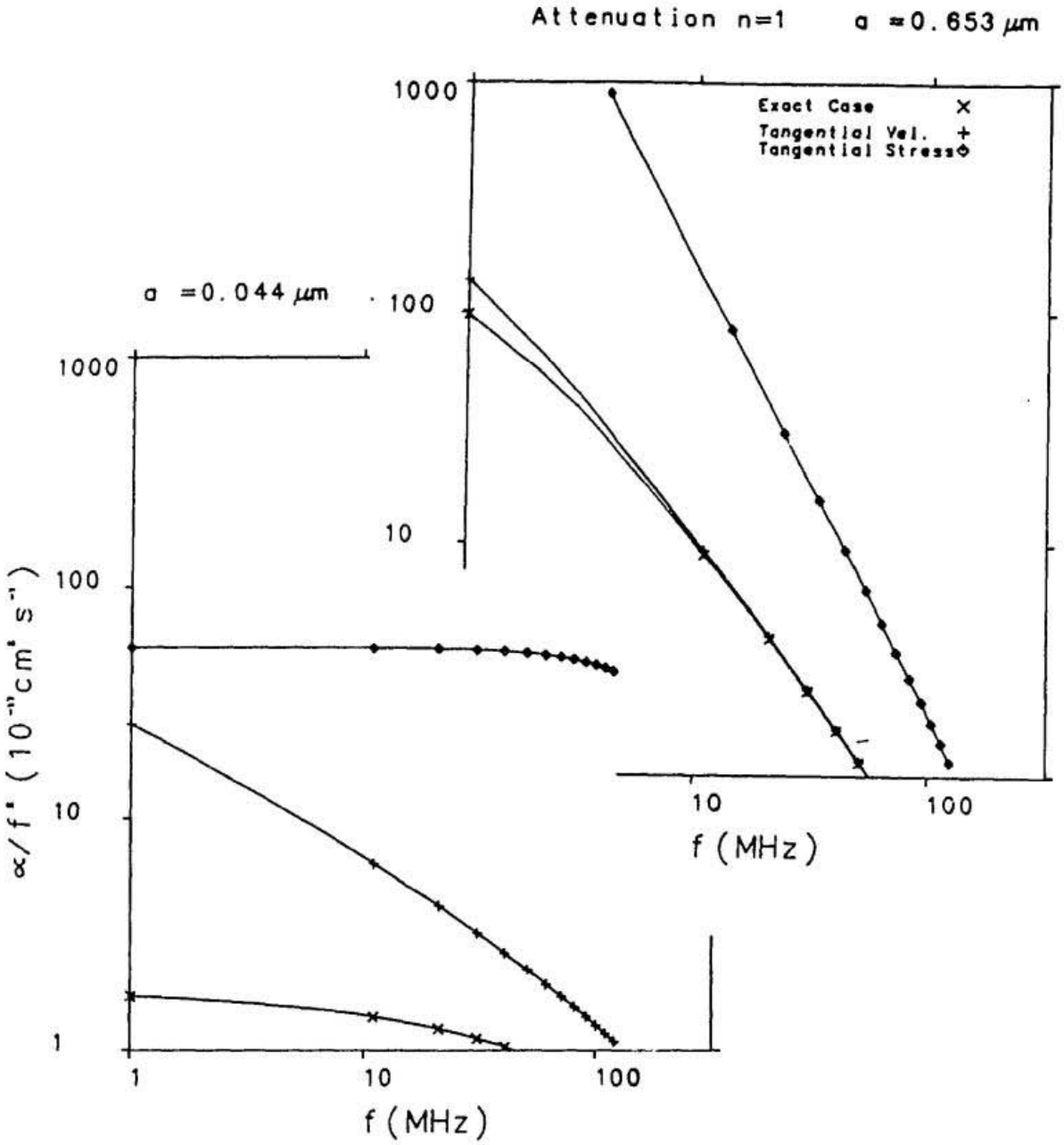

Figure 3.11. The $n = 1$ contribution to total attenuation, second boundary layer approximation, viscous conducting case, polystyrene spheres in water at 20 ^{0}C. Particle radii are given. The exact result (2.3.3), and the second boundary layer approximations (3.3.22) are shown, except for the approximate radial stress result.

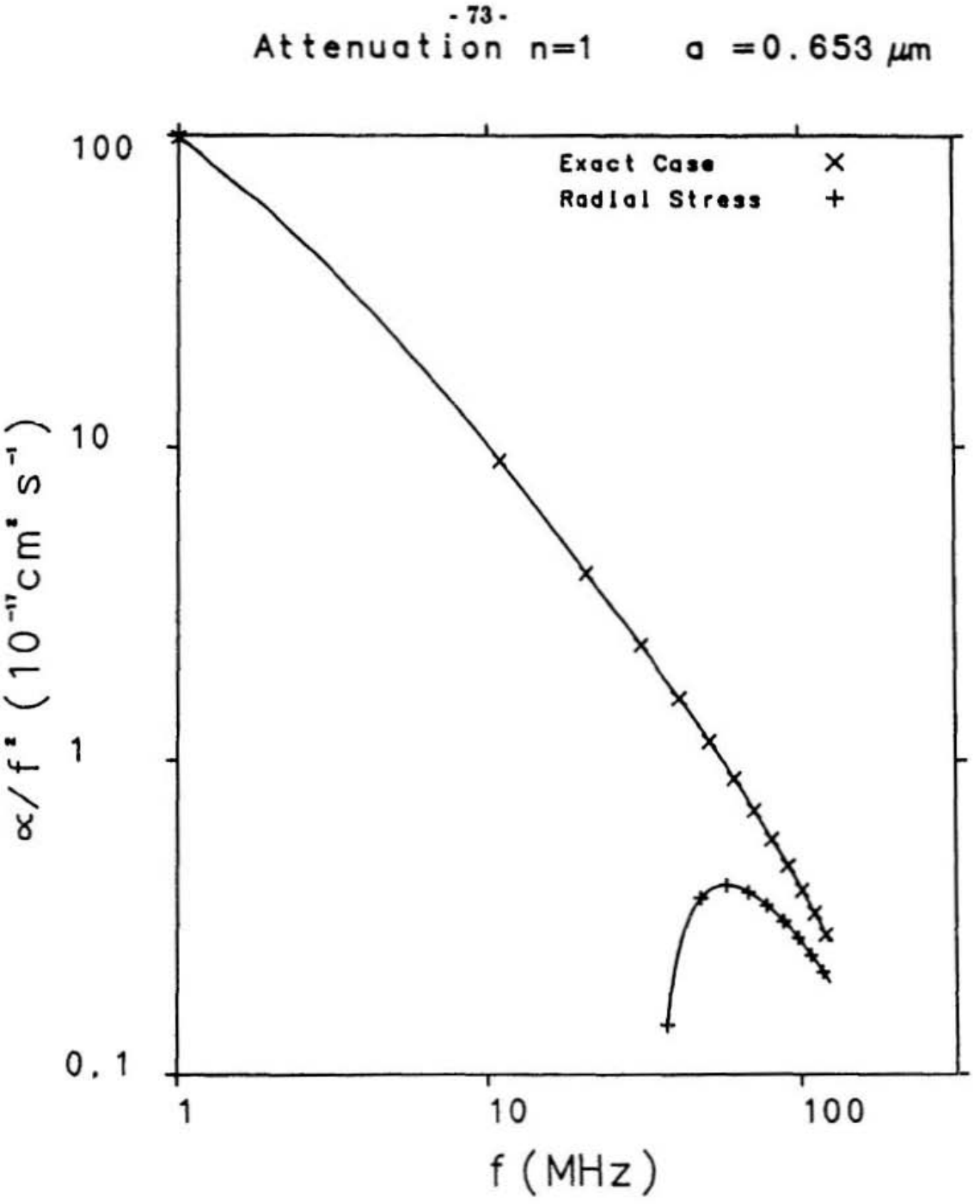

Figure 3.12. The $n = 1$ contribution to total attenuation, second boundary layer approximation, viscous conducting case, polystyrene spheres in water at 20 ^{0}C. Particle radii are given. The exact result (2.3.3), and the result of the second boundary layer approximation (3.3.22c) to the radial stress, are shown.

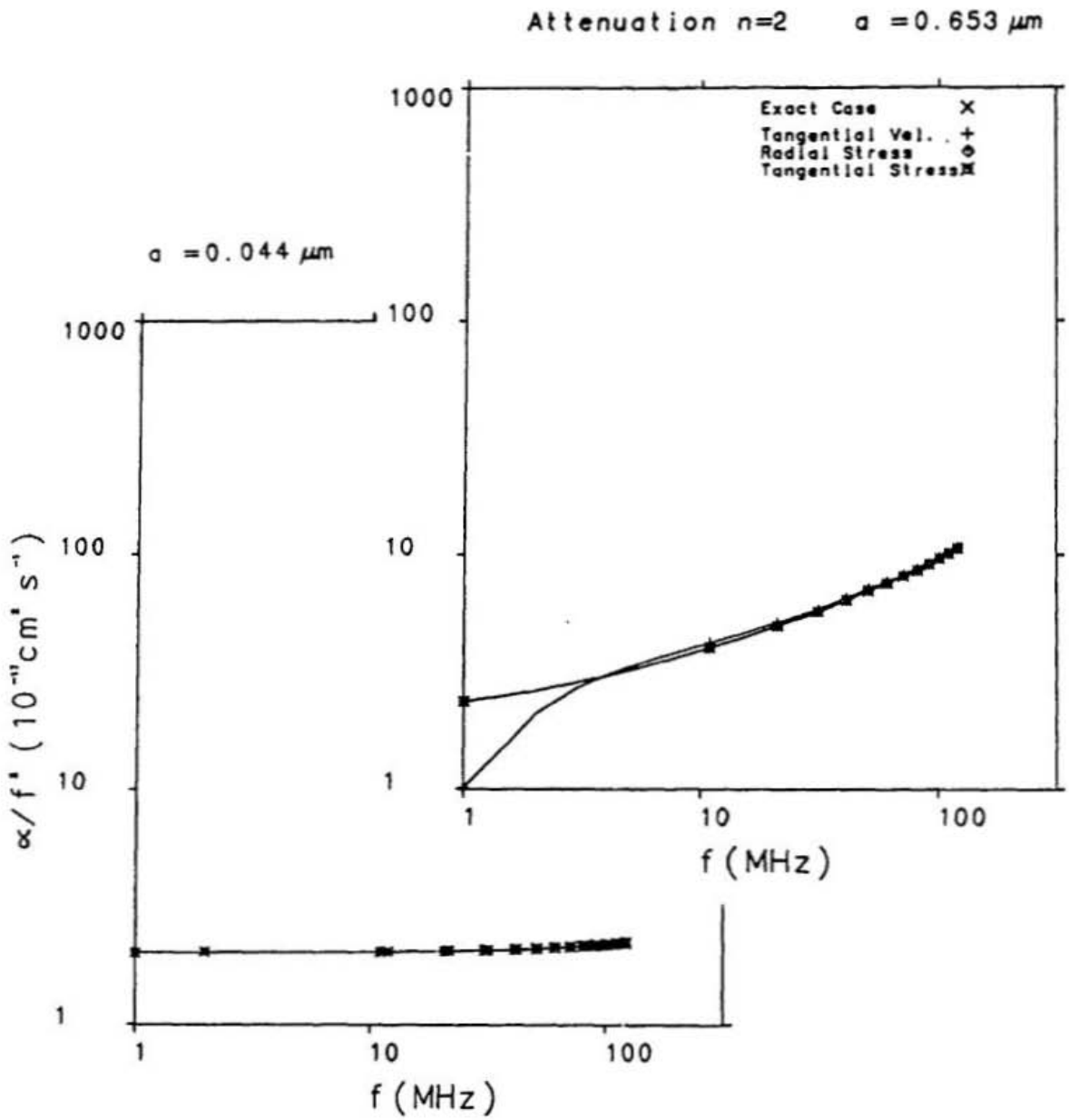

Figure 3.13. The $n = 2$ contribution to total attenuation, second boundary layer approximation, viscous conducting case, polystyrene spheres in water at 20 ^{0}C. Particle radii are given. The exact result (2.3.3), and the second boundary layer approximations (3.3.22) are shown.

CHAPTER 4 SUMMARY AND CONCLUSIONS

Boundary layer approximation techniques have been applied to the problem of sound scattering by an elastic, heat conducting sphere in a viscous, heat conducting fluid. The approximate results are compared to exact calculations, and to measurements of attenuation made by Allegra and Hawley [1972] in aqueous suspensions of polystyrene spheres at long wavelengths. Computations are therefore made only for the $n = 0, 1, 2$ in the partial wave expansion of the acoustic field.

Both the Allegra and Hawley [1972] and the Pierce [1981] modal decompositions of the acoustic field into compression and shear wave modes were used. In the fluid, this results in viscous shear waves and thermal compression waves in addition to the usual acoustic compression wave. In the solid, a thermal wave exists in addition to the usual elastic compression and shear waves. These modes are uncoupled to lowest order except at boundaries. Pierce's approach has been generalized here to include the solid case, and has been adapted to spherical geometry. The boundary conditions at the surface of a sphere obtained using the two modal separations are shown to be comparable in form. One of the main differences between the two approaches results from Pierce's assumption that the thermal wave in the fluid does not contribute significantly to the normal stress.

Pierce's modal decomposition has two main advantages. First, by not introducing vector and scalar potentials the governing equations are easier to interpret physically, and the relationships between different physical variables are clearer.

Second, the modal relations reveal the relative importance of the different field quantities in each modal wave. For example, the viscous wave has no first order effect on pressure, entropy, temperature, or density. The importance of this here is that some terms can be justifiably dropped from the boundary conditions at a fluid-solid interface.

To test the accuracy of our computational procedures prior to making any approximations, comparisons were made with Urick's [1948] result for rigid, movable particles in the viscous, non-heat-conducting case, and with the exact calculations made by Allegra and Hawley [1972] for polystyrene spheres. Good agreement was obtained with Urick [1948]. For the viscous conducting case, we were able to obtain equivalent results to those of Allegra and Hawley [1972], except that at high frequencies the contribution from the $n = 0$ term is lower in our case.

In general, solving for the attenuation coefficient in the viscous heat-conducting case involves solving six-by-six matrices, in which the matrix elements are the coefficients in the six boundary conditions for the nth-order partial waves. In order to simplify the computational problem, approximate forms for the boundary conditions were found by using boundary layer approximation techniques. Two types of boundary layer approximation were introduced. The so-called first boundary layer approximation involves only the radial stress in the fluid, and in the first instance all terms involving viscosity and heat conduction were removed. In the so-called second boundary layer approximation, radial gradients of the thermal and viscous waves are assumed to be large compared to their tangential gradients, and are scaled by the imaginary parts of their respective wavenumbers (which are the reciprocals of the corresponding boundary layer thicknesses).

For the first boundary layer approximation we obtained the following results. For $n = 2$, the agreement was good for the full frequency and particle

size range considered. The approximate attenuation for $n = 1$ was larger than the exact result, and the relative error increased with increasing frequency. By reintroducing the viscous terms for the incident wave, improved agreement was obtained. The results for $n = 1$ and $n = 2$ in the viscous conducting case and in the viscous non-conducting case are the same, indicating that thermal effects are unimportant for $n \geq 1$. This confirms the result derived in Section 3.1.5, which indicated that the thermal wave should be isotropic and therefore contribute only to the $n = 0$ term. The results for $n = 0$ in the first boundary layer approximation showed that in order to obtain a reasonable approximation to thermal absorption, it is necessary that the thermal pressure in the fluid be included in the radial stress, at least for polystyrene.

Next we consider the second boundary layer approximation, and consider the contribution of the various boundary conditions separately. For α_0, the approximate radial velocity condition yields values for the smallest particles which are too large, but converges to the exact result at high frequencies, and provides a good match for the larger particle size. The approximation for this boundary condition is in the thermal terms, and t and t' are too small for good accuracy, which accounts for the large difference at low frequencies for the small particle (see Tables 3.2-3). The temperature boundary condition involves no gradients, and therefore has no approximate form here. Heat flux, on the other hand, is approximated, and strongly depends on the values of t and t' being large. Since they are not at low frequencies for the smallest particle considered, we get poor agreement with the exact case in this size/frequency range. However, much better agreement is obtained for larger particles and higher frequencies. For the radial stress condition, the results are similar to the first boundary layer approximation: that is, the thermal terms in the fluid must be retained, although approximate forms of these terms may be used.

For $n \geq 1$ all thermal wave terms are dropped in the second boundary layer approximation, and an approximation is made to radial gradients of the viscous shear wave. When the boundary conditions for $n = 1$ are approximated, we find that the resultant attenuation converges towards the exact case for the larger particle as the frequency increases, which we expect. Although the approximate radial stress boundary condition in the second boundary layer approximation produces an attenuation coefficient that converges as the boundary layer thickness decreases, the approximate radial stress in the fluid in the first boundary layer approximation results in much better agreement with the exact case. Why the first boundary layer approximation produces better agreement with the exact case for the attenuation is not clear, and merits further research. The approximation for $n = 2$ produces good agreement with the exact case, except for the attenuation due to modifying the tangential stress boundary condition, and even this converges for the large particle for increasing frequency.

In the Pierce approach $p_t \approx 0$, which results in no thermal terms in the radial stress boundary condition in the fluid. But we have shown in both the first and second boundary layer approximation that neglecting thermal terms decreases the attenuation, and that (in the first boundary layer approximation) when thermal terms are reintroduced into the fluid radial stress, reasonably good agreement with the exact result is obtained. This approximation is also the major difference between the boundary conditions of Allegra and Hawley, and Pierce. The rationale was that p_t, within the thermal mode, was negligible, and thus was neglectable overall. In order to obtain a better scaling for p_t, the boundary conditions could be solved explicitly, but this was not the objective here. This would be a potential area for further work.

To conclude, thermal effects are important only in the $n = 0$ term of the attenuation, and the viscous nonconducting treatment is sufficient elsewhere, at

least for polystyrene in water. A good approximation for the radial stress in the fluid for $n = 1$ requires that the radial stress due to the incident wave be unchanged, and the reason for this is not fully understood. The approximation $p_t \approx 0$ in the $n = 0$ radial stress did not work well for the data set considered. Additional measurements using larger particles over a similar frequency range would provide a useful test of the boundary layer approximation as larger values of n become important with increasing $k_c a$.

REFERENCES

Abramowitz, M. and Stegun, I.A., *Handbook of Mathematical Functions* , National Bureau of Standards, Applied Mathematics Series, Dover, **55** , 1968.

Allegra, J.R., *Theoretical and Experimental Investigation of the Attenuation of Sound In Suspensions and Emulsions* , Ph.D. thesis, Phys. Dept., Harvard Univ., Cambridge, Mass., 1970.

Allegra, J. R. and S. A. Hawley, Attenuation of Sound in Suspensions and Emulsions: Theory and Experiment, *J. Acoust. Soc. Am.* , **51** , 1545-1564, 1972.

Arfken, G., *Mathematical Methods For Physicists* , Second Edition, Academic Press, New York, 1970, 815 pp.

Batchelor, G.K., *An Introduction To Fluid Dynamics* , Cambridge University Press, Cambridge, 353-355, 1967, 614 pp.

Davis, M.C., Attenuation of Sound In Highly Concentrated Suspensions and Emulsions, *J. Acoust. Soc. Am.* , **65** , 387-390, 1979.

Epstein, P.S. and Carhart, R.R., The Absorption of Sound In Suspensions and Emulsions. I. Water Fog In Air,*J. Acoust. Soc. Am.* , **25**, 553-565, 1953.

Faran, J.J. Jr., Sound Scattering By Solid Cylinders and Spheres, *J. Acoust. Soc. Am.* , **23,** 405-418, 1951.

Hawley, S.A., *Ultrasonic Absorption In Aqueous Suspensions of Small Elastic Particles* , Ph.D. thesis, Dept. Biophys., Univ. of Illinois, Urbana, Ill., 1967.

Hay, A. E. and R. W. Burling, On Sound Scattering and Attenuation in Suspensions. with Marine Applications, *J. Acoust. Soc. Am.*, **72,** 950-959, 1982.

Hay, A.E. and Mercer, D.G., A Note on the Viscous Attenuation of Sound In Suspensions,*J. Acoust. Soc. Am.* , **85**, 2215-2216, 1989.

Hay, A. E. and Mercer, D.G., On the Theory of Sound Scattering and Viscous Absorption in Aqueous Suspensions at Medium and Short Wavelengths, *J. Acoust. Soc. Am.*, **78** , 1761-1771, 1985.

Hickling, R., Analysis of Echoes From a Solid Elastic Sphere In Water, *J. Acoust. Soc. Am.*, **34,** 1582-1592, 1962.

Hickling, R., and Wang, N.M., Scattering of Sound By a Rigid Movable Sphere, *J. Acoust. Soc. Am.* , **39**, 276-279, 1966.

Isakovitch, M.A., *Zh. Eksperim. i Teor. Fiz., 18*, 907, 1948.

Lamb, H., *Hydrodynamics*, Sixth Editition, Dover, New York, 1945, 738 pp.

Landau, L.D., and Lifshitz, E.M., *Theory of Elasticity*, Third Edition, Pergamon Press, Great Britain, 1986, 187 pp.

Morse, P.M., *Vibration and Sound*, American Institute of Physics for the Acoustical Society of America, U.S., 1986, 468 pp.

Morse, P.M. and Ingard, K.U., *Theoretical Acoustics*, McGraw-Hill, New York, 1968, 927 pp.

Neubauer, W.G., Vogt, R.H., and Dragonette, L.R., Acoustic Reflection from Elastic Spheres. I. Steady-State Signals, *J. Acoust. Soc. Am.*, **55**, 1123-1129, 1974.

Pierce, A.D., *ACOUSTICS: An Introduction to Its Physical Principles and Applications*, McGraw-Hill, New York, 1981, 642 pp.

Prandtl, L., *Verhandlungen des dritten internationalin Mathematiker-Kongresses*, (Heidelberg 1904), Leipzig, 484-491, 1905.

Rayleigh, Lord (J.W. Strutt), *Theory of Sound*, volume 2, Second Edition, Dover, New York, 1945, 504 pp.

Schlichting, H., *Boundary-Layer Theory*, Sixth Edition, McGraw-Hill, New York, 1968, 747pp.

Tritton, D.J., *Physical Fluid Dynamics*, Van Nostrand Reinhold, Cambridge, 1977, 362 pp.

Truesdell, C., Precise Theory of the Absorption and Dispersion of Forced Plane Infinitesimal Waves According To the Navier-Stokes Equation, *J. Ration. Mech. Anal.*, **2**, 643-730, 1953.

Urick, R.J., The Absorption of Sound In Suspensions of Irregular Particles, *J. Acoust. Soc. Am.*, **20**, 283-289, 1948.

Appendix 1 Linearisation of Governing Equations

We consider the governing equations for the solid (2.1.1); conservation of mass,

$$\frac{\partial \rho'}{\partial t} + \vec{\nabla} \cdot (\rho' \dot{\vec{u}}) = 0 \qquad \text{A1.1a}$$

conservation of momentum,

$$\rho' \ddot{u}_j + \rho' (\dot{\vec{u}} \cdot \vec{\nabla}) \dot{u}_j = \frac{\partial \sigma'_{ij}}{\partial x_i} \qquad \text{A1.1b}$$

and conservation of energy,

$$\rho' \frac{\partial U'}{\partial t} + \rho' \dot{u}_i \frac{\partial U'}{\partial x_i} + p' \vec{\nabla} \cdot \dot{\vec{u}} \qquad \text{A1.1c}$$

$$= \Phi + K' \nabla^2 T'$$

We assume that any motion in the solid is a small perturbation from an equilibrium state of no motion, and express the seven unknowns as

$$\rho' = \rho_0' + \rho_1' \qquad \text{A1.2a}$$

$$p' = p_0' + p_1' \qquad \text{A1.2b}$$

$$T' = T_0' + T_1' \qquad \text{A1.2c}$$

$$U' = U_0' + U_1' \qquad \text{A1.2d}$$

$$\vec{u} = \vec{u}_0 + \vec{u}_1 \qquad \text{A1.2e}$$

where the subscript 0 denotes the equilibrium value of the appropriate variable, and where the subscript 1 refers to the perturbation from equilibrium of that quantity. We further assume that the solid is homogeneous and isotropic.

Now we consider the conservation of mass equation A1.1a, which we may rewrite

$$\frac{\partial \rho'}{\partial t} + \rho' \vec{\nabla} \cdot \dot{\vec{u}} + \dot{\vec{u}} \cdot \vec{\nabla} \rho' = 0 \qquad \text{A1.3a}$$

We now substitute the density, pressure, and displacement from A1.2a, A1.2b, and A1.2e, respectively, into A1.3a to obtain

$$\frac{\partial}{\partial t}(\rho_0' + \rho_1') + (\rho_0' + \rho_1')\vec{\nabla} \cdot (\dot{\vec{u}}_0 + \dot{\vec{u}}_1) + (\dot{\vec{u}}_0 + \dot{\vec{u}}_1) \cdot \vec{\nabla}(\rho_0' + \rho_1') = 0 \qquad \text{A1.3b}$$

First we note that $\dot{\vec{u}}_0$ and $\frac{\partial \rho_0'}{\partial t}$ are zero since the equilibrium state is not time-dependent. Next we expand to first order in small quantities, noting that $\vec{\nabla}\rho_0'$ is zero by homogeneity, and obtain

$$\frac{\partial \rho_1'}{\partial t} + \rho_0' \vec{\nabla} \cdot \dot{\vec{u}}_1 = 0 \qquad \text{A1.4}$$

Next we consider the conservation of momentum equation (A1.1b). We consider the stress tensor explicitly, using the form (2.1.2c)

$$\sigma_{ij}' = -p'\delta_{ij} + \mu' \left\{ \frac{\partial u_i}{\partial x_j} + \frac{\partial u_j}{\partial x_i} - \frac{2}{3}\frac{\partial u_i}{\partial x_i}\delta_{ij} \right\} \qquad \text{A1.5}$$

$$= -(p_0' + p_1')\delta_{ij} + \mu' \left\{ \frac{\partial u_{0,i}}{\partial x_j} + \frac{\partial u_{0,j}}{\partial x_i} - \frac{2}{3}\frac{\partial u_{0,i}}{\partial x_i}\delta_{ij} \right\}$$

$$+ \mu' \left\{ \frac{\partial u_{1,i}}{\partial x_j} + \frac{\partial u_{1,j}}{\partial x_i} - \frac{2}{3}\frac{\partial u_{1,i}}{\partial x_i}\delta_{ij} \right\}$$

We substitute this into the momentum equation A1.1b.

To zero order in small quantities the momentum equation becomes

$$\rho_0' \ddot{u}_{0,j} + \rho_0' \dot{\vec{u}}_0 \cdot \vec{\nabla} \dot{u}_{0,j} \qquad \text{A1.6}$$

$$= \frac{\partial}{\partial x_j} \left\{ -p_0'\delta_{ij} + \mu' \left[\frac{\partial u_{0,i}}{\partial x_j} + \frac{\partial u_{0,j}}{\partial x_i} - \frac{2}{3}\frac{\partial u_{0,i}}{\partial x_i}\delta_{ij} \right] \right.$$

Time independance eliminates the left side. The pressure p_0' is the same throughout the solid and thus has no gradient. Isotropy eliminates the non-diagonal ($i <> j$) terms in square brackets There are no diagonal terms in the brackets because the tensor quantity in the brackets is defined so as to be traceless [Landau and Lifshitz, 1986, p.10]. Therefore the equilibrium momentum equation drops out as expected.

To first order in perturbation quantities we obtain

$$\rho_0' \ddot{u}_{1,j} = \qquad \text{A1.7a}$$

$$\frac{\partial}{\partial x_j} \left\{ -p_1'\delta_{ij} + \mu' \left[\frac{\partial u_{1,i}}{\partial x_j} + \frac{\partial u_{1,j}}{\partial x_i} - \frac{2}{3}\frac{\partial u_{1,i}}{\partial x_i}\delta_{ij} \right] \right\}$$

or in vector notation

$$\rho_0' \ddot{\mathbf{u}}_1 = -\vec{\nabla} p_1' + \frac{\mu'}{3} \vec{\nabla} (\vec{\nabla} \cdot \mathbf{u}_1) + \mu' \nabla^2 \mathbf{u}_1 \qquad \text{A1.7b}$$

Finally we consider the energy equation A1.1c. Expanding as before we obtain

$$(\rho_0' + \rho_1')\frac{\partial}{\partial t}(U_0' + U_1') + (p_0' + p_1)\vec{\nabla}\cdot(\dot{\mathbf{u}}_0 + \dot{\mathbf{u}}_1) \qquad \text{A1.8}$$
$$= \Phi + K'\nabla^2(T_0' + T_1')$$

Zero order terms again vanish, and to first order we find

$$\rho_0'\frac{\partial U_1'}{\partial t} + p_0'\vec{\nabla}\cdot\dot{\mathbf{u}}_1 = K'\nabla^2 T_1' \qquad \text{A1.9}$$

The viscous dissipation function Φ is a function of velocities [Landau and Lifshitz, 1986, p.137], and therefore $\mathbf{u}_0$ is eliminated from it. Also, the viscous dissipation function is composed of terms to second order in velocities, and therefore is eliminated from the first order equation A1.9.

A similar decomposition can be made for the fluid governing equations. We eliminate the subscript 1 for perturbation results from the remainder of the thesis, but retain the subscript 0, which represents equilibrium quantities.

Appendix 2 Derivation of Helmholtz Equations

Here we show, for the fluid case, how to obtain (2.1.12) using vector and scalar potentials (2.1.8). The same procedure will yield equivalent results for the solid case.

Introducing (2.1.8) into (2.1.7a) results in

$$-\omega^2 \vec{\nabla}\bar{\phi} - \left(\frac{c^2}{\gamma} - \frac{i\omega\mu_0}{3\rho_0} \right) \vec{\nabla}(\nabla^2 \bar{\phi}) + i\omega \frac{\mu_0}{\rho_0} \nabla^2 (\vec{\nabla}\bar{\phi}) + i\omega \frac{c^2\beta}{\gamma} \vec{\nabla} T$$
$$= i\omega \frac{\mu_0}{\rho_0} \left[i\omega \frac{\mu_0}{\rho_0} \vec{\nabla}\times\vec{A} + \nabla^2 (\vec{\nabla}\times\vec{A}) \right] \qquad \text{A2.1}$$

Both sides of (A2.1) vanish separately, yielding

$$\nabla^2 (\vec{\nabla}\times\vec{A}) + i\omega \frac{\rho_0}{\mu_0} \vec{\nabla}\times\vec{A} = 0 \qquad \text{A2.2}$$

and

$$\vec{\nabla} \left\{ -\omega^2 \bar{\phi} - \left(\frac{c^2}{\gamma} - i\omega \frac{4}{3} \frac{\mu_0}{\rho_0} \right) \nabla^2 \bar{\phi} + i\omega \frac{c^2\beta}{\gamma} T \right\} = 0 \qquad \text{A2.3}$$

Consider A2.2 first. Recalling that (Arfken, 1970, p. 42)

$$\nabla^2 (\vec{\nabla}\times\vec{A}) = \vec{\nabla} [\vec{\nabla} \cdot (\vec{\nabla}\times\vec{A})] - \vec{\nabla}\times[\vec{\nabla}\times(\vec{\nabla}\times\vec{A})] \qquad \text{A2.4}$$

The first term on the right hand side clearly vanishes, therefore A2.2 reduces to

$$\vec{\nabla}\times\vec{\nabla}\times\vec{A} - i\omega \frac{\rho_0}{\mu_0} \vec{A} = 0 . \qquad \text{A2.5}$$

Recalling that $\vec{A} = (0, 0, A_\phi)$ and that by symmetry there is no ϕ dependance, we obtain the following using the separation of variables technique (Arfken, 1970, pp. 87, 383):

$$A_\phi = - \sum_{n=0}^{\infty} i^n (2n + 1) C_n h_n(k_s r) \frac{dP_n(\cos\theta)}{d\theta} \qquad \text{A2.6}$$

where $k_s^2 = i\omega\rho_0/\mu_0$.

Taking the divergance of (A2.5) yields

$$\vec{\nabla} \cdot \vec{A} = 0 \qquad \text{A2.7}$$

and combining this with the identity used in (A2.4) on (A2.5) gives

$$\nabla^2 \vec{A} + k_s^2 \vec{A} = 0 \qquad \text{A2.8}$$

Therefore equation (A2.5) requires that (A2.7) be satisfied, and that although $\vec{A}$ satisfies the Helmholtz equation, we obtain $dP_n/d\theta$ instead of P_n in our series expansion (A2.6).

From (A2.3) we have

$$T = \frac{\gamma}{i\omega c^2 \beta}\left[\omega^2 \bar{\phi} + \left(\frac{c^2}{\gamma} - i\omega \frac{4}{3}\frac{\mu_0}{\rho_0}\right)\nabla^2 \bar{\phi}\right]. \qquad \text{A2.9}$$

then we substitute (2.1.8) with (2.1.7b), obtaining

$$\frac{(\gamma - 1)}{\beta}\nabla^2 \bar{\phi} + i\omega T + \gamma\sigma\nabla^2 T = 0. \qquad \text{A2.10}$$

Eliminating T from (A2.9) and (A2.10), we obtain the following biquadratic equation

$$(\nabla^2 + k_c^2)(\nabla^2 + k_t^2)\bar{\phi} = 0 \qquad \text{A2.11}$$

where k_c^2 and k_t^2 are equations (2.1.13) and (2.1.14), respectively. It is easily shown that $k_c^2 \neq k_t^2$ and thus we get two solutions ϕ_c and ϕ_t corresponding to k_c and k_t respectively, such that

$$\bar{\phi} = \phi_c + \phi_t , \qquad \text{A2.12}$$

$$(\nabla^2 + k_c^2)\phi_c = 0 , \qquad \text{A2.13}$$

$$(\nabla^2 + k_t^2)\phi_t = 0 , \qquad \text{A2.14}$$

where each of the above solutions have the form

$$\phi = \sum_{n=0}^{\infty} i^n (2n + 1) D_n h_n(kr) P_n(\cos\theta) \qquad \text{A2.13}$$

and where the terms D_n are constants.

Thus we get the three Helmholtz equations (2.1.12) and indicate why the series solution for the vector potential differs in form from those for the scalar solution.

Appendix 3 Derivation of v_t Polarization Relationship

We are required to show that for the entropy mode in section (2.1.2), that the thermal velocity is not negligible, and is in fact equal to

$$\vec{v}_t = \left[\frac{\beta T_0 K}{\rho_0 C_p^2}\right] \nabla S_t \qquad \text{A3.1}$$

Using (2.1.26b) and setting $p \approx 0$ is insufficient, since $|\vec{k}|$ is large, and thus we need more care. By $|\vec{k}|$ being large, we mean that the relation $k^2 = i\omega\rho_0 C_p / K$ allows the possibility that $|\nabla s_t| >> (\omega/c)\,|s_t|$. Take equation (2.1.27b) and substitute this into (2.1.26b), obtaining

$$\begin{aligned} -i\omega\rho_0 (\omega\rho_0 + i(4/3)\mu_0 k^2)\vec{v} &= -i\vec{k}\dot{p}\ (\omega\rho_0 + i(4/3)\mu_0 k^2) \\ &\quad - \mu_0[k^2(\omega\rho_0 + i(4/3)\mu_0 k^2)\vec{v} - \vec{k}\dot{p}\,[(1/3)\mu_0 k^2] \end{aligned} \qquad \text{A3.2}$$

which reduces to

$$(\omega\rho_0 + i\omega(4/3)\mu_0 k^2)\vec{v} = \vec{k}\dot{p}\ . \qquad \text{A3.3}$$

Then using the modal relation (2.1.33b)

$$\beta\frac{\dot{p}}{\rho_0} = (\gamma - 1)(\epsilon_t - \epsilon_s)\,\dot{S} \qquad \text{A3.4}$$

where ϵ_s and ϵ_t are defined by (2.1.30), the relation

$$X = -\frac{1}{\epsilon_t} \qquad \text{A3.5}$$

and the relation

$$\gamma - 1 = \frac{\beta^2 T_0 c^2}{C_p}\ . \qquad \text{A3.6}$$

We substitute A3.5 into A3.3 to obtain

$$(\omega\rho_0 + i\frac{4}{3}\mu_0 k^2)\vec{v} = \frac{\rho_0}{\beta}(\gamma - 1)(\epsilon_t - \epsilon_s)\dot{S}\vec{k}\ . \qquad \text{A3.7}$$

The trick here is to make

$$\frac{(\rho_0/\beta)(\gamma-1)(\epsilon_t - \epsilon_s)}{(\omega\rho + i\frac{4}{3}\mu_0 k^2)} = \frac{i\beta T_0 K}{\rho_0 C_p^2}\ . \qquad \text{A3.8}$$

For convenience, calling the left hand side (LHS), we get

$$LHS = \frac{\rho_0(\epsilon_t - \epsilon_s)}{(\omega\rho_0 + i\frac{4}{3}\mu_0 k^2)} \frac{\beta^2 T_0 c^2}{C_p} \qquad \text{A3.9}$$

$$= \frac{\beta T_0 \omega}{C_p} \frac{(\epsilon_t - \epsilon_s)}{\left(\frac{\omega^2}{c^2} + i\frac{4}{3}\frac{\mu_0 \omega}{\rho_0 c^2} k^2\right)}$$

$$= \frac{\beta T_0 \omega}{C_p} \frac{(\epsilon_t - \epsilon_s)}{\left(\frac{k^2}{X} + \epsilon_s k^2\right)}$$

$$= \frac{\beta T_0 \omega}{C_p k^2} \frac{(\epsilon_t - \epsilon_s)}{(\epsilon_s - \epsilon_t)}$$

and using A3.5 we get that

$$LHS = \frac{iK\beta T_0}{\rho_0 C_p^2} . \qquad \text{A3.10}$$

Therefore we obtain the relation A3.1.

Appendix 4 Error in Allegra's Solution of Kirchhoff's Dispersion Relation

The positive root from (2.1.43), to low order in ϵ_t', is

$$\frac{1}{X'_+} = 1 + \epsilon_s' - \gamma'\epsilon_t' + \frac{\epsilon_t'(1 + \gamma'\epsilon_s')}{1 + \epsilon_s' - \gamma'\epsilon_t'} \qquad \text{A4.1}$$

Since ϵ_t' is small, then

$$1/X'_+ \approx 1 + \epsilon_s' - \gamma'\epsilon_t' + \frac{\epsilon_t'(1 + \gamma'\epsilon_s')}{1 + \epsilon_s'} \qquad \text{A4.2}$$

Since $\gamma' \approx 1$ then $1 + \gamma'\epsilon_s' \approx 1 + \epsilon_s'$ and

$$\frac{1}{X'_+} \approx 1 + \epsilon_s' - \epsilon_t'(\gamma'\epsilon_s' - 1)\,, \qquad \text{A4.3}$$

which is Allegra's result. The difference between this and our result lies in writing

$$\frac{1 + \gamma'\epsilon_s'}{1 + \epsilon_s'} = \gamma' - \frac{(\gamma' - 1)}{1 + \epsilon_s'} \qquad \text{A4.4}$$

or

$$= 1 + \frac{(\gamma' - 1)\epsilon_s'}{1 + \epsilon_s'} \qquad \text{A4.5}$$

Allegra seems to have ignored the second term of equation A4.5. If we make no other approximations except for small ϵ_t', we get equation A4.4, which can be markedly different. In our treatment we will use A4.4, and our result is

$$\frac{1}{X'_+} \approx 1 + \epsilon_s' - \frac{\epsilon_t'(\gamma' - 1)}{1 + \epsilon_s'}\,. \qquad \text{A4.6}$$

Appendix 5 Thermal Dispersion Relationship for Solid

We need to start with the negative root of the Kirchhoff dispersion equation. This is

$$\frac{1}{X'_-} \approx -\epsilon_t' \left(\frac{1 + \gamma' \epsilon_s'}{1 + \epsilon_s'} \right) \qquad \text{A5.1}$$

which reduces to

$$k'^2 \approx \left(\frac{i\omega}{\sigma'} \right) \left(\frac{1 + \epsilon_s'}{1 + \gamma' \epsilon_s'} \right) \qquad \text{A5.2}$$

$$\approx \frac{i\omega}{\sigma'} \frac{c'^2}{c_1'^2 [1 + e + (\gamma' - 1)\epsilon_s']}$$

which reduces to

$$\approx \frac{i\omega}{\sigma'} \left[\frac{1}{1 + (\gamma' - 1) e \frac{c_1'^2}{c'^2}} \right]$$

If the second term in the denominator is small, which is true for the materials of interest to us, then equation A5.2 becomes, to first order in small quantities

$$k'^2 \approx \frac{i\omega}{\sigma'} \left[1 - (\gamma' - 1)\epsilon_s' \frac{c_1'^2}{c'^2} \right] \qquad \text{A5.3}$$

which becomes to lowest order in small quantities

$$k'^2 \approx \frac{i\omega}{\sigma'} \qquad \text{A5.4}$$

We call this the thermal wavenumber, and write it k'_t.

Appendix 6 Allegra and Hawley [1972] Attenuation Data Set

The following five figures, presented by Allegra and Hawley [1972], show experimental results and theoretical calculations of sound attenuation by small polystyrene spheres in water. Figure A6.4 has experimental data for a heterodisperse suspension of particles with a mean particle radius of 0.110 μm. The other four figures have experimental data for monodisperse suspensions.

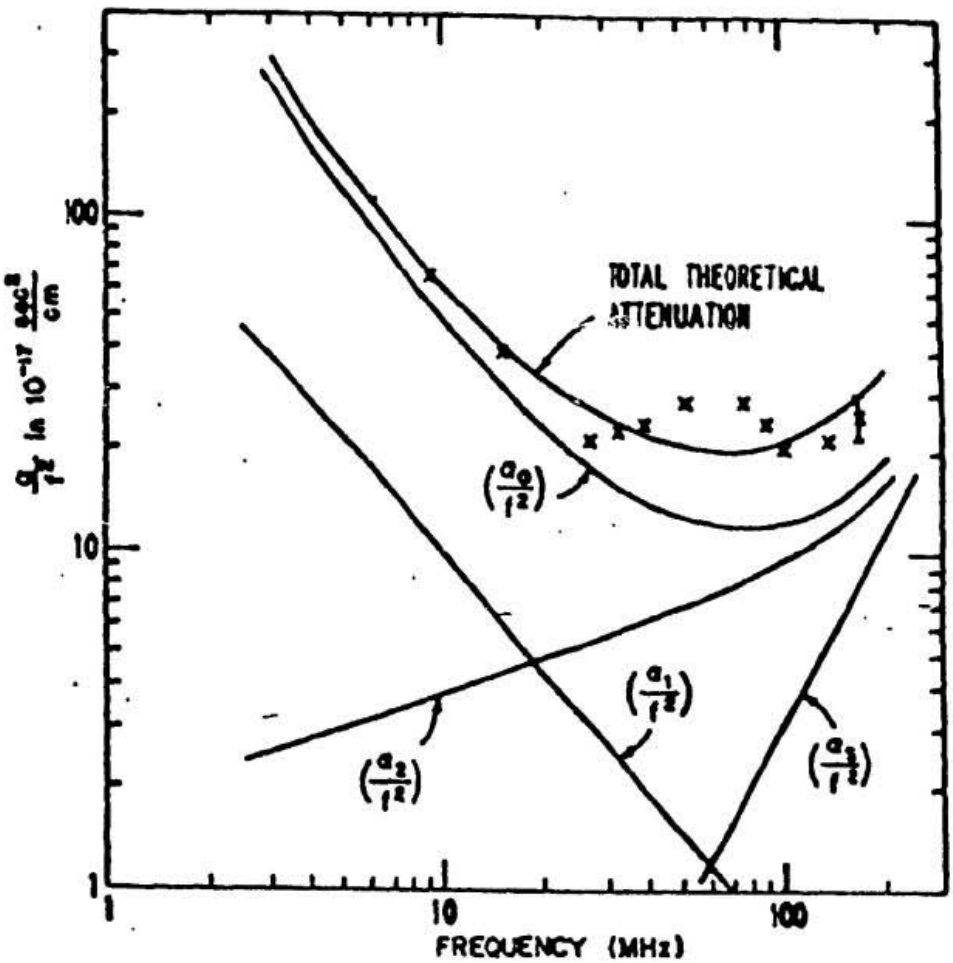

Figure A6.1. Excess attenuation versus frequency for an aqueous suspension of polystyrene spheres at 20° C, $a = 0.653\ \mu m$. Points are measured excess attenuation . [Allegra and Hawley, 1972]. α_s is the attenuation due to scattering alone.

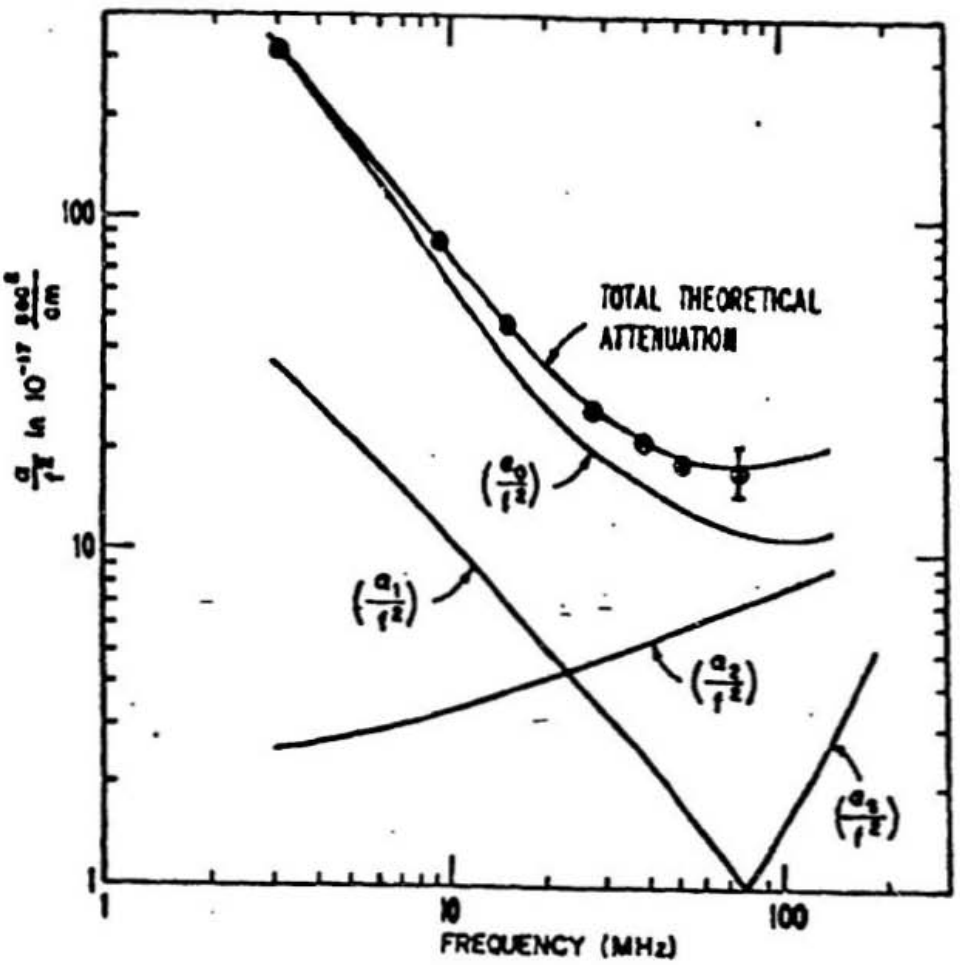

Figure A6.2. Excess attenuation versus frequency for an aqueous suspension of polystyrene spheres at 20° C, $a = 0.504\ \mu m$. Points are measured excess attenuation . [Allegra and Hawley, 1972]. α_s is the attenuation due to scattering alone.

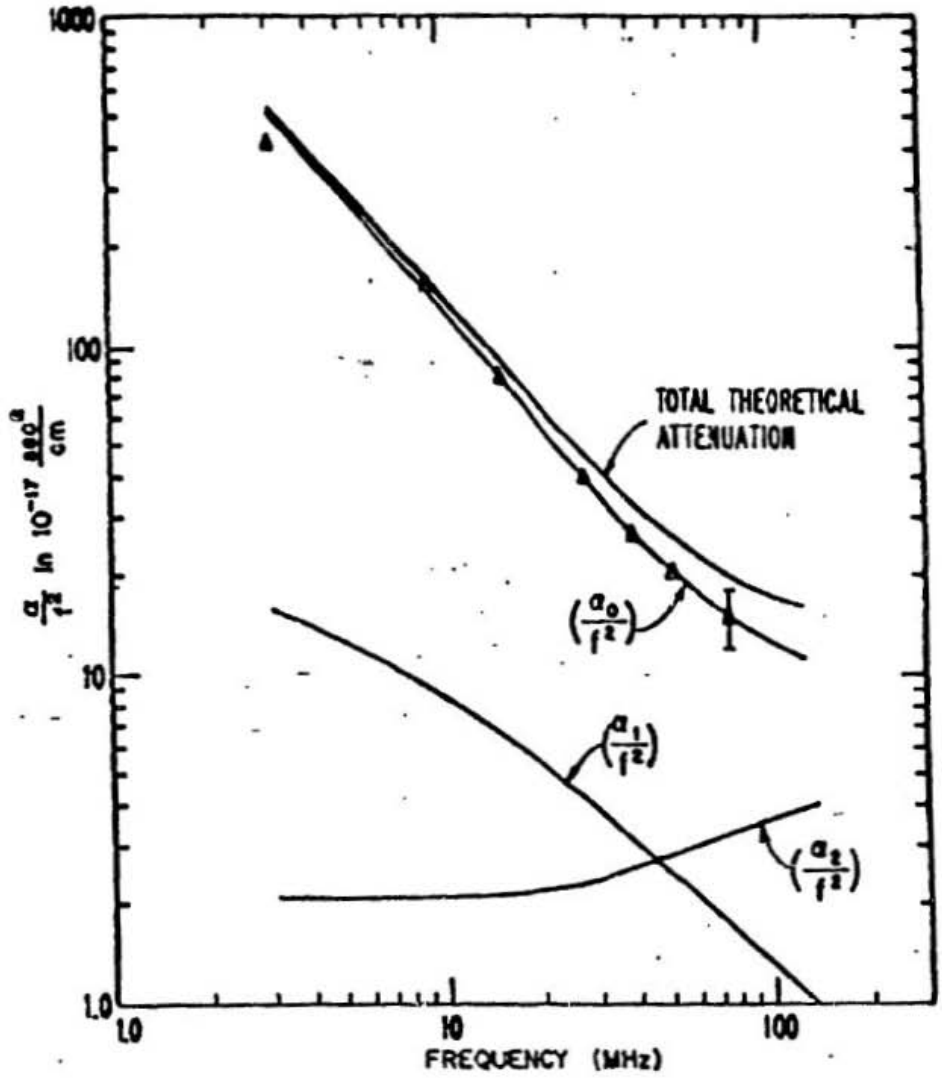

Figure A6.3. Excess attenuation versus frequency for an aqueous suspension of polystyrene spheres at 20° C, $a = 0.178\ \mu m$. Points are measured excess attenuation . [Allegra and Hawley, 1972].

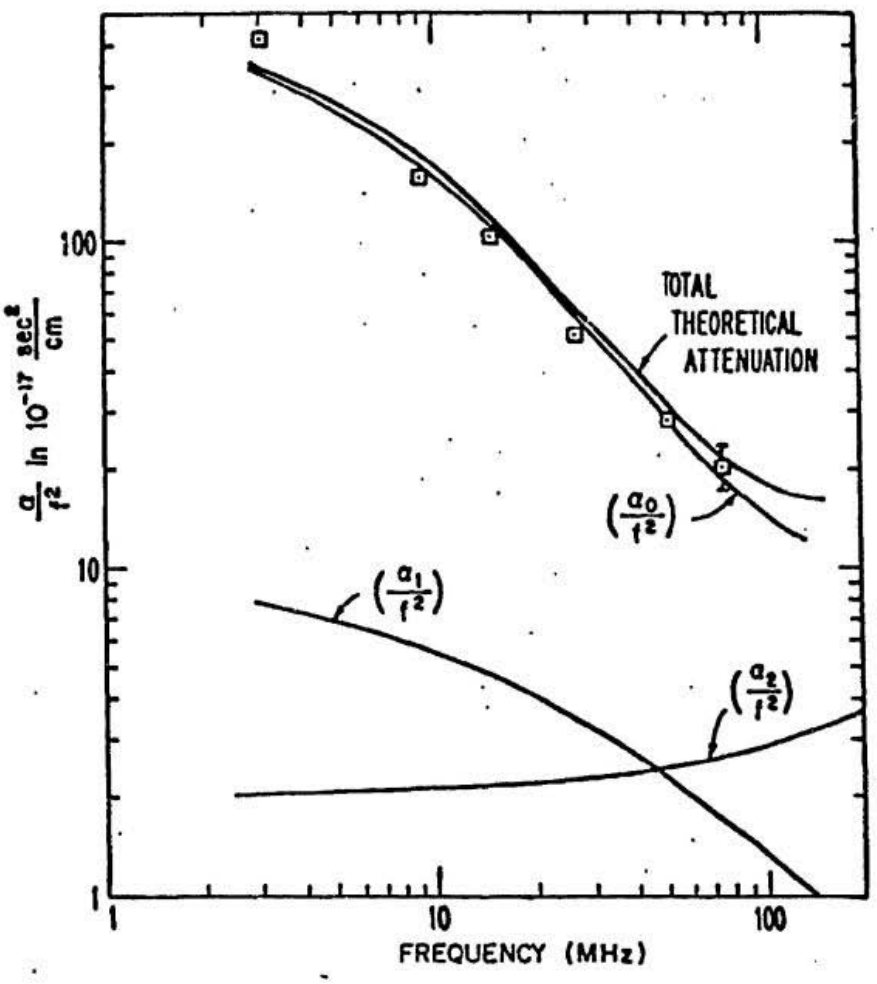

Figure A6.4. Excess attenuation versus frequency for an aqueous suspension of polystyrene spheres at 20° C, $a = 0.110\ \mu m$. Points are measured excess attenuation . [Allegra and Hawley, 1972].

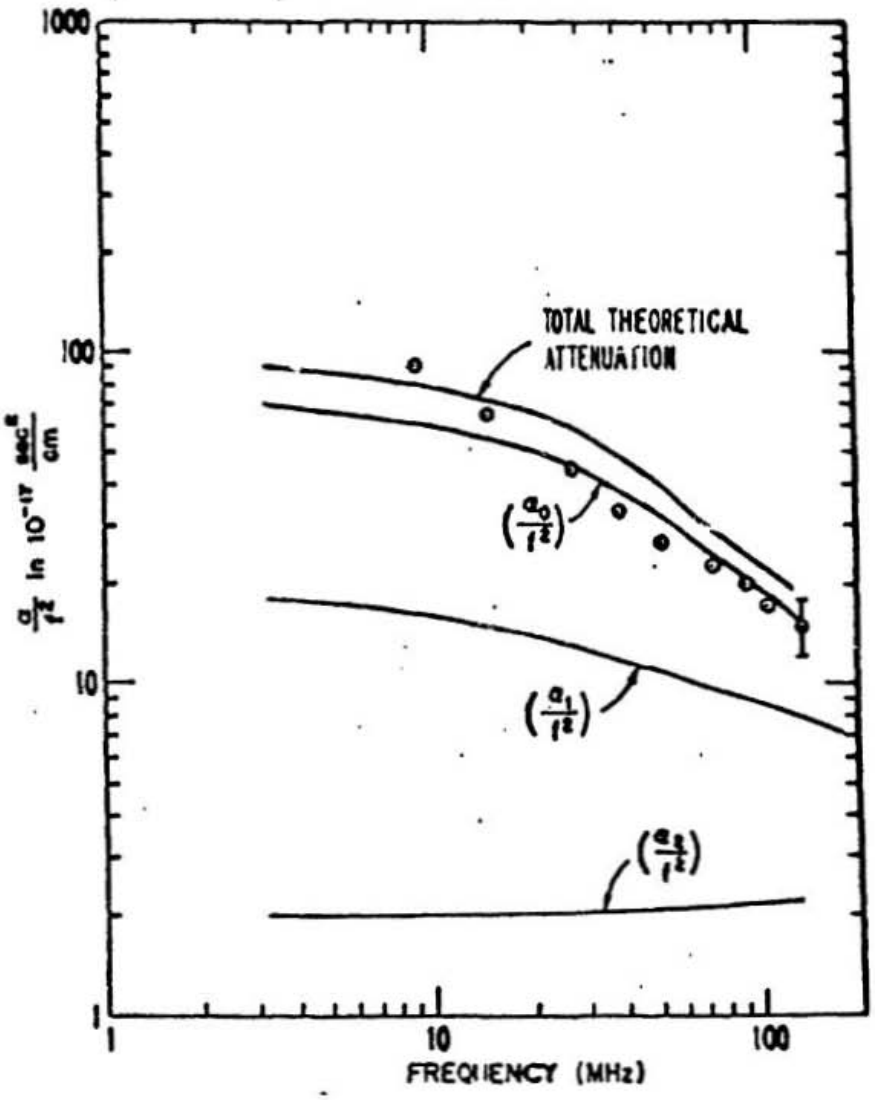

Figure A6.5. Excess attenuation versus frequency for an aqueous suspension of polystyrene spheres at 20° C, $a = 0.044\ \mu\text{m}$. Points are measured excess attenuation. [Allegra and Hawley, 1972].

Appendix 7 Simplification of the Tangential Stress Boundary Condition

For both the acoustic and the thermal mode the condition $\nabla \times \vec{v} = 0$ holds. Since for us the velocity is $\vec{v} = (v_r, v_\theta, 0)$, then we get (Arfken, 1970, p.81)

$$\vec{\nabla} \times \vec{v} = \frac{\hat{\phi}}{r}\left[\frac{\partial}{\partial r}(r v_\theta) - \frac{\partial v_r}{\partial \theta}\right] = 0 . \qquad \text{A7.1}$$

and then we obtain

$$\frac{\partial v_r}{\partial \theta} = \frac{\partial}{\partial r}(r v_\theta) . \qquad \text{A7.2}$$

Note that for the tangential stress boundary condition there is a relation of the form

$$\begin{aligned} r\,\frac{\partial}{\partial r}\left(\frac{v_\theta}{r}\right) + \frac{1}{r}\frac{\partial}{\partial \theta}(v_r) &= r\,\frac{\partial}{\partial r}\left(\frac{v_\theta}{r}\right) + \frac{1}{r}\frac{\partial}{\partial r}(r v_\theta) \qquad \text{A7.3} \\ &= 2\frac{\partial v_\theta}{\partial r} + \frac{v_\theta}{r} - \frac{v_\theta}{r} \\ &= 2\frac{\partial v_\theta}{\partial r} . \end{aligned}$$

This holds for both $\vec{v}_c$ and $\vec{v}_t$, but by the boundary layer theory $v_{t,\theta} = 0$, therefore we neglect it and the tangential stress is effectively independent of thermal effects, both in the fluid and the solid.

Appendix 8 Approximate Forms of b_c, b_t, b_c', and b_t'

We approximate the Allegra-Hawley results for b_c , b_t, b_c', and b_t'. In the fluid, Allegra and Hawley obtained (2.1.17) for b_c in the fluid, which is

$$b_c = \left(-\frac{\gamma}{c^2\beta} \right) \left[\omega^2 - \left(\frac{c^2}{\gamma} - \frac{4\, i\, \omega\, \mu_0}{3\, \rho_0} \right) k_c^2 \right]. \qquad \text{A8.1}$$

Using $k_c^2 c^2 \approx \omega^2$, equation A8.1 becomes

$$b_c \approx \frac{-\gamma k_c^2}{\beta} \left(1 - \frac{1}{\gamma} + \frac{4}{3} \frac{i\omega\mu_0}{\rho_0 c^2} \right) \qquad \text{A8.2}$$

where we can identify the last term in the equation as the scaling parameter ϵ_s (see 2.1.30b), which we know to be much less than one. Therefore equation A8.2 may be approximated by

$$b_c \approx -(\gamma-1)\frac{k_c^2}{\beta} . \qquad \text{A8.3}$$

Next we consider b_t. The Allegra and Hawley result is (2.1.18), which is

$$b_t = \left(-\frac{\gamma}{c^2\beta} \right) \left[\omega^2 - \left(\frac{c^2}{\gamma} - \frac{4\, i\, \omega\, \mu_0}{3\, \rho_0} \right) k_t^2 \right]. \qquad \text{A8.4}$$

We again assume that $k_c^2 c^2 \approx \omega^2$, and obtain

$$b_t \approx \frac{-\gamma k_c^2}{\beta} \left[1 - \frac{k_t^2}{k_c^2} \left(\frac{1}{\gamma} - \epsilon_s \right) \right] \qquad \text{A8.5}$$

which, since ϵ_s is small, is

$$b_t \approx \frac{-\gamma k_c^2}{\beta} \left(1 - \frac{1}{\gamma} \frac{k_t^2}{k_c^2} \right) \qquad \text{A8.6}$$

and since the second term is much larger than the first, we obtain

$$b_t \approx \frac{k_t^2}{\beta} \qquad \text{A8.7}$$

Now we approximate b_c' and b_t' in a similar fashion. The exact result for b_c' is (2.1.23) which is written

$$b_c' = \frac{-\gamma'}{c_1'^2 \beta'} \left[\omega^2 - \left(\frac{c_1'^2}{\gamma'} + \frac{4}{3}\frac{\mu'}{\rho_0'} \right) k_c'^2 \right], \qquad \text{A8.8}$$

and we then assume $k_c'^2 c'^2 \approx \omega^2$ to obtain

$$b_c' \approx \frac{-\gamma'}{\beta'} \frac{\omega^2}{c'^2} \left[\frac{c'^2}{c_1'^2} - \left(\frac{1}{\gamma'} + \frac{4}{3}\frac{\mu'}{\rho_0' c_1'^2} \right) \right] \qquad \text{A8.9}$$

$$= \frac{(1-\gamma')}{\beta'} \frac{\omega^2}{c'^2} \qquad \text{A8.10}$$

where we use $c'^2 = \frac{\lambda'+2\mu'}{\rho_0'}$ and $c_1'^2 = \frac{\lambda'+2/3\mu'}{\rho_0'}$.

Next we consider b_t'. The exact result is (2.1.24), which is

$$b_t' = \frac{-\gamma'}{c_1'^2 \beta'} \left[\omega^2 - \left(\frac{c_1'^2}{\gamma'} + \frac{4}{3}\frac{\mu'}{\rho_0'} \right) k_t'^2 \right]. \qquad \text{A8.11}$$

We make the approximation $k_c'^2 c'^2 \approx \omega^2$ to rewrite A8.11 as

$$b_t' \approx \frac{-\gamma'}{\beta'} \frac{c'^2}{c_1'^2} k_t'^2 \left[\frac{k_c'^2}{k_t'^2} - \left(\frac{1}{\gamma'}\frac{c_1'^2}{c'^2} + \frac{4}{3}\frac{\mu'}{\rho_0' c'^2} \right) \right] \qquad \text{A8.12}$$

Using the definitions of c' and c_1' given above, equation A8.12 can be rewritten as

$$b_t' = \frac{-\gamma'}{\beta'} \frac{c'^2}{c_1'^2} k_t'^2 \left[\frac{k_c'^2}{k_t'^2} - \frac{1}{\gamma'} \left(1 + (\gamma'-1)\frac{4/3\mu'}{\lambda'+2\mu'} \right) \right] \qquad \text{A8.13}$$

Knowing that both $(\gamma' - 1)$ and $k_c'^2/k_t'^2$ are much less than one, we may approximate A8.13 as

$$b_t' \approx \frac{c'^2}{c_1'^2} \frac{k_t'^2}{\beta'} \qquad \text{A8.14}$$